

CERN-TH/2002-264, SLAC-PUB-9604

# Present Status of Inclusive Rare B Decays

Tobias Hurth\*

*CERN, Theory Division*

*CH-1211 Geneva 23, Switzerland*

*tobias.hurth@cern.ch*

*and*

*SLAC, Stanford University*

*Stanford, CA 94309, USA*

*hurth@slac.stanford.edu*

## Abstract

We give a status report on inclusive rare  $B$  decays, highlighting recent developments and open problems. We focus on the decay modes  $B \rightarrow X_{s,d}\gamma$ ,  $B \rightarrow X_s\ell^+\ell^-$  and  $B \rightarrow X_s\nu\bar{\nu}$  and on their role in the search for new physics.

Most of the inclusive rare  $B$  decays are important modes of flavour physics due to the small hadronic uncertainties. They can be regarded as laboratories to search for new physics.

We collect the experimental data already available from CLEO and the  $B$  factories BABAR and BELLE. We review the NLL and NNLL QCD calculations of the inclusive decay rates that were recently completed, and discuss future prospects, especially the issue of the charm mass scheme ambiguity. Finally, we analyse the phenomenological impact of these decay modes, in particular on the CKM phenomenology and on the indirect search for supersymmetry.

We also briefly discuss direct CP violation in inclusive rare  $B$  decays, as well as the rare kaon decays  $K^+ \rightarrow \pi^+\nu\bar{\nu}$  and  $K_L \rightarrow \pi^0\nu\bar{\nu}$ , which offer complementary theoretically clean information.

## Invited Contribution to Reviews of Modern Physics

---

\*Heisenberg Fellow

## Contents

<b>I</b>	<b>Introduction</b>	<b>3</b>
<b>II</b>	<b>Strong interaction in <math>B</math> decays</b>	<b>6</b>
<b>III</b>	<b>Experimental status</b>	<b>10</b>
A	Experimental data on $B \rightarrow X_s \gamma$ . . . . .	10
B	Photon spectrum of $B \rightarrow X_s \gamma$ . . . . .	15
C	Experimental status of $B \rightarrow X_s \ell^+ \ell^-$ and $B \rightarrow X_d \gamma$ . . . . .	18
<b>IV</b>	<b>Perturbative calculations in <math>B \rightarrow X_{s,d} \gamma</math></b>	<b>21</b>
<b>V</b>	<b>Perturbative calculations in <math>B \rightarrow X_s \ell^+ \ell^-</math> and <math>B \rightarrow X_s \bar{\nu} \nu</math></b>	<b>26</b>
<b>VI</b>	<b>Non-perturbative contributions</b>	<b>31</b>
A	Inclusive decay rates of $B$ mesons . . . . .	31
B	Non-perturbative corrections to $B \rightarrow X_{s,d} \gamma$ and $B \rightarrow X_s \ell^+ \ell^-$ . . . . .	32
<b>VII</b>	<b>Phenomenology</b>	<b>35</b>
A	SM prediction of $B \rightarrow X_s \gamma$ . . . . .	35
B	CKM phenomenology with $B \rightarrow X_{s,d} \gamma$ . . . . .	37
C	Role of $b \rightarrow s$ gluon for $B \rightarrow X_{nocharm}$ . . . . .	38
D	Phenomenology of $B \rightarrow X_s \ell^+ \ell^-$ . . . . .	39
E	Golden mode $B \rightarrow X_s \bar{\nu} \nu$ . . . . .	43
<b>VIII</b>	<b>Indirect search for supersymmetry</b>	<b>45</b>
A	Generalities . . . . .	45
B	Constraints from $B \rightarrow X_s \gamma$ . . . . .	46
C	Constraints from $B \rightarrow X_s \ell^+ \ell^-$ . . . . .	54
<b>IX</b>	<b>Direct CP violation in <math>b \rightarrow s</math> transitions</b>	<b>56</b>
<b>X</b>	<b>Further opportunities</b>	<b>60</b>
A	$K_L \rightarrow \pi^0 \nu \bar{\nu}$ and $K^+ \rightarrow \pi^+ \nu \bar{\nu}$ . . . . .	60
<b>XI</b>	<b>Summary</b>	<b>65</b>

## I. INTRODUCTION

The precise test of the flavour structure and the mechanism of CP violation of the standard model (SM) is at the centre of today's research in high-energy physics. By definition, flavour physics deals with that part of the SM that distinguishes between the three generations of fundamental fermions. It is still a mystery why there are exactly three generations. Also the origin of the fermion masses and their mixing is unknown; in particular, the SM does not explain the hierarchical pattern of these parameters. Flavour physics can be regarded as the least tested part of the SM. This is reflected in the rather large error bars of several flavour parameters such as the mixing parameters at the 20% level [1].

However, the experimental situation concerning flavour physics is drastically changing. Several  $B$  physics experiments are successfully running at the moment and, in the upcoming years, new facilities will start to explore  $B$  physics with increasing sensitivity and within various experimental settings: apart from the CLEO experiment (Cornell, USA), located at the Cornell Electron–Positron Storage Ring (CESR) [2], two  $B$  factories, operating at the  $\Upsilon(4S)$  resonance in an asymmetric mode, are successfully obtaining data: the BABAR experiment at SLAC (Stanford, USA) [3] and the BELLE experiment at KEK (Tsukuba, Japan) [4]. Besides the hadronic  $B$  physics program at FERMILAB (Batavia, USA) [5] there are  $B$  physics experiments planned at the hadronic colliders. Within the LHC project at CERN in Geneva [6] all three experiments have strong  $B$  physics programs. Also at FERMILAB an independent  $B$  physics experiment,  $B\text{TeV}$ , is planned [7]. The main motivation for a  $B$  physics program at hadron colliders is the huge  $b$  quark production cross section with respect to the one at  $e^+e^-$  machines.

While the time of electroweak precision physics focusing on the *gauge* sector of the SM, draws to a close with the completion of the LEP experiments at CERN and the SLC experiment in Stanford, the era of precision flavour physics, focusing on the *scalar* sector of the SM, has just begun with the start of the  $B$  factories.

The  $B$  system represents an ideal framework for the study of flavour physics. Since the  $b$  quark mass is much larger than the typical scale of the strong interaction  $\Lambda_{QCD}$ , long-distance strong interactions are generally less important and are under better control than in kaon physics, thanks to the expansion in that heavy mass. Moreover, GIM suppression is not active in loop diagrams involving the top quarks, which leads to experimentally accessible rare decays and to large CP violating effects within  $B$  physics. Thus, the CP violation in the  $B$  system represents an important independent test of the SM description of CP violation (see [8–10]).  $B$  meson decays also allow for a rich CKM phenomenology and stringent tests of the unitarity.

The so-called rare decays are of particular interest. These processes represent flavour changing neutral currents (FCNCs) and occur in the SM only at the loop level. They also run under the name of ‘penguin decays’ (see fig. 1 [33]), first introduced in [11] as a result of a bet.

In contrast to the exclusive rare  $B$  decay modes, the inclusive ones are theoretically clean observables, because no specific model is needed to describe the hadronic final states. For instance the decay width  $\Gamma(B \rightarrow X_s \gamma)$  is well approximated by the partonic decay rate

$\Gamma(b \rightarrow X_s^{parton} \gamma)$ , which can be analysed within the framework of renormalization-group-improved perturbation theory. Non-perturbative contributions play only a subdominant role and can be calculated in a model-independent way by using the heavy-quark expansion.

The role of inclusive rare  $B$  decays is twofold: on the one hand they are relevant to the determination of CKM matrix elements. On the other hand they are particularly sensitive to new physics beyond the SM, since additional contributions to the decay rate, in which SM particles are replaced by new particles, such as the supersymmetric charginos or gluinos, are not suppressed by additional factors  $\alpha/(4\pi)$  relative to the SM contribution. This makes it possible to observe new physics indirectly - a strategy complementary to the direct production of new (supersymmetric) particles. The latter production is reserved for the planned hadronic machines such as the LHC at CERN, while the indirect search of the  $B$  factories already implies significant restrictions for the parameter space of supersymmetric models and, thus, lead to important clues for the direct search of supersymmetric particles.

It is even possible that these rare processes lead to the first evidence of new physics outside the neutrino sector by a significant deviation from the SM prediction, for example in the observables concerning direct CP violation within the  $\Delta F = 1$  sector; such a measurement would definitely not be in conflict with the recent measurements of CP violation in the  $B_d$  system, which confirms the SM predictions at the 10% level [8,9]. But also in the long run, after new physics has already been discovered, inclusive rare  $B$  decays will play an important role in analysing in greater detail the underlying new dynamics.

The expression *inclusive rare  $B$  decay* is loosely defined and calls for a precise definition. Within the present paper it is understood as a FCNC process  $B \rightarrow X Y$ , where  $B$  denotes a  $B^\pm$ ,  $B_d$  or  $B_s$  meson.  $X$  is an inclusive hadronic state containing no charmed particles, and  $Y$  is a state built out of leptons, neutrinos and photons. The possibilities for  $Y$  are for example  $\gamma$  (one particle),  $\ell^+ \ell^-$ ,  $\gamma \gamma$  or  $\nu \bar{\nu}$  (two particles), etc. The most interesting ones are  $B \rightarrow X_{s,d} \gamma$ ,  $B \rightarrow X_s \ell^+ \ell^-$ ,  $B \rightarrow X_s \nu \bar{\nu}$ , on which we will focus in this paper. Clearly, the cases with  $X = \emptyset$  are regarded as exclusive decay modes. Nevertheless, for example the rare decay  $B_{s,d} \rightarrow \ell^+ \ell^-$  is also theoretically rather clean, in contrast to other exclusive  $B$  rare modes.

In 1993, the first evidence for a rare  $B$  meson decay was found by the CLEO collaboration. At CESR, the exclusive electromagnetic penguin process  $B \rightarrow K^* \gamma$  was measured [12]. Among inclusive rare  $B$  decays, the  $B \rightarrow X_s \gamma$  mode is the most prominent, because it was already measured by several independent experiments [37,39–42] and the stringent bounds obtained from that mode on various non-standard scenarios (see e.g. [13–16]) are a clear example of the importance of theoretically clean FCNC observables in discriminating new-physics models. Also the inclusive  $B \rightarrow X_s \ell^+ \ell^-$  transition is already accessible at  $B$  factories [55]. It represents a new source of theoretically clean observables, complementary to the  $B \rightarrow X_s \gamma$  rate. In particular, kinematic observables such as the invariant dilepton mass spectrum and the forward–backward (FB) asymmetry in  $B \rightarrow X_s \ell^+ \ell^-$ , provide clean information on short-distance couplings not accessible in  $B \rightarrow X_s \gamma$  [18].

Although the general focus within flavour physics is at present on  $B$  systems, kaon physics offers interesting complementary opportunities in the new physics search, such as the exclusive rare decays  $K^+ \rightarrow \pi^+ \nu \bar{\nu}$  and  $K_L \rightarrow \pi^0 \nu \bar{\nu}$ . They are specifically interesting in view

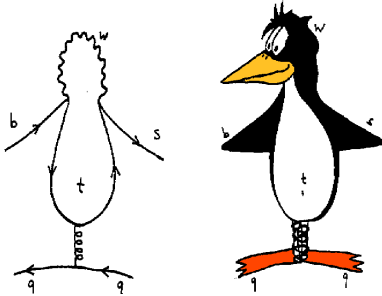


FIG. 1. Penguin decays of  $B$  mesons.

of the current experiments at the Brookhaven National Laboratory (USA) and suggested experiments at FERMILAB (USA) and at KEK (Japan). They are also theoretically clean observables.

This present paper is meant as a status report to highlight recent developments and open problems; for the technical tools the reader is often guided to excellent reviews that already exist in the literature. The paper is organized as follows: in section II we briefly discuss the role of the strong interaction within flavour physics. In section III the experimental status of rare  $B$  decays is summarized. In section IV and V we focus on the perturbative calculations; in section VI we discuss the non-perturbative corrections. Phenomenological implications are discussed in section VII. In section VIII we explore the implications of these decays for our search of physics beyond the SM. In section IX we discuss direct CP violation and in section X the complementary role of rare kaon decays in precision flavour physics. In section XI, we present our summary.

## II. STRONG INTERACTION IN $B$ DECAYS

Flavour physics is governed by the interplay of strong and weak interactions. One of the main difficulties in examining the observables in flavour physics is the influence of the strong interaction. As is well known, for matrix elements dominated by long-distance strong interactions, there is no adequate quantitative solution available in quantum field theory. The resulting hadronic uncertainties restrict the opportunities in flavour physics significantly, in particular within the indirect search for new physics.

The present discussion on the new  $g - 2$  muon data [19] also reflects this issue (for a recent review, see [20]): the hadronic self-energy contribution to the  $g - 2$  observable can be determined by experimental data, however, the results found from  $e^+e^-$ -based data and from the  $\tau$ -based data differ from each other. Furthermore the well-known light-by-light scattering contribution can only be modelled at present. It is obvious that these hadronic uncertainties make it difficult to deduce strict constraints on a new physics scenario from this measurement.

There are several fundamental tools available, which are directly based on QCD. High hopes for precise QCD predictions are placed on lattice gauge theoretical calculations. While there are competitive predictions from lattice gauge theory for form factors of semi-leptonic  $B$  decays, pure hadronic decays are less accessible to these methods [21].

Another approach is the method of factorization [22]. This method has recently been systemized for non-leptonic decays in the heavy quark limit [23,24]. However, within this approach, a quantitative method to estimate the  $1/m_b$  corrections to this limit is missing [25]. A promising step in this direction was recently presented in [26].

Further well-known fundamental methods whose applications and precision are also somewhat restricted are chiral perturbation theory [27], heavy quark effective theory (HQET) [29], QCD sum rules [28] and the  $1/N$  expansion [30].

In view of this, the goal must be to minimize theoretical uncertainties with the help of an optimized combination of different fundamental methods solely based on QCD. This can only be done for a selected number of observables in flavour physics. It is also clear that an active cooperation between theory and experiment is necessary in order to make progress on this issue.

There are a few golden channels in which the hadronic physics can be disentangled and clean tests of the SM are possible. Moreover, there are also observables, dominated by perturbative contributions, which make precision flavour physics possible in the near future. Among them inclusive rare  $B$  decays play the most important role. Inclusive decay modes are theoretically clean and represent a theoretical laboratory of perturbative QCD. In particular, the decay width  $\Gamma(B \rightarrow X_s \gamma)$  is well approximated by the partonic decay rate  $\Gamma(b \rightarrow X_s^{\text{parton}} \gamma)$ , which can be analysed in renormalization-group-improved perturbation theory:

$$\Gamma(B \rightarrow X_s \gamma) = \Gamma(b \rightarrow X_s^{\text{parton}} \gamma) + \Delta^{\text{nonpert.}} \quad (\text{II.1})$$

Non-perturbative effects,  $\Delta^{\text{nonpert.}}$ , play a subdominant role and are under control thanks to the heavy mass expansion [31] and the assumption of quark–hadron duality [32].

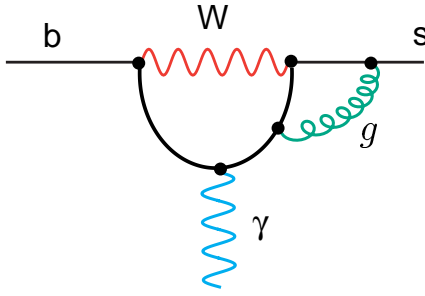


FIG. 2. QCD corrections to the decay  $B \rightarrow X_s \gamma$ .

Thus, in general, inclusive decay modes should be preferred to exclusive ones from the theoretical point of view. The inclusive modes  $B \rightarrow X_{s(d)}\gamma$  and  $B \rightarrow X_{s(d)}\ell^+\ell^-$  can be measured by the electron–positron experiments ( $B$  factories, CLEO) with their kinematic constraints and their controlled background, while they are more difficult to measure at hadronic machines. Exclusive decay modes, however, are more accessible to experiments, in particular at hadronic machines. But in contrast to the inclusive modes, they have in general large non-perturbative QCD contributions, which makes it difficult to deduce valuable information on new physics from those decay modes. However, as mentioned in the introduction, the exclusive decays  $B_{d,s} \rightarrow \mu^+\mu^-$  are distinguished observables at hadronic colliders.

Within inclusive  $B$  decay modes, short-distance QCD effects turn out to be very important. For example, in the decay  $B \rightarrow X_s \gamma$  they lead to a tremendous rate enhancement. These effects are induced by hard–gluon exchange between the quark lines of the one-loop electroweak diagrams (fig. 2).

The QCD radiative corrections bring in large logarithms of the form  $\alpha_s^n(m_b) \log^m(m_b/M)$ , where  $M = m_t$  or  $M = m_W$  and  $m \leq n$  (with  $n = 0, 1, 2, \dots$ ). This is a natural feature in any process where two different mass scales are present. In order to get a reasonable result at all, one has to resum at least the leading-log (LL) series

$$\alpha_s^n(m_b) \log^n(m_b/M), \text{ (LL)} \quad (\text{II.2})$$

with the help of renormalization–group techniques. Working to next-to-leading-log (NLL) precision means that one is also resumming all the terms of the form

$$\alpha_s(m_b) \alpha_s^n(m_b) \log^n(m_b/M), \text{ (NLL).} \quad (\text{II.3})$$

A suitable framework to achieve the necessary resummations of the large logs is an effective low-energy theory with five quarks, obtained by integrating out the heavy particles, which, in the SM, are the electroweak bosons and the top quark. The standard method of the operator product expansion (OPE) allows for a separation of the meson decay amplitude into two distinct parts, the long-distance contributions contained in the operator matrix elements and the short-distance physics described by the so-called Wilson coefficients (see

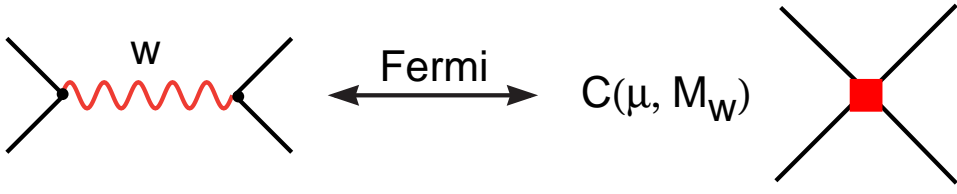


FIG. 3. Operator product expansion: full versus effective theory.

fig. 3). In the case of  $B$  decays, the  $W$  boson and the top quark with mass larger than the factorization scale are integrated out, that is removed from the theory as dynamical fields. The effective Hamiltonian can be written

$$H_{eff} = -\frac{4G_F}{\sqrt{2}} \sum C_i(\mu, M_{heavy}) \mathcal{O}_i(\mu), \quad (\text{II.4})$$

where  $\mathcal{O}_i(\mu)$  are the relevant operators and  $C_i(\mu, M_{heavy})$  are the corresponding Wilson coefficients. As the heavy fields are integrated out, the complete top and  $W$  mass dependence is contained in the Wilson coefficients. Working out a convenient set of quantities, both in the effective (low-energy) theory and in the full (standard model) theory, and requiring equality (matching) up to terms suppressed by higher powers of  $m_W$  or  $m_t$ , these coefficients can be determined. At the high scale  $\mu_W \approx m_W, m_t$ , the matrix elements of the operators in the effective theory lead to the same logarithms as the full theory calculation. Consequently, the Wilson coefficients  $C_i(\mu_W)$  only pick up small QCD corrections, which can be calculated in fixed-order perturbation theory.

Within this framework QCD corrections for the decay rates are twofold: the ingredients are the order  $\alpha_s$  corrections to the matrix elements of the various operators and the order  $\alpha_s$  corrections to the Wilson coefficients, of course both at the low-energy scale  $\mu_b \approx m_b$ . Only the sum of the two contributions is renormalization-scheme- and scale-independent; in fact, from the  $\mu$ -independence of the effective Hamiltonian, one can derive a renormalization group equation (RGE) for the Wilson coefficients  $C_i(\mu)$ :

$$\mu \frac{d}{d\mu} C_i(\mu) = \gamma_{ji} C_j(\mu) \quad , \quad (\text{II.5})$$

where the matrix  $\gamma$  is the anomalous dimension matrix of the operators  $\mathcal{O}_i$ , which describes the anomalous scaling of the operators with respect to the one at the classical level. At leading order, the solution is given by

$$\tilde{C}_i(\mu) = \left[ \frac{\alpha_s(\mu_W)}{\alpha_s(\mu)} \right]^{\frac{\tilde{\gamma}_{ii}^{(0)}}{2\beta_0}} \tilde{C}_i(\mu_W) = \left[ \frac{1}{1 + \beta_0 \frac{\alpha_s(\mu)}{4\pi} \ln \frac{\mu_W^2}{\mu^2}} \right]^{\frac{\tilde{\gamma}_{ii}^{(0)}}{2\beta_0}} \tilde{C}_i(\mu_W) \quad (\text{II.6})$$

with  $\mu d/d\mu\alpha_s = -2\beta_0\alpha_s^2/(4\pi)$ ;  $\beta_0$  and  $\tilde{\gamma}_{ii}^0$  correpond to the leading anomalous dimension of the coupling constant and the operators, respectively. The tilde indicates that the diagonalized anomalous dimension matrix is used. The formula (II.6) to LL precision makes the renormalization-group improvement transparent. It represents a summation of the form of the Eq. (II.2).

There are three principal calculational steps leading to the leading-log (next-to-leading-log) result within the effective field theory approach (for a pedagogical review see [34]):

- Step 1: The full SM theory has to be matched with the effective theory at the scale  $\mu = \mu_W$ , where  $\mu_W$  denotes a scale of order  $m_W$  or  $m_t$ . As mentioned above, the Wilson coefficients  $C_i(\mu_W)$  only pick up small QCD corrections, which can be calculated in fixed-order perturbation theory. In the LL (NLL) program, the matching has to be worked out at the  $O(\alpha_s^0)$  ( $O(\alpha_s^1)$ ) level.
- Step 2: Then the evolution of these Wilson coefficients from  $\mu = \mu_W$  down to  $\mu = \mu_b$  has to be performed with the help of the renormalization group, where  $\mu_b$  is of the order of  $m_b$ . As the matrix elements of the operators evaluated at the low scale  $\mu_b$  are free of large logarithms, the latter are contained in resummed form in the Wilson coefficients. For a LL (NLL) calculation, this RGE step has to be done using the anomalous-dimension matrix up to order  $\alpha_s^1$  ( $\alpha_s^2$ ).
- Step 3: To LL (NLL) precision, the corrections to the matrix elements of the operators  $\langle s\gamma|\mathcal{O}i(\mu)|b\rangle$  at the scale  $\mu = \mu_b$  have to be calculated to order  $\alpha_s^0$  ( $\alpha_s^1$ ) precision. This includes also bremsstrahlung corrections.

Finally, we stress that the step from the leading (LL) to the next-to-leading (NLL) order within the framework of the renormalization-group-improved perturbation theory is not only a quantitative one, increasing the precision of the theoretical prediction, but also a qualitative one, which tests the validity of the perturbative approach in the given problem.

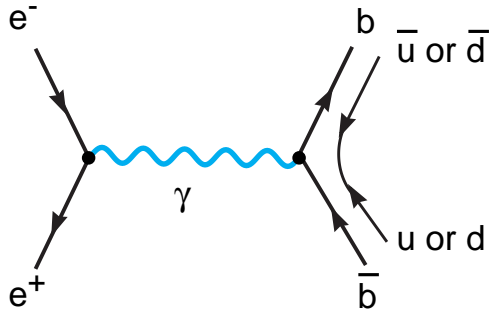


FIG. 4.  $e^+e^- \rightarrow \Upsilon(4S) \rightarrow B^+B^-, B^0\bar{B}^0$ .

### III. EXPERIMENTAL STATUS

#### A. Experimental data on $B \rightarrow X_s\gamma$

Among inclusive rare  $B$  decays, the  $B \rightarrow X_s\gamma$  mode is the most prominent because it was already measured by several independent  $e^+e^-$ -experiments, mostly at the  $\Upsilon(4S)$  resonance, fig. 4 [37,39–42] (see also [43–45]). In 1993, the first evidence for a penguin-induced  $B$  meson decay was found by the CLEO collaboration. At CESR, they measured the exclusive electromagnetic penguin process  $B \rightarrow K^*\gamma$  [12]. The inclusive analogue  $B \rightarrow X_s\gamma$ , which is the quantity of theoretical interest, was also found by the CLEO collaboration through the measurement of its characteristic photon energy spectrum in 1994. As this process is dominated by the two-body decay  $b \rightarrow s\gamma$ , its photon energy spectrum is expected to be a smeared delta function centred at  $E_\gamma \approx m_b/2$ , where the smearing is due to perturbative gluon bremsstrahlung and to the non-perturbative motion of the  $b$  quark within the  $B$  meson.

Only the high part of the  $B \rightarrow X_s\gamma$  photon spectrum is observed. Some lower cut-off in the photon energy was imposed in order to suppress the background from other  $B$  decay processes. The  $B\bar{B}$  background mainly arises from the processes  $B \rightarrow \pi^0X$  and  $\pi^0 \rightarrow \gamma_1\gamma_2$  or  $B \rightarrow \eta X$  and  $\eta \rightarrow \gamma_1\gamma_2$ , where  $\gamma_1$  has high energy and  $\gamma_2$  either has energy too low to be observed or is not in the geometric acceptance of the detector. Moreover, there is a small component ( $\sim 5\%$ ) from the process  $B \rightarrow \bar{n}X$  or  $B \rightarrow K_LX$ , where the anti-neutron or the neutral kaon interacts hadronically with the electromagnetic calorimeter, faking a photon.

Therefore only the ‘kinematic’ branching ratio for  $B \rightarrow X_s\gamma$  in the range between  $E_\gamma = 2.2$  GeV and the kinematic endpoint at  $E_\gamma = 2.7$  GeV could be measured directly within this first measurement. To obtain from this measurement the ‘total’ branching ratio, one has to know the fraction  $R$  of the  $B \rightarrow X_s\gamma$  events with  $E_\gamma \geq 2.2$  GeV. This was first done in [35] where the motion of the  $b$  quark in the  $B$  meson was taken into account by using a phenomenological model [36] and taking into account a large systematic error for this model dependence. Using this *theoretical* input regarding the photon energy spectrum the value  $R = 0.87 \pm 0.06$  was used by the CLEO collaboration, leading to the CLEO branching ratio [37]

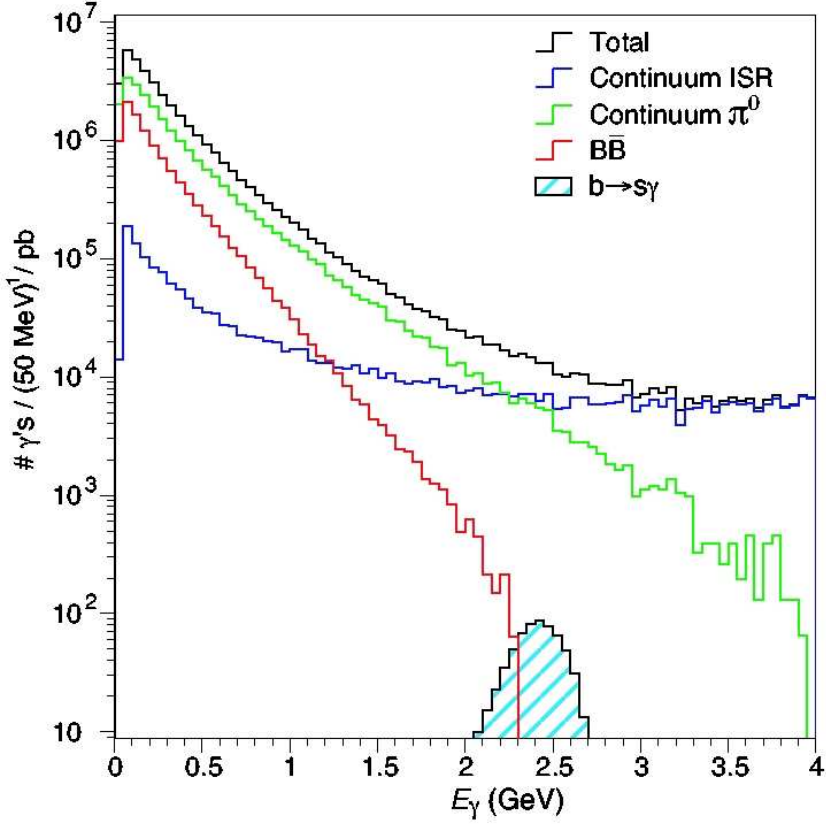


FIG. 5. Levels of inclusive photons from various background processes at  $\Upsilon(4S)$  and the expected signal from  $b \rightarrow s\gamma$ : ISR,  $B\bar{B}$  and  $\pi^0$  backgrounds are shown (from the bottom to the top at  $E_\gamma = 0.5$ ), from [45].

$$\mathcal{B}(B \rightarrow X_s \gamma) = (2.32 \pm 0.57_{stat} \pm 0.35_{syst}) \times 10^{-4}. \quad (\text{III.1})$$

The first error is statistical and the second is systematic (including model dependence). This measurement was based on a sample of  $2.2 \times 10^6 B\bar{B}$  events.

Besides the high energy cut-off to suppress the background from other  $B$  decays, two different techniques were used to suppress the continuum background in this first CLEO measurement. In the first (semi-inclusive) technique all products were reconstructed as in the exclusive measurement. The background in the measurement of exclusive modes is naturally low, because of kinematical constraints and of the beam energy constraint. In order to reduce the combinatoric background, only  $K(n\pi)\gamma$ , with  $n \leq 4$  and at most one  $\pi^0$ , were chosen as final states in this analysis, which accounts for  $\sim 50\%$  of the inclusive rate. In the second (fully inclusive) technique, only the photon was explicitly reconstructed. As shown in fig. 5, there are very large backgrounds, both from the initial-state-radiation (ISR) process  $e^+e^- \rightarrow q\bar{q}\gamma$ , where one of the beam electrons radiates a hard photon before annihilation, and from inclusive  $\pi^0/\eta$  production in which one of the photons from the decay is not detected. Background suppression was therefore more difficult with this technique. For this purpose, topological differences between the spherical  $B\bar{B}$  events and the two jets

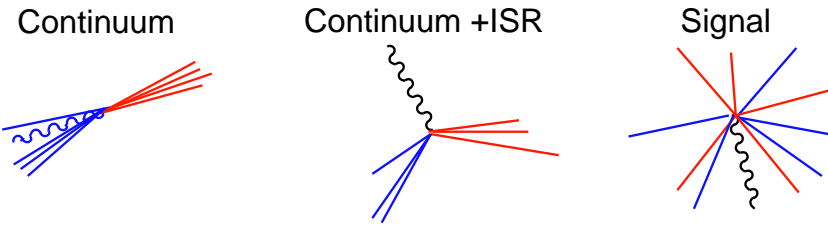


FIG. 6. Examples of idealized event shapes. The straight lines indicate hadrons and the wavy lines photons, from [44].

$e^+e^- \rightarrow q\bar{q}$  as shown in fig. 6 were used. While the signal events are spherical because the  $B$  mesons are almost at rest at the  $\Upsilon(4S)$  resonance, the continuum events have a jet-like structure. With the help of a neural network, several event-shape variables were combined into a single one, which tends towards +1 for  $b \rightarrow s\gamma$  and towards -1 for the ISR and  $q\bar{q}$  processes; the signal was extracted from a one-parameter fit to that variable.

The signal efficiency (32%) was very high with respect to the first technique (9%). However the first technique has a better signal-to-noise ratio, so that the two methods had nearly equal sensitivity. In the first CLEO measurement in 1994, they found  $\mathcal{B}(B \rightarrow X_s\gamma) = (2.75 \pm 0.67_{\text{stat}}) \times 10^{-4}$  with the first technique and  $\mathcal{B}(B \rightarrow X_s\gamma) = (1.88 \pm 0.74_{\text{stat}}) \times 10^{-4}$  using the second technique. The branching ratio stated above (III.1) represents the average of the two measurements, taking into account the correlation between the two techniques.

In 1999, CLEO had presented a preliminary improved measurement [38], which was based on 53% more data ( $3.3 \times 10^6$  events). They also used the slightly wider  $E_\gamma$  window starting at 2.1 GeV. The relative error dropped by a factor of almost  $\sqrt{3}$  already. In 2002, CLEO published a new measurement [39], based on three times more data ( $10 \times 10^6$  events). The spectrum down to 2.0 GeV was used, which includes almost 90% of the  $B \rightarrow X_s\gamma$  yield. This also leads to a significant background from  $B$  decay processes other than  $B \rightarrow X_s\gamma$ , located within 2.0 – 2.2 GeV. This  $B\bar{B}$  background arises from two components. First the inclusive  $\pi^0/\eta$  decays which account for  $\sim 90\%$  of the background. This is estimated by Monte Carlo in which the inclusive  $\pi^0/\eta$  spectra have been tuned with independent processes to replicate the data. Second, hadronic interactions of anti-neutrons and neutral kaons in the electromagnetic calorimeter may fake a photon candidate. However, their lateral profile is different from that of real photons, which allows a background subtraction. The continuum background was suppressed with the same two approaches as in the first measurement, but within a fully integrated analysis. What remained of the continuum background was subtracted using off-resonance data.

In order to obtain the corrected branching ratio of  $B \rightarrow X_s\gamma$ , two extrapolations were necessary. What was directly measured was the branching fraction for  $B \rightarrow X_s\gamma$  plus  $B \rightarrow X_d\gamma$ . The  $B \rightarrow X_d\gamma$  part was subtracted by using the theory input that, according to the SM expectation, the  $B \rightarrow X_d\gamma$  and the  $B \rightarrow X_s\gamma$  branching fractions are in the ratio  $|V_{td}/V_{ts}|^2$ . Therefore the branching ratio was corrected down by  $(4.0 \pm 1.6)\%$  of itself - assuming the validity of the SM suppression factor  $|V_{td}/V_{ts}|^2$ . Moreover, one has to know again the fraction  $R$  of the  $B \rightarrow X_s\gamma$  events with  $E_\gamma \geq 2.0$  GeV. In this measurement,

the corresponding fraction was estimated to be  $R = 0.915^{+0.027}_{-0.055}$  using the model of Kagan and Neubert (see also section III B), which allowed for the extrapolation of the measured branching ratio to the ‘total’  $B \rightarrow X_s \gamma$  branching ratio ( $E_\gamma > 0.25$  GeV). With these two theoretical corrections, the present CLEO measurement for the  $B \rightarrow X_s \gamma$  branching ratio is

$$\mathcal{B}(B \rightarrow X_s \gamma) = (3.21 \pm 0.43_{stat} \pm 0.27_{syst}^{+0.18}_{-0.10_{mod}}) \times 10^{-4}. \quad (\text{III.2})$$

The errors represent statistics, systematics, and the model dependence (due to the extrapolation below  $E_\gamma = 2.0$  GeV) respectively.

There are also data at the  $Z^0$  peak from the LEP experiments. The ALEPH collaboration [40] has measured the inclusive branching ratio based on  $0.8 \times 10^6 b\bar{b}$  pairs.

$$\mathcal{B}(H_b \rightarrow X_s \gamma) = (3.11 \pm 0.80_{stat} \pm 0.72_{syst}) \times 10^{-4}. \quad (\text{III.3})$$

The signal was isolated in lifetime-tagged  $b\bar{b}$  events by the presence of a hard photon associated with a system of high momentum and high rapidity hadrons. It should be noted that the branching ratio in (III.3) involves a weighted average of the  $B$  mesons and  $\Lambda_b$  baryons produced in  $Z^0$  decays (hence the symbol  $H_b$ ) different from the corresponding one given by CLEO, which has been measured at the  $\Upsilon(4S)$  resonance. High luminosity is more difficult to obtain at higher  $e^+e^-$  collision energies. Thus,  $B\bar{B}$  samples obtained by the LEP experiments are rather small. The rate measured by ALEPH is consistent with the CLEO measurement, with an error twice as large as the present CLEO measurement.

BELLE has also presented a measurement [41] based on  $6.07 \times 10^{-6} B\bar{B}$  events at the  $\Upsilon(4S)$  resonance. A semi-inclusive analysis was used to reconstruct the  $B \rightarrow X_s \gamma$  decay from a primary photon, a kaon and multiple pions (no more than one  $\pi^0$ ). The background reduction includes an effective  $E_\gamma > 2.24$  GeV photon energy cut-off which corresponds to a cut in the hadronic mass spectrum of  $M_{X_s} = 2.05$  GeV as quoted in [41];  $E_\gamma = (M_B^2 - M_{X_s}^2)/(2M_B)$ :

$$\mathcal{B}(B \rightarrow X_s \gamma) = (3.37 \pm 0.53_{stat} \pm 0.42_{syst} \pm 0.54_{mod}) \times 10^{-4}, \quad (\text{III.4})$$

which is consistent with previous measurements.

BABAR presented two preliminary analyses on the  $B \rightarrow X_s \gamma$  branching ratio, a fully inclusive and a semi-inclusive one [42]. The fully inclusive BABAR measurement has used the largest number of  $B$  mesons, so far. It is based on almost  $60 \times 10^6 B\bar{B}$  events at the  $\Upsilon(4S)$  resonance. The method of extracting the signal from the data is similar to what was done for previous measurements: the continuum background was subtracted with the help of off-resonance data. The  $B\bar{B}$  contribution was deduced from Monte Carlo predictions.

Nevertheless, the high statistics available in this BABAR measurement allowed for additional techniques: a lepton tag on a high-momentum electron or muon was also required to suppress continuum backgrounds. For the  $B \rightarrow X_s \gamma$  signal events, the lepton arises from the semi-leptonic decay of the other  $B$  meson. Leptons also occur in the continuum background, most notably from the semi-leptonic decays of charm hadrons, but their production is significantly less frequent and their momentum lower than those from a  $B$  decay. Because a lepton tag is imposed on the other  $B$  meson, not on the signal  $B$ , one can reject the

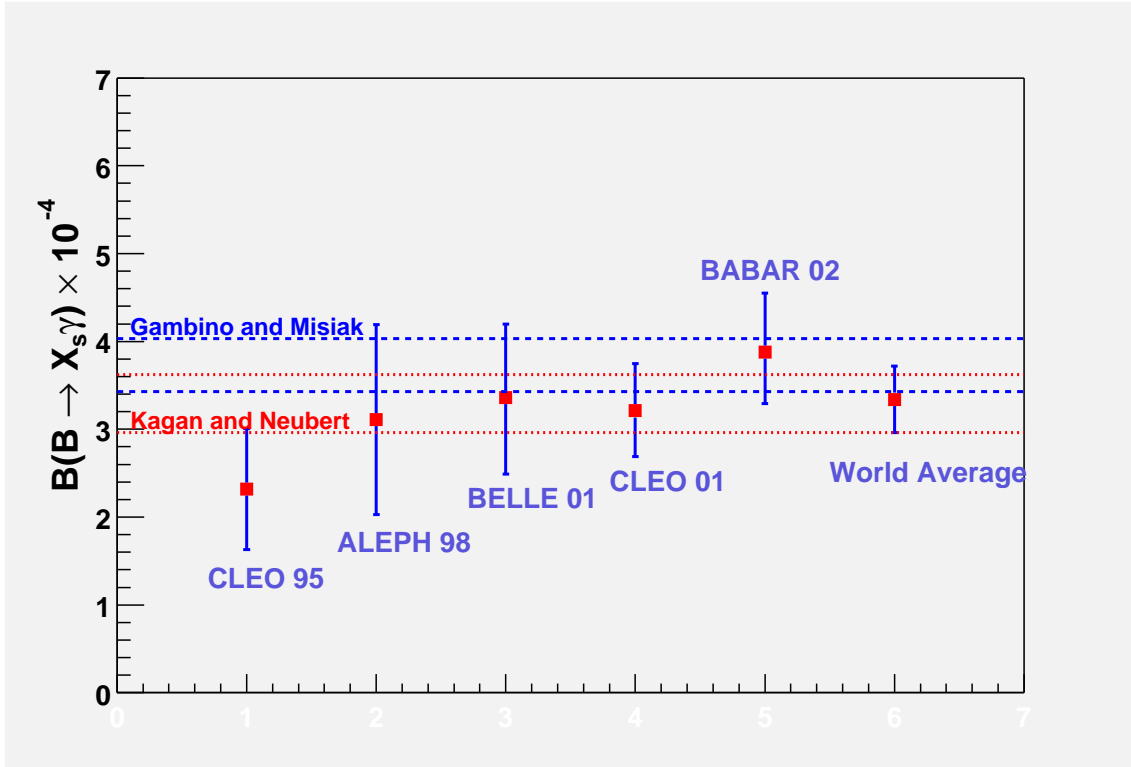


FIG. 7.  $B \rightarrow X_s \gamma$  measurements versus theoretical predictions (see section VII A), from [42].

continuum background without introducing any model dependence because one does not impose any requirements on the signal decay. A  $\times 1200$  reduction of the background was achieved by 5% efficiency of the lepton tag. This effective method to suppress the continuum background was possible because of the high statistics of the new BABAR measurement.

The systematic precision was limited by the size of the  $B\bar{B}$  background control samples scaling in proportion to the signal sample. The systematic precision limited the lower bound to  $E_\gamma > 2.1$  GeV (measured in the  $e^+e^-$  centre-of-mass system). The preliminary BABAR measurement is

$$\mathcal{B}(B \rightarrow X_s \gamma) = (3.88 \pm 0.36_{stat} \pm 0.37_{syst}^{+0.43}_{-0.23_{mod}}) \times 10^{-4}. \quad (\text{III.5})$$

Besides this fully inclusive analysis, BABAR also presented a semi-inclusive analysis where twelve exclusive  $b \rightarrow s\gamma$  decays were fully reconstructed, which led to the following measurement of the inclusive branching ratio:

$$\mathcal{B}(B \rightarrow X_s \gamma) = (4.4 \pm 0.5_{stat} \pm 0.8_{syst} \pm 1.3_{mod}) \times 10^{-4}. \quad (\text{III.6})$$

The error is much larger than the one of the previous semi-inclusive measurements, but includes also less final states; only states including 1 – 3 pions rather than 1 – 4 pions were reconstructed.

When much more statistics is available, the fully-inclusive strategy using the lepton tag will get the priority in the future measurements of the  $B \rightarrow X_s \gamma$  branching ratio because

model dependence and systematic errors can be reduced significantly compared to the semi-inclusive method.

As fig. 7 shows, all the measurements of the ‘total’  $B \rightarrow X_s\gamma$  branching ratio available so far are consistent with each other and also consistent with the SM predictions (see section VII A). A weighted average of the available experimental measurements is problematic, because the model dependence errors (and also the systematic errors) are correlated and differ within the various measurements. A recent analysis taking into account the correlations leads to the following world average [50]:

$$\mathcal{B}(B \rightarrow X_s\gamma) = (3.34 \pm 0.38) \times 10^{-4}. \quad (\text{III.7})$$

With the expected high luminosity of the  $B$ -factories, the systematic uncertainty in the  $B\bar{B}$  background will be reduced along with statistical uncertainties. This reduction in the systematic uncertainty will also allow for a lower photon energy cut-off, which will further reduce the model dependence from the theory-based interpolation to the whole energy spectrum [42]. Thus, in the future the lower energy cut-off in a fully inclusive analysis has to balance the systematic error due to the  $B\bar{B}$  background and the model dependence due to the extrapolation. An experimental accuracy below 10% in the inclusive  $B \rightarrow X_s\gamma$  mode is possible in the near future.

### B. Photon spectrum of $B \rightarrow X_s\gamma$

The uncertainty regarding the fraction  $R$  of the  $B \rightarrow X_s\gamma$  events above the chosen lower photon energy cut-off  $E_\gamma$  GeV quoted in the experimental measurement, also cited as model dependence, should be regarded as a purely *theoretical* uncertainty: in contrast to the ‘total’ branching ratio of  $B \rightarrow X_s\gamma$ , the photon energy spectrum cannot be calculated directly using the heavy mass expansion, because the operator product expansion breaks down in the high-energy part of the spectrum, where  $E_\gamma \approx m_b/2$ . Therefore, the fraction  $R$  was calculated in [35] using a phenomenological model [36], where the motion of the  $b$  quark in the  $B$  meson is characterized by two parameters, the average momentum  $p_F$  of the  $b$  quark and the average mass  $m_q$  of the spectator quark.

The error on the fraction  $R$  is essentially obtained by varying the model parameters  $p_F$  and  $m_q$  in the range for which the model correctly describes the energy spectrum of the charged lepton in the semi-leptonic decays  $B \rightarrow X_c\ell\nu$  and  $B \rightarrow X_u\ell\nu$ , measured by CLEO and ARGUS. In [35] a first comparison between the calculated photon energy spectrum and the one measured by the CLEO collaboration was presented. The (normalized) measured photon energy spectrum and the theoretical one were in agreement for those values of  $p_F$  and  $m_q$  that correctly describe the inclusive semi-leptonic CLEO data on  $B \rightarrow X_c\ell\nu$  and  $B \rightarrow X_u\ell\nu$ .

Besides this phenomenological model, more fundamental theoretical methods are available today to implement the bound-state effects, namely by making use of operator product expansion techniques in the framework of the heavy quark effective theory (HQET). An analysis along these lines was presented in [46]. As mentioned above, the operator product expansion breaks down near the endpoint of the photon energy spectrum; therefore, an

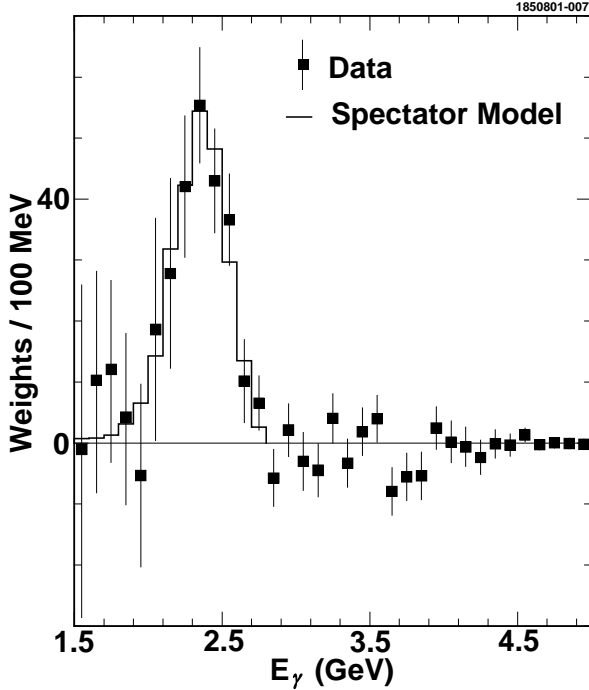


FIG. 8. Photon energy spectrum measured by CLEO and spectrum from Monte Carlo simulation of the spectator model with parameters  $\hat{m}_b = 4.690$  GeV,  $p_F = 410$  MeV/c, a good fit to the data, from [39].

infinite number of leading-twist corrections have to be resummed into a non-perturbative universal shape function, which determines the light-cone momentum distribution of the  $b$  quark in the  $B$  meson [47]. The physical decay distributions are then obtained from a convolution of parton model spectra with this shape function. At present this function cannot be calculated, but there is at least some information on the moments of the shape function, which are related to the forward matrix elements of local operators. Ansätze for the shape function, constrained by the latter information, are used. In contrast to the older analysis based on the phenomenological model proposed in [36], the analysis of Kagan and Neubert [46] includes the full NLL information.

In the latest CLEO measurement [39], the phenomenological spectator model [36,35] was used first. The momentum parameter  $p_F$  and the  $b$  quark average mass  $\hat{m}_b$  were treated as free parameters, which allowed the mean and the width of the photon energy spectrum to be varied: see fig. 8. The Kagan–Neubert approach was also used by CLEO: the simple two-parameter shape function was fitted to the measured photon spectrum and very similar results to those obtained using the spectator model were obtained.

An important observation is that the shape of the photon spectrum is practically insensitive to physics beyond the SM. As can be seen in fig. 9, all different contributions to the spectrum (corresponding to the interference terms of the various operators involved, see section IV) have a very similar shape besides the small 8–8 contribution. This implies that

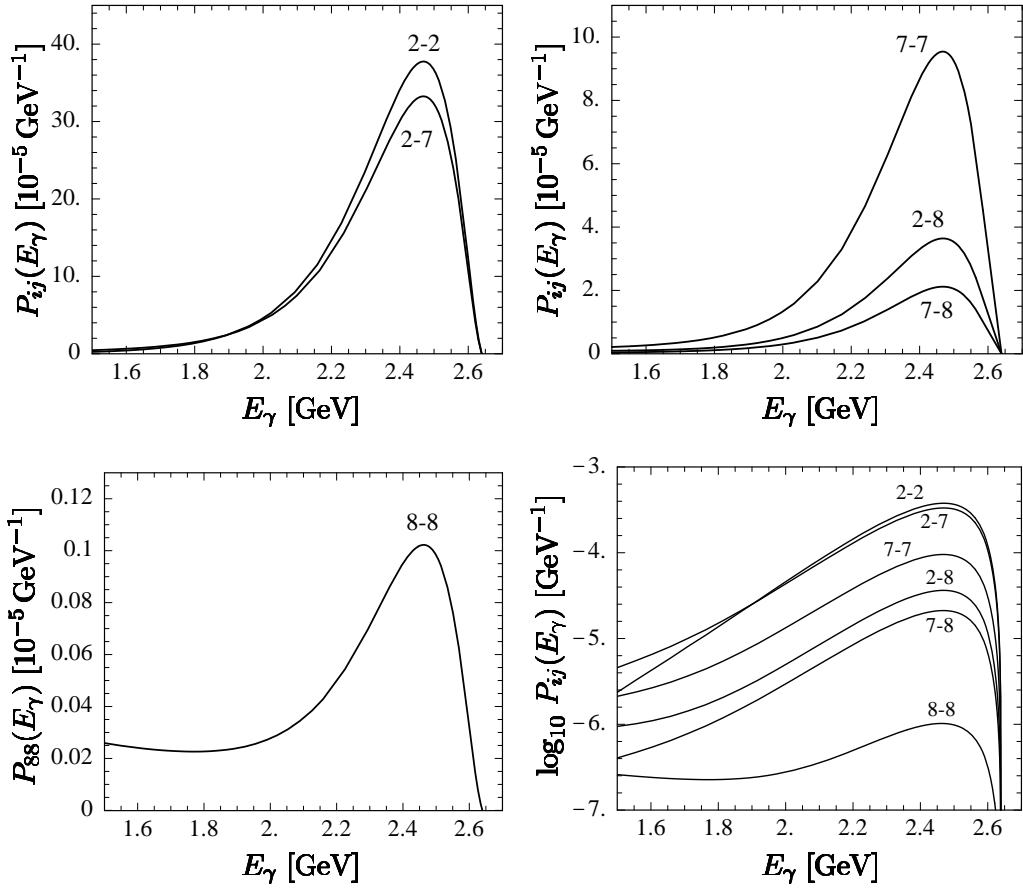


FIG. 9. Different components of the photon spectrum in the  $B \rightarrow X_s \gamma$  decay, from [46].

we do not have to assume the correctness of the SM in the experimental analysis.

A precise measurement of the photon spectrum allows to determine the parameters of the shape function. The latter information is an important input for the determination of the CKM matrix element  $V_{ub}$ . One takes advantage of the universality of the shape function to lowest order in  $\Lambda_{QCD}/m_b$ . The same shape function occurs in the description of nonperturbative effects in the endpoint region of the  $B \rightarrow X_s \gamma$  photon spectrum and of the  $B \rightarrow X_u \ell \nu$  charged-lepton spectrum up to higher  $1/m_b$  corrections [47]. Thus, from the photon spectrum one can determine the shape function; with the help of the latter and of the measurement of the charged-lepton spectrum of  $B \rightarrow X_u \ell \nu$ , one can extract a value for  $V_{ub}$ . This method represents one of the best ways to measure the CKM matrix element  $V_{ub}$ . Following this strategy, CLEO has presented the following measurement [48]:

$$V_{ub} = (4.08 \pm 0.56_{exp} \pm 0.29_{th}). \quad (\text{III.8})$$

The impact of the higher-order corrections in  $1/m_b$  was quite recently investigated [49].

The future aim should be to determine the shape function by using the high-precision measurements of the photon energy spectrum more precisely.

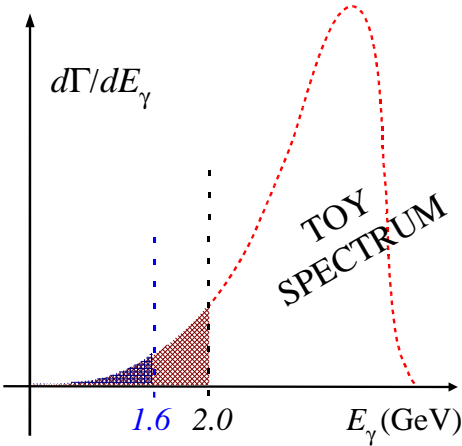


FIG. 10. Schematic photon spectrum of  $B \rightarrow X_s \gamma$ .

Moreover, the first and the second moment of the photon spectrum can be determined within the measurement of  $B \rightarrow X_s \gamma$ . These results can be used to extract values for the HQET parameters  $\bar{\Lambda}$  and  $\lambda_1$  (see [51]). CLEO has measured these moments and extracted for example from the first moment  $\bar{\Lambda} = 0.35 \pm 0.08 \pm 0.10 \text{ GeV}$ , where the first error is from the experimental error and the second error is from the theoretical expression, in particular from neglected higher-order terms [39].

A lower experimental cut in the photon energy spectrum within the measurement of  $B \rightarrow X_s \gamma$  decreases the sensitivity to the parameters of the shape function and therefore the model dependence. With respect to this, the ideal energy cut would be 1.6 GeV (see fig. 10). But in this case a better understanding of the  $\psi$  background would be mandatory. The intermediate  $\psi$  background, namely  $B \rightarrow \psi X_s$  followed by  $\psi \rightarrow X' \gamma$ , is more than  $4 \times 10^{-4}$  in the ‘total’ branching ratio. With the present energy cut of 2.0 GeV, this contribution is suppressed and estimated to be less than 1.5%; for 2.1 GeV it is 0.6% [60].

### C. Experimental status of $B \rightarrow X_s \ell^+ \ell^-$ and $B \rightarrow X_d \gamma$

The inclusive  $B \rightarrow X_s \ell^+ \ell^-$  transition also starts to be accessible at the  $B$  factories. BELLE and also BABAR have already established measurements of the exclusive mode  $B \rightarrow K \ell^+ \ell^-$  [52,54]. The two measurements are compatible with each other.

Quite recently, BELLE has also announced the first measurement of the inclusive  $B \rightarrow X_s \ell^+ \ell^-$  mode based on a semi-inclusive analysis [55,56]. The hadronic system  $X_s$  is reconstructed from a kaon with 0 to 4 pions (at most one  $\pi^0$ ). The used data sample contains  $65.4 \times 10^6 B\bar{B}$  pairs.

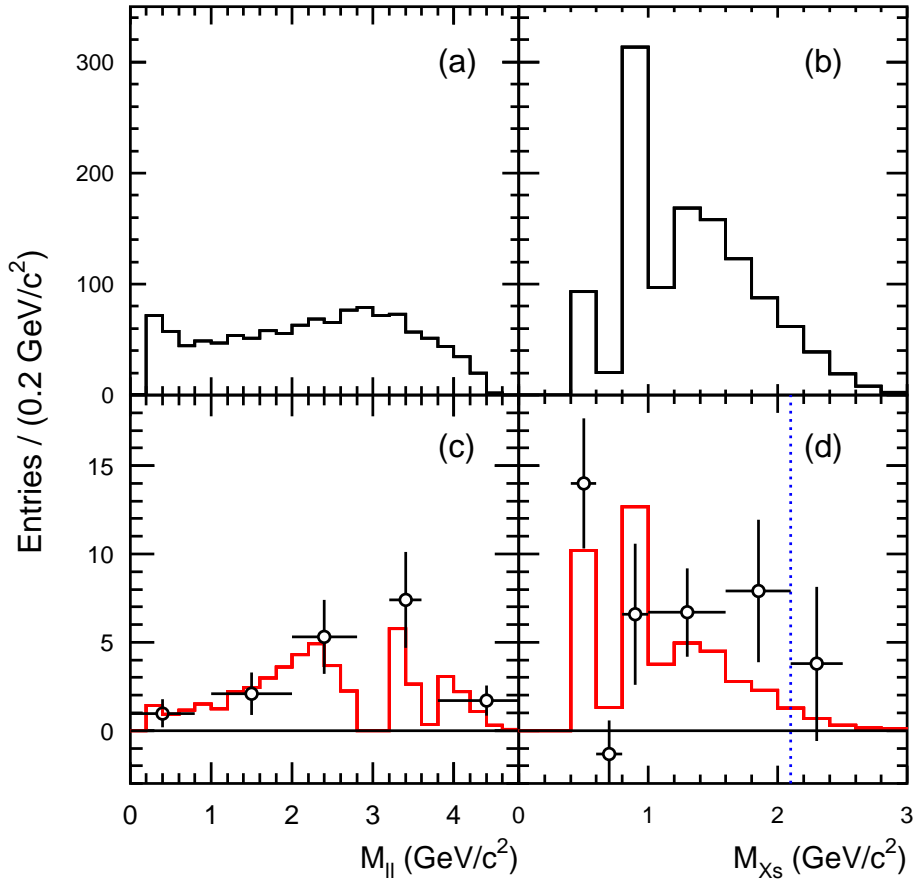


FIG. 11. SM expectations for the (a) dilepton and (b) recoil mass spectra; the observed (c) dilepton and (d) recoil mass spectra (circles). The histograms in (c), (d) show the SM expectations after all the selections are applied; histograms are normalized to the expected branching fractions. The dotted line in (d) indicates the  $M_{Xs} < 2.1$   $\text{GeV}$  requirement, from [55].

The signal characteristics within this semi-inclusive analysis is determined by modelling the invariant mass  $M_{X_s}$  spectrum using the phenomenological model first proposed in [36]. The reconstruction efficiencies of the signal are determined by the MC samples based on this model, leading to a large part of the systematic uncertainty.

The non-peaking backgrounds are estimated by sideband subtraction. But there are two peaking backgrounds: the first one is the process  $B \rightarrow X_s \pi^+ \pi^-$ , where the two pions are misidentified as leptons. This background is estimated explicitly by reconstructing the  $B \rightarrow X_s \pi^+ \pi^-$  and multiplying the yield by  $(f_\pi^\mu)^2$ , where  $f_\pi^\mu$  is the probability of a pion faking a muon measured in an independent data set. The second source are the charmonium decays  $B \rightarrow \psi(\rightarrow \ell^+ \ell^-) X_s$  and  $B \rightarrow \psi'(\rightarrow \ell^+ \ell^-) X_s$ . They are vetoed by excluding lepton combinations whose invariant mass falls within a window around the nominal  $\psi$  and  $\psi'$  mass.

The continuum background and the  $B\bar{B}$  background, however, can be suppressed by the kinematical constraints. Further suppression is achieved with methods similar to those in the  $B \rightarrow X_s \gamma$  analysis.

Moreover, there is a cut used in the  $X_s$  invariant mass spectrum at 2.1 GeV. This removes a large part of the combinatorial background while a model calculation determines that  $(93 \pm 5)\%$  of the signal is within this experimental window (leading to an additional model dependence). Events with a dilepton mass  $M_{\ell^+\ell^-}$  less than 0.2 GeV are also rejected in order to suppress electron pairs from  $\pi^0 \rightarrow e^+e^-\gamma$  and  $\gamma \rightarrow e^+e^-$  conversion.

A comparison of the histograms in fig. 11, (a) and (c), indicates that the efficiency within this measurement is much higher in the high dilepton mass region.

The uncertainty of this first measurement of the inclusive decay is still at the 30% level and in agreement with the SM expectations. One can expect much higher accuracy from the  $B$  factories in the near future.

Also the inclusive decay  $B \rightarrow X_d\gamma$  is within reach of the high-luminosity  $B$  factories. Such a measurement will rely on high statistics and on powerful methods for the kaon–pion–discrimination. At present only upper bounds on corresponding exclusive modes are available from CLEO [57], BELLE [58] and also from BABAR [59].

#### IV. PERTURBATIVE CALCULATIONS IN $B \rightarrow X_{S,D} \gamma$

The inclusive decay  $B \rightarrow X_s \gamma$  is a laboratory for perturbative QCD. Non-perturbative effects (see section VI) play a subdominant role and are well under control thanks to the heavy quark expansion. The dominant short-distance QCD corrections enhance the partonic decay rate  $\Gamma(b \rightarrow X_s^{\text{parton}} \gamma)$  by a factor of more than 2. The corresponding large logarithms of the form  $\alpha_s^n(m_b) \log^m(m_b/M)$ , where  $M = m_t$  or  $M = m_W$  and  $m \leq n$  (with  $n = 0, 1, 2, \dots$ ), have to be summed with the help of the renormalization-group-improved perturbation theory, as presented in section II.

The effective Hamiltonian relevant to  $B \rightarrow X_s \gamma$  in the SM reads

$$H_{\text{eff}}(B \rightarrow X_s \gamma) = -\frac{4G_F}{\sqrt{2}} \lambda_t \sum_{i=1}^8 C_i(\mu) \mathcal{O}_i(\mu) \quad , \quad (\text{IV.9})$$

where  $\mathcal{O}_i(\mu)$  are the relevant operators,  $C_i(\mu)$  are the corresponding Wilson coefficients, which contain the complete top- and  $W$ -mass dependence (see fig. 12), and  $\lambda_q = V_{qb} V_{qs}^*$  with  $V_{ij}$ , the CKM matrix elements. The CKM dependence globally factorizes, if one works in the approximation  $\lambda_u = 0$ <sup>1</sup>. One neglects the operators with dimension  $> 6$ , which are suppressed by higher powers of  $1/m_W$ .

Using the equations of motion for the operators, one arrives at the following basis of dimension-6 operators [61,62]:

$$\begin{aligned} \mathcal{O}_1 &= (\bar{s}\gamma_\mu T^a P_L c) (\bar{c}\gamma^\mu T_a P_L b) , & \mathcal{O}_2 &= (\bar{s}\gamma_\mu P_L c) (\bar{c}\gamma^\mu P_L b) , \\ \mathcal{O}_3 &= (\bar{s}\gamma_\mu P_L b) \sum_q (\bar{q}\gamma^\mu q) , & \mathcal{O}_4 &= (\bar{s}\gamma_\mu T^a P_L b) \sum_q (\bar{q}\gamma^\mu T_a q) , \\ \mathcal{O}_5 &= (\bar{s}\gamma_\mu \gamma_\nu \gamma_\rho P_L b) \sum_q (\bar{q}\gamma^\mu \gamma^\nu \gamma^\rho q) , & \mathcal{O}_6 &= (\bar{s}\gamma_\mu \gamma_\nu \gamma_\rho T^a P_L b) \sum_q (\bar{q}\gamma^\mu \gamma^\nu \gamma^\rho T_a q) , \\ \mathcal{O}_7 &= \frac{e}{16\pi^2} \bar{m}_b(\mu) (\bar{s}\sigma^{\mu\nu} P_R b) F_{\mu\nu} , & \mathcal{O}_8 &= \frac{g_s}{16\pi^2} \bar{m}_b(\mu) (\bar{s}\sigma^{\mu\nu} T^a P_R b) G_{\mu\nu}^a , \end{aligned} \quad (\text{IV.10})$$

In the dipole-type operators  $\mathcal{O}_7$  and  $\mathcal{O}_8$ ,  $e$  and  $F_{\mu\nu}$  ( $g_s$  and  $G_{\mu\nu}^a$ ) denote the electromagnetic (strong) coupling constant and field strength tensor, respectively.  $T^a$  ( $a = 1, 8$ ) denote  $SU(3)$  colour generators and  $P_{R,L} = (1 \pm \gamma_5)/2$ .

The error of the leading logarithmic (LL) result [63] was dominated by a large renormalization scale dependence at the  $\pm 25\%$  level, which already indicated the importance of the NLL series. By convention, the dependence on the renormalization scale  $\mu_b$  is obtained by the variation  $m_b/2 < \mu_b < 2m_b$ . The former measurement of the CLEO collaboration (see (III.1)) overlaps with the estimates based on LL calculations, and the experimental and theoretical errors are comparable. In view of the expected increase in the experimental precision, it became clear that a systematic inclusion of the NLL corrections was becoming necessary. Moreover, such a NLL program was also important in order to ensure the validity of renormalization-group-improved perturbation theory in this specific phenomenological application.

---

<sup>1</sup>This approximation is not used within the recent theoretical predictions.

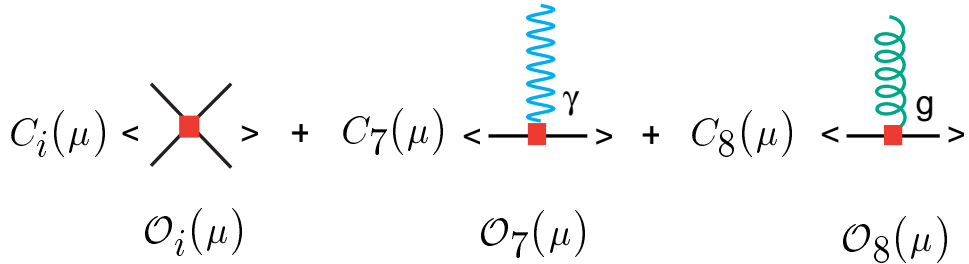


FIG. 12. Effective Hamiltonian in the case of  $B \rightarrow X_{s,d}\gamma$ .

This ambitious NLL enterprise was completed some years ago. This was a joint effort of many different groups ([35], [65], [66], [67]). The theoretical error of the previous LL result was substantially reduced, to  $\pm 10\%$ , and the central value of the partonic decay rate increased by about 20%. All three steps to NLL precision listed below (II.5) involve rather difficult calculations (see fig. 13).

- The most difficult part in Step 1 is the two-loop (or order  $\alpha_s$ ) matching of the dipole operators  $\mathcal{O}_7$  and  $\mathcal{O}_8$ . It involves two-loop diagrams both in the full and in the effective theory. It was first worked out by Adel and Yao [66]. As this is a crucial step in the NLL program, Greub and Hurth confirmed their findings in a detailed recalculation using a different method [71]. Two further complete [72,136] and one partial recalculations [73] of this result were presented in the meanwhile, confirming the original results in [66]. In order to match the dimension-6 operators  $\mathcal{O}_7$  and  $\mathcal{O}_8$ , it is sufficient to extract the terms of order  $\frac{m_b^2}{M^2}$  ( $M = m_W, m_t$ ) from the SM matrix elements for  $b \rightarrow s\gamma$  and  $b \rightarrow sg$ . Terms suppressed by additional powers of  $m_b/M$  correspond to higher-dimensional operators in the effective theory. In [71] the finite parts of the two-loop diagrams in the SM were calculated by means of the well-known method of asymptotic mass expansions, which naturally leads to a systematic expansion of Feynman diagrams in inverse powers of  $M$ .
- The order  $\alpha_s^2$  anomalous dimension matrix (Step 2) has been worked out by Chetyrkin, Misiak and Münz [67]. In particular, the calculation of the elements  $\gamma_{i7}$  and  $\gamma_{i8}$  ( $i = 1, \dots, 6$ ) in the  $\mathcal{O}(\alpha_s^2)$  anomalous dimension matrix involves a huge number of three-loop diagrams from which the pole parts (in the  $d - 4$  expansion) have to be extracted. This extraction was simplified by a clever decomposition of the scalar propagator [68]. Moreover, the number of necessary evanescent operators was reduced by a new choice of a basis of dimension-6 operators [69]. Using the matching result (Step 1), these authors obtained the NLL correction to the Wilson coefficient  $C_7(\mu_b)$ . Numerically, the LL and NLL values for  $C_7(\mu_b)$  turn out to be rather similar; the NLL corrections to the Wilson coefficient  $C_7(\mu_b)$  lead to a change of the  $B \rightarrow X_s\gamma$  decay rate that does not exceed 6% in the  $\overline{MS}$  scheme [67].

It should be stressed that the result of Step 2, in particular the entries  $\gamma_{i7}$  and  $\gamma_{i8}$  ( $i = 1, \dots, 6$ ) of the anomalous dimension matrix to NLL precision, is the only part of

the complete NLL enterprise that has not been confirmed by an independent group. An independent check of this important part of the NLL program is already on the way [70].

- Step 3 basically consists of bremsstrahlung corrections and virtual corrections. While the bremsstrahlung corrections were worked out some time ago by Ali and Greub [35], and were confirmed and extended by Pott [64], a complete analysis of the virtual two-loop corrections (up to the contributions of the four-quark operators with very small coefficients) was presented by Greub, Hurth and Wyler [65]. This calculation involves two-loop diagrams, where the full charm dependence has to be taken into account. By using Mellin–Barnes techniques in the Feynman parameter integrals, the result of these two-loop diagrams was obtained in the form

$$c_0 + \sum_{n=0,1,2,\dots; m=0,1,2,3} c_{nm} \left( \frac{m_c^2}{m_b^2} \right)^n \log^m \frac{m_c^2}{m_b^2}, \quad (\text{IV.11})$$

where the quantities  $c_0$  and  $c_{nm}$  are independent of  $m_c$ . The convergence of the Mellin–Barnes series was proved; the practical convergence of the series (IV.11) was also checked explicitly. Moreover, a finite result is obtained in the limit  $m_c \rightarrow 0$ , as there is no naked logarithm of  $m_c^2/m_b^2$ . This observation is of some importance in the  $b \rightarrow d\gamma$  process, where the  $u$ -quark propagation in the loop is not CKM-suppressed (see below). The main result of Step 3 consists in a drastic reduction of the renormalization scale uncertainty from about  $\pm 25\%$  to about  $\pm 6\%$ . The central value was shifted by about 20%.

In [65] these results are presented also in the 't Hooft–Veltman scheme, which may be regarded as a first step towards a cross-check of the complete NLL calculation prediction in a different renormalization scheme. Recently, the results of the  $\mathcal{O}_{1,2}$  matrix elements in the  $\overline{MS}$  scheme calculated in [65] were confirmed by an independent group [74] with the help of the method of asymptotic expansions. Also two further calculations with the help of a direct analytical [80] and of a numerical method [78] confirmed these results. The direct analytical method also allowed control over the matrix elements of the penguin operators  $\mathcal{O}_{3-6}$ . As expected from the smallness of the corresponding Wilson coefficients, their effect on the branching ratio does not exceed 1%.

Combining the NLL calculations of the three steps, the first practically complete theoretical prediction to NLL precision for the branching ratio of  $B \rightarrow X_s\gamma$  was presented in [67] (see also [81]):

$$\mathcal{B}(B \rightarrow X_s\gamma) = (3.28 \pm 0.33) \times 10^{-4}. \quad (\text{IV.12})$$

The theoretical error had two dominant sources,  $\mu$  dependence, which was reduced to about 6%, and the  $m_c/m_b$  dependence. This first theoretical NLL prediction already included the non-perturbative correction scaling with  $1/m_b^2$ , which are rather small (at the 1% level) (see section VI). Surprisingly, these first NLL predictions, [67] and [81], are almost identical to

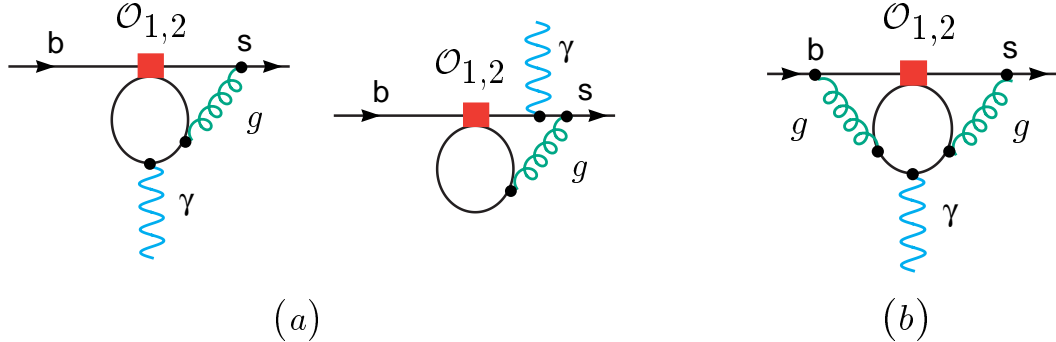


FIG. 13. (a) Typical diagrams (finite parts) contributing to the matrix element of the operator  $\mathcal{O}_2$  at the NLL level, Step 3; (b) typical diagram (infinite part) contributing to the NLL anomalous dimension matrix, Step 2; see fig.2 for a typical diagram (finite part) contributing to the NLL matching calculation, Step 1.

the present predictions (VII.31) using the charm pole mass, in spite of so many important additional refinements such as the electroweak two-loop corrections and the non-perturbative corrections, which will be discussed below.

Detailed studies of the two-loop electroweak corrections in the decay  $B \rightarrow X_s \gamma$  were performed. In [103] part of the electroweak two-loop contributions, namely contributions from fermion loops in gauge boson propagators ( $\gamma$  and  $W$ ) and from short-distance photonic loop corrections, were calculated. Moreover, it was observed that the on-shell value of the fine structure constant  $1/\alpha_{em} = 137$  is more appropriate for real photon emission than the value  $1/\alpha_{em} = (130.3 \pm 2.3)$  used in previous analyses. The QED loop calculations in [103] confirmed this expectation. This change in  $\alpha_{em}$  leads to a reduction of 5% in the perturbative contribution. In [105] a calculation of the heavy top and the heavy Higgs corrections in the gaugeless limit  $m_W \rightarrow 0$  was presented. In [46] the QED analysis made in [103] was improved by resumming the contributions of order  $\alpha_{em} \log(\mu_b/M)(\alpha_s \log(\mu_b/M))^n$  to all orders (while in [103] only the  $n = 0$  contribution was included). This resummation decreases the QED corrections. In [104] the same calculation was performed taking into account the complete relevant set of operators. It was explicitly shown that the truncation of the operator basis in [46] turns out to be a correct approximation and that these corrections lead to a 0.8% correction only.

The first (practically) complete analysis of the electroweak contributions to order  $\alpha_{em}(\alpha_s \log(\mu/M))^n$  was performed in [107]. This includes a two-loop matching to order  $\alpha_{em}$ , the QED–QCD running of the Wilson coefficients down to the  $b$  quark and one- and two-loop QED matrix elements. While in [106] only the so-called purely electroweak contributions were considered where terms vanishing in the limit  $\sin \theta \rightarrow 0$  were neglected if they are not enhanced by powers of the top mass, in [107] the complete two-loop matching conditions to order  $\alpha_{em}$  were presented. It was shown that the electroweak two-loop corrections of order  $\alpha_{em}(\alpha_s \log(\mu/M))^n$  lead, because of accidental cancellations, to a 1.6% reduction of the branching ratio of  $B \rightarrow X_s \gamma$  only. Thus, the electroweak corrections are well under control and shown to play a subdominant role.

It is clear that many parts of the perturbative calculations at the partonic level in the

case of  $B \rightarrow X_s \gamma$  can be taken over to the cases  $B \rightarrow X_d \gamma$  and  $B \rightarrow X_s \ell^+ \ell^-$ ; the latter case, however, needs some modifications, in particular the operator basis gets enlarged as will be discussed in the next subsection.

The perturbative QCD corrections in the decay  $b \rightarrow d\gamma$  can be treated in complete analogy to the ones in the decay  $b \rightarrow s\gamma$  [82]: the effective Hamiltonian is the same in the processes  $b \rightarrow s\gamma$  and  $b \rightarrow d\gamma$  up to the obvious replacement of the  $s$ -quark field by the  $d$ -quark field. But as  $\lambda_u = V_{ub}V_{ud}^*$  for  $b \rightarrow d\gamma$  is not small with respect to  $\lambda_t = V_{tb}V_{td}^*$  and  $\lambda_c = V_{cb}V_{cd}^*$ , one also has to take into account the operators proportional to  $\lambda_u$ . The matching conditions  $C_i(m_W)$  and the solutions of the RG equations, yielding  $C_i(\mu_b)$ , coincide with those needed for the process  $B \rightarrow X_s \gamma$ .

The perturbative calculations at the partonic level of  $B \rightarrow X_s \gamma$  can also be used for the partonic process  $c \rightarrow u\gamma$ . As FCNC process, it does not occur at the tree level in the SM either. Moreover, it is strongly GIM-suppressed at one-loop. The leading QCD logarithms are known to enhance the one-loop amplitude by more than one order of magnitude. It was shown in [83] that the amplitude increases further by two orders of magnitude after including the formally NLL QCD effects. So the  $c \rightarrow u\gamma$  process is completely dominated by a two-loop term. However, this is only of theoretical interest, because the  $\Delta S = 0$  radiative decays of charmed hadrons remain dominated by the  $c \rightarrow d\bar{d}u\gamma$  and  $c \rightarrow s\bar{s}u\gamma$  subprocesses.

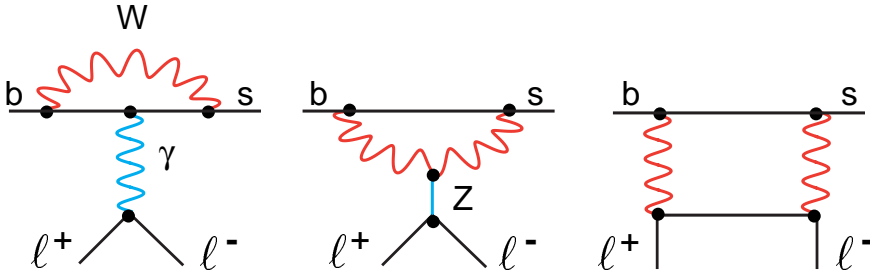


FIG. 14. One-loop contributions to the decay  $B \rightarrow X_s \ell^+ \ell^-$ .

## V. PERTURBATIVE CALCULATIONS IN $B \rightarrow X_s \ell^+ \ell^-$ AND $B \rightarrow X_s \bar{\nu}\nu$

In comparison with the  $B \rightarrow X_s \gamma$  decay, the inclusive  $B \rightarrow X_s \ell^+ \ell^-$  decay presents a complementary and also more complex test of the SM, since different contributions add to the decay rate (fig. 14).

It is particularly attractive because of kinematic observables such as the invariant dilepton mass spectrum and the forward–backward (FB) asymmetry. It is also dominated by perturbative contributions, if one eliminates  $c\bar{c}$  resonances with the help of kinematic cuts (see section VII D).

The effective Hamiltonian relevant to  $B \rightarrow X_s \ell^+ \ell^-$  in the SM reads

$$H_{eff}(B \rightarrow X_s \ell^+ \ell^-) = -\frac{4G_F}{\sqrt{2}} \lambda_t \sum_{i=1}^{10} C_i(\mu) \mathcal{O}_i(\mu). \quad (\text{V.13})$$

Compared with the decay  $B \rightarrow X_s \gamma$  (see (IV.9)), the effective Hamiltonian (V.13) contains two additional operators  $\mathcal{O}(\alpha_{em})$  (see fig. 15):

$$\begin{aligned} \mathcal{O}_9 &= \frac{e^2}{16\pi^2} (\bar{s}\gamma_\mu P_L b) (\bar{l}\gamma^\mu l), \\ \mathcal{O}_{10} &= \frac{e^2}{16\pi^2} (\bar{s}\gamma_\mu P_L b) (\bar{l}\gamma^\mu \gamma_5 l). \end{aligned} \quad (\text{V.14})$$

It turns out that the first large logarithm of the form  $\log(m_b/M)$  ( $M = m_W$ ) already arises without gluons, because the operator  $\mathcal{O}_2$  mixes into  $\mathcal{O}_9$  at one loop via the diagram given in fig. 16.

This possibility, which has no equivalent in the  $b \rightarrow s\gamma$  case, leads to the following ordering of contributions to the decay amplitude (which should be compared with (II.2) and (II.3)):

$$\begin{aligned} [\alpha_{em} \log(m_b/M)] \alpha_s^n(m_b) \log^n(m_b/M) &\quad [\text{LL}] , \\ [\alpha_{em} \log(m_b/M)] \alpha_s^{n+1}(m_b) \log^n(m_b/M) &\quad [\text{NLL}] , \dots \end{aligned} \quad (\text{V.15})$$

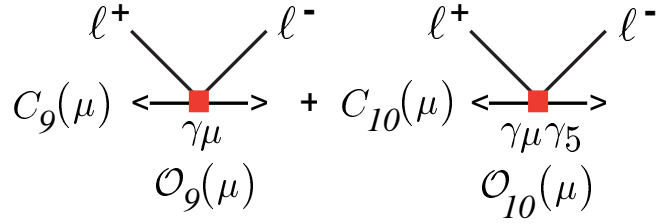


FIG. 15. Additional operators in the effective Hamiltonian in the case of  $B \rightarrow X_{s,d}\ell^+\ell^-$ .

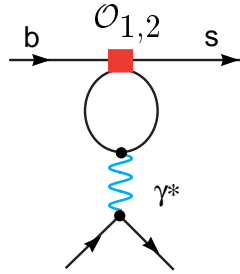


FIG. 16. Mixing of the operator  $\mathcal{O}_2$  into  $\mathcal{O}_9$  at one loop.

Technically, to perform the resummation, it is convenient to transform these series into the standard form (II.2). This can be achieved by redefining magnetic, chromomagnetic and lepton-pair operators as follows [86,87]:

$$\mathcal{O}_i^{new} = \frac{16\pi^2}{g_s^2} \mathcal{O}_i^{old}, \quad C_i^{new} = \frac{g_s^2}{(4\pi)^2} C_i^{old}, \quad (i = 7, \dots, 10). \quad (\text{V.16})$$

This redefinition enables one to proceed in the standard way, or as in  $b \rightarrow s\gamma$ , in the three calculational steps discussed at the end of section II. At the high scale, the *new* Wilson coefficients can be computed at a given order in perturbation theory and expanded in powers of  $\alpha_s$ :

$$C_i^{new} = C_i^{(0)} + \frac{\alpha_s}{(4\pi)} C_i^{(1)} + \frac{\alpha_s^2}{(4\pi)^2} C_i^{(2)} + \dots \quad (\text{V.17})$$

Obviously, the Wilson coefficients of the *new* operators  $\mathcal{O}_{7-10}$  at the high scale start at order  $\alpha_s$  only. Then the anomalous-dimension matrix has the canonical expansion in  $\alpha_s$  and starts with a term proportional to  $\alpha_s$ :

$$\gamma^{new} = \frac{\alpha_s}{4\pi} \gamma^{(0)} + \frac{\alpha_s^2}{(4\pi)^2} \gamma^{(1)} + \frac{\alpha_s^3}{(4\pi)^3} \gamma^{(2)} + \dots \quad (\text{V.18})$$

In particular, after the reshufflings in (V.16), the one-loop mixing of the operator  $\mathcal{O}_2$  with  $\mathcal{O}_9$  formally appears at order  $\alpha_s$ .

The last of the three steps, however, requires some care: among the *new* operators with a non-vanishing tree-level matrix element, only  $\mathcal{O}_9$  has a non-vanishing coefficient at the LL level. Therefore, at this level, only the tree-level matrix element of this operator ( $\langle \mathcal{O}_9 \rangle$ ) has to be included. At NLL accuracy the QCD one-loop contributions to  $\langle \mathcal{O}_9 \rangle$ , the tree-level contributions to  $\langle \mathcal{O}_7 \rangle$  and  $\langle \mathcal{O}_{10} \rangle$ , and the electroweak one-loop matrix elements of the four-quark operators have to be calculated. Finally, at NNLL precision, one should in principle take into account the QCD two-loop corrections to  $\langle \mathcal{O}_9 \rangle$ , the QCD one-loop corrections to  $\langle \mathcal{O}_7 \rangle$  and  $\langle \mathcal{O}_{10} \rangle$ , and the QCD corrections to the electroweak one-loop matrix elements of the four-quark operators.

The present status of these perturbative contributions to decay rate and FB asymmetry of  $B \rightarrow X_s \ell^+ \ell^-$  is the following: the complete NLL contributions to the decay amplitude have been found in [86,87]. Since the LL contribution to the rate turns out to be numerically rather small, NLL terms represent an  $\mathcal{O}(1)$  correction to this observable. On the other hand, since a non-vanishing FB asymmetry is generated by the interference of vector ( $\sim \mathcal{O}_{7,9}$ ) and axial-vector ( $\sim \mathcal{O}_{10}$ ) leptonic currents, the LL amplitude leads to a vanishing result and NLL terms represent the lowest non-trivial contribution to this observable.

In view of the forthcoming precise measurements at the  $B$  factories, a computation of NNLL terms in  $B \rightarrow X_s \ell^+ \ell^-$  is needed if one aims at the same numerical accuracy as achieved by the NLL analysis of  $B \rightarrow X_s \gamma$ . Large parts of the latter can be taken over and used in the NNLL calculation of  $B \rightarrow X_s \ell^+ \ell^-$ . But this is not the full story.

- (Step 1) The full computation of initial conditions to NNLL precision was presented in Ref. [84]. The authors did the two-loop matching for all the operators relevant to  $b \rightarrow s \ell^+ \ell^-$  (including a confirmation of the  $b \rightarrow s \gamma$  NLL matching results of [66,71]). The inclusion of this NNLL contribution removes the large matching scale uncertainty (around 16%) of the NLL calculation of the  $b \rightarrow s \ell^+ \ell^-$  decay rate.
- (Step 2) Thanks to the reshufflings of the LL series, most of the NNLL contributions to the anomalous-dimension matrix can be derived from the NLL analysis of  $b \rightarrow s \gamma$ . In particular the three-loop mixing of the four-quark operators  $\mathcal{O}_{1-6}$  into  $\mathcal{O}_7$  and  $\mathcal{O}_8$  can be taken over from Ref. [67], which allows an evaluation of the matrix element  $U_{72}^{(2)}$  (using the usual convention  $C_i(\mu_b) = U_{ij}C_j(\mu_W)$ ). The only missing piece for a full NNLL analysis of the  $b \rightarrow s \ell^+ \ell^-$  decay rate is the matrix element  $U_{92}^{(2)}$  (see fig. 18).

In [84] an estimate was made, which suggests that the numerical influence of  $U_{92}^{(2)}$  on the branching ratio of  $b \rightarrow s \ell^+ \ell^-$  is small. Interestingly, since the FB asymmetry has no contributions proportional to  $|\langle \mathcal{O}_9 \rangle|^2$ , this missing term is not needed for a NNLL analysis of this observable.

- (Step 3) Within the  $B \rightarrow X_s \gamma$  calculation at NLL, the two-loop matrix elements of the four-quark operator  $\mathcal{O}_2$  for an on-shell photon were calculated in [65], using Mellin–Barnes techniques. This calculation was extended in [85] to the case of an off-shell photon (see fig. 17) with the help of a double Mellin–Barnes representation which corresponds to a NNLL contribution relevant to the decay  $B \rightarrow X_s \ell^+ \ell^-$ . The

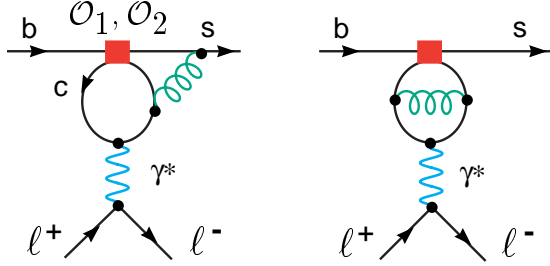


FIG. 17. Typical diagrams (finite parts) contributing to the matrix element of the operator  $\mathcal{O}_2$  at the NNLL level (Step 3).

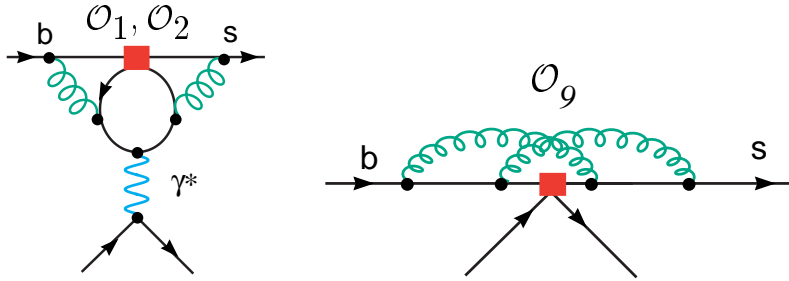


FIG. 18. Parts still missing in a complete canonical NNLL analysis of the dilepton mass spectrum. Left: typical diagram (infinite part) contributing to the NNLL mixing  $U_{92}^{(2)}$ , Step 2. Right: typical diagram (finite piece) contributing to the NNLL matrix element of the operator  $\mathcal{O}_9$ , Step 3.

validity of these analytical results given in [85] is restricted to small dilepton masses  $q_{\ell^+\ell^-}^2/m_b^2 < 0.25$ . An independent numerical check of these results has been performed in [78]. Moreover, the NNLL calculation in [78] is also valid for high dilepton masses for which the experimental methods have an efficiency much higher than the one at low dilepton masses. Step 3 also includes the bremsstrahlung contributions which were calculated for the dilepton mass spectrum (symmetric part) in [76,75] and for the FB asymmetry in [75,77]. In the low dilepton spectrum, these matrix element calculations reduce the error corresponding to the uncertainty of the low-scale dependence from  $\pm 13\%$  down to  $\pm 6.5\%$ .

In principle, a complete NNLL calculation of the  $B \rightarrow X_s \ell^+ \ell^-$  rate would require also the calculation of the renormalization-group-invariant two-loop matrix element of the operator  $\mathcal{O}_9$  (see fig. 18). But its impact to the dilepton mass spectrum is expected to be small. Similarly to the missing piece of the anomalous-dimension matrix, also this (scale-independent) contribution does not enter the FB asymmetry at NNLL accuracy.

As anticipated, the canonical LL expansion is numerically not well justified, since the formally-leading  $\mathcal{O}(1/\alpha_s)$  term in  $C_9$  is numerically close to the  $\mathcal{O}(1)$  term. For this reason, it has been proposed in Ref. [85] to use a different counting rule, where the  $\mathcal{O}(1/\alpha_s)$  term of  $C_9$  is treated as  $\mathcal{O}(1)$ . This approach, although it cannot be consistently extended at

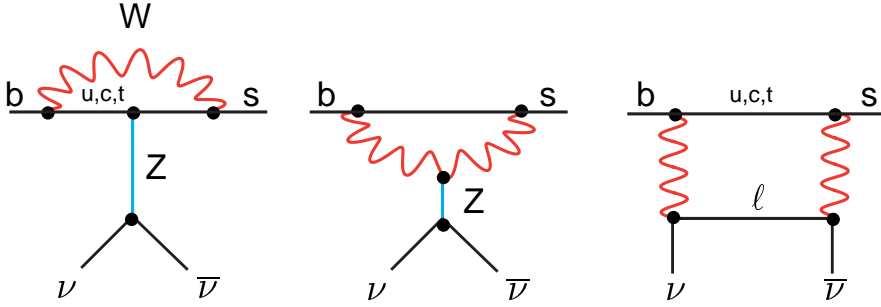


FIG. 19. One-loop contributions to the decay  $B \rightarrow X_s \nu \bar{\nu}$ .

higher orders, seems to be well justified at the present status of the calculation. Within this approach, the two missing ingredients for a NNLL calculation of the dilepton mass spectrum (see fig. 18) would be of higher order.

The decay  $B \rightarrow X_{s,d} \nu \bar{\nu}$  is induced by  $Z^0$  penguin and box diagrams (see fig. 19). The main difference to the semi-leptonic decay  $B \rightarrow X_{s,d} \ell^+ \ell^-$  is the absence of a photon penguin contribution. The latter implies only a logarithmic GIM suppression, while the former contributions have a quadratic GIM suppression. As a consequence, the decay  $B \rightarrow X_{s,d} \nu \bar{\nu}$  is completely dominated by the internal top contribution.

The effective Hamiltonian reads

$$H_{eff}(B \rightarrow X_s \nu \bar{\nu}) = -\frac{4G_F}{\sqrt{2}} \frac{\alpha}{2\pi \sin^2 \Theta_W} V_{tb} V_{ts}^* C(m_t^2/m_W^2) (\bar{s} \gamma_\mu P_L b)(\bar{\nu} \gamma^\mu P_L \nu) + h.c. \quad (\text{V.19})$$

For the decay  $B \rightarrow X_d \nu \bar{\nu}$  the obvious changes have to be made.

The hard (quadratic) GIM mechanism leads to  $C(m_c^2/m_W^2)/C(m_t^2/m_W^2) \approx O(10^{-3})$ . Moreover, the corresponding CKM factors in the top and the charm contribution are both of order  $\lambda^2$ . Therefore the charm contribution (and also the up quark contribution) can safely be neglected.

The NLL QCD contributions to the partonic decay rate were presented in [88]. The perturbative error, namely the one due to the renormalization scale, was reduced from  $O(10\%)$  at the LL level to  $O(1\%)$  at the NLL level.

## VI. NON-PERTURBATIVE CONTRIBUTIONS

### A. Inclusive decay rates of $B$ mesons

In contrast to the exclusive rare  $B$  decays, the inclusive ones are theoretically clean observables and dominated by the partonic contributions. Bound-state effects of the final states are eliminated by averaging over a specific sum of hadronic states. Moreover, also long-distance effects of the initial state are accounted for, through the heavy mass expansion in which the inclusive decay rate of a heavy  $B$  meson is calculated using an expansion in inverse powers of the  $b$  quark mass [31].

This heavy-mass expansion is now a well-known method to calculate the inclusive decay rates of a hadron containing a heavy quark, especially a  $b$  quark. The optical theorem relates the *inclusive* decay rate of a hadron  $H_b$  to the imaginary part of certain forward scattering amplitudes

$$\Gamma(H_b \rightarrow X) = \frac{1}{2m_{H_b}} \text{Im} \langle H_b | \mathbf{T} | H_b \rangle, \quad (\text{VI.20})$$

where the transition operator  $\mathbf{T}$  is given by  $\mathbf{T} = i \int d^4x T[H_{eff}(x)H_{eff}(0)]$ . The insertion of a complete set of states,  $X\rangle\langle X$ , leads to the standard formula for the decay rate:

$$\Gamma(H_b \rightarrow X) = \frac{1}{2m_{H_b}} \sum_X (2\pi)^4 \delta^4(p_i - p_f) |\langle X | H_{eff} | H_b \rangle|^2. \quad (\text{VI.21})$$

It is then possible to construct an operator product expansion (OPE) of the operator  $\mathbf{T}$ , which gets expressed as a series of *local* operators - suppressed by powers of the  $b$  quark mass and written in terms of the  $b$  quark field:

$$T[H_{eff}H_{eff}] \stackrel{OPE}{=} \frac{1}{m_b} (\mathcal{O}_0 + \frac{1}{m_b} \mathcal{O}_1 + \frac{1}{m_b^2} \mathcal{O}_2 + \dots). \quad (\text{VI.22})$$

This construction is based on the parton–hadron duality [32], using the facts that the sum is done over all exclusive final states and that the energy release in the decay is large with respect to the QCD scale,  $m_b \ll \Lambda_{QCD}$ .

With the help of the HQET, namely the new heavy-quark spin-flavour symmetries arising in the heavy quark limit  $m_b \rightarrow \infty$  [29], the hadronic matrix elements within the OPE,  $\langle H_b | \mathcal{O}_i | H_b \rangle$ , can be further simplified.

The crucial observations within this well-defined procedure, which are important for the application to the inclusive rare  $B$  decays, are the following: the free quark model turns out to be the first term in the constructed expansion in powers of  $1/m_b$  and therefore the dominant contribution. This contribution can be calculated in perturbative QCD. Second, in the applications to inclusive rare  $B$  decays one finds no correction of order  $1/m_b$  to the free quark model approximation, and the corrections to the partonic decay rate start with  $1/m_b^2$  only. The latter fact implies the rather small numerical impact of the non-perturbative corrections to the decay rate of inclusive modes.

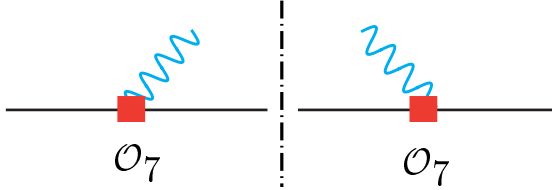


FIG. 20. Relevant cut diagram for the  $(\mathcal{O}_7, \mathcal{O}_7)$  contribution.

### B. Non-perturbative corrections to $B \rightarrow X_{s,d}\gamma$ and $B \rightarrow X_s\ell^+\ell^-$

These techniques can directly be used in the decay  $B \rightarrow X_s\gamma$ , in order to single out non-perturbative corrections to the branching ratio. They are also applicable to the case of  $B \rightarrow X_d\gamma$  and, with some modifications, to the case of  $B \rightarrow X_s\ell^+\ell^-$ .

If one neglects perturbative QCD corrections and assumes that the decay  $B \rightarrow X_s\gamma$  is due to the operator  $\mathcal{O}_7$  only, then one has to consider the time-ordered product  $T\mathcal{O}_7^+(x)\mathcal{O}_7(0)$  (see fig. 20). Using the OPE for  $T\mathcal{O}_7^+(x)\mathcal{O}_7(0)$  and heavy quark effective theory methods as discussed above, the decay width  $\Gamma(B \rightarrow X_s\gamma)$  reads [89,90] (modulo higher terms in the  $1/m_b$  expansion):

$$\begin{aligned} \Gamma_{B \rightarrow X_s\gamma}^{(\mathcal{O}_7, \mathcal{O}_7)} &= \frac{\alpha G_F^2 m_b^5}{32\pi^4} |V_{tb} V_{ts}|^2 C_7^2(m_b) \left(1 + \frac{\delta_{rad}^{NP}}{m_b^2}\right) , \\ \delta_{rad}^{NP} &= \frac{1}{2}\lambda_1 - \frac{9}{2}\lambda_2 , \end{aligned} \quad (\text{VI.23})$$

where  $\lambda_1$  and  $\lambda_2$  are the HQET parameters for the kinetic and the chromomagnetic energy. Using  $\lambda_1 = -0.5 \text{ GeV}^2$  and  $\lambda_2 = 0.12 \text{ GeV}^2$ , one gets  $\delta_{rad}^{NP} \simeq -3\%$ .

The  $B \rightarrow X_s\gamma$  decay width is usually normalized by the semi-leptonic one. The semi-leptonic decay width gets  $1/m_b^2$  corrections, which are also negative:

$$\delta_{semilept}^{NP} = \frac{1}{2}\lambda_1 - \left(\frac{3}{2} - \frac{6(1-z)^4}{g(z)}\right)\lambda_2, \quad (\text{VI.24})$$

where  $g(z)$  is a phase-space factor and  $z$  the ratio  $m_{c,pole}^2/m_{b,pole}^2$ .

The non-perturbative corrections scaling with  $1/m_b^2$  tend to cancel in the branching ratio  $\mathcal{B}(B \rightarrow X_s\gamma)/\mathcal{B}(B \rightarrow X_c\ell\nu)$ , and only about 1% remains: the HQET parameter  $\lambda_1$  cancels out in the ratio and the HQET parameter  $\lambda_2$  is known from  $B^* - B$  mass splitting,

$$\lambda_2 = \frac{1}{4}(m_{B^*}^2 - m_B^2). \quad (\text{VI.25})$$

Voloshin [91] considered the non-perturbative effects that arise when including also the operator  $\mathcal{O}_2$ . This effect is generated by the diagram in fig. 21a (and by the one, not shown, where the gluon and the photon are interchanged);  $g$  is a soft gluon interacting with the charm quarks in the loop. Up to a characteristic Lorentz structure, this loop is given by the integral

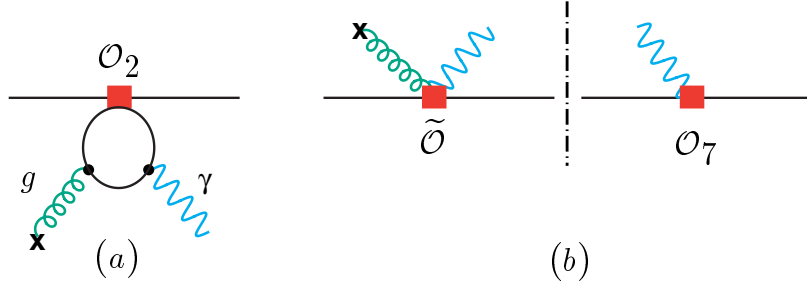


FIG. 21. a) Feynman diagram from which the operator  $\tilde{\mathcal{O}}$  arises. b) Relevant cut diagram for the  $(\tilde{\mathcal{O}}, \mathcal{O}_7)$  interference.

$$\int_0^1 dx \int_0^{1-x} dy \frac{xy}{m_c^2 - k_g^2 x(1-x) - 2xyk_gk_\gamma} \quad . \quad (\text{VI.26})$$

As the gluon is soft, i.e.  $k_g^2, k_gk_\gamma \approx \Lambda_{QCD} m_b/2 \ll m_c^2$ , the integral can be expanded in  $k_g$ . The (formally) leading operator, denoted by  $\tilde{\mathcal{O}}$ , is

$$\tilde{\mathcal{O}} = \frac{G_F}{\sqrt{2}} V_{cb} V_{cs}^* C_2 \frac{eQ_c}{48\pi^2 m_c^2} \bar{s} \gamma_\mu (1 - \gamma_5) g_s G_{\nu\lambda} b \epsilon^{\mu\nu\rho\sigma} \partial^\lambda F_{\rho\sigma} \quad . \quad (\text{VI.27})$$

Then working out the cut diagram shown in fig. 21b, one obtains the non-perturbative contribution  $\Gamma_{B \rightarrow X_s \gamma}^{(\tilde{\mathcal{O}}, \mathcal{O}_7)}$  to the decay width, which is due to the  $(\mathcal{O}_2, \mathcal{O}_7)$  interference. Normalizing this contribution by the LL partonic width, one obtains [94]

$$\frac{\Gamma_{B \rightarrow X_s \gamma}^{(\tilde{\mathcal{O}}, \mathcal{O}_7)}}{\Gamma_{b \rightarrow s \gamma}^{LL}} = -\frac{1}{9} \frac{C_2}{C_7} \frac{\lambda_2}{m_c^2} \simeq +0.03 \quad . \quad (\text{VI.28})$$

As the expansion parameter is  $m_b \Lambda_{QCD}/m_c^2 \approx 0.6$  (rather than  $\Lambda_{QCD}^2/m_c^2$ ), it is not a priori clear whether, formally, higher order terms in the  $1/m_c$  expansion are numerically suppressed. More detailed investigations [92–94] have shown that higher order terms are indeed suppressed, because the corresponding expansion coefficients are small.

The analogous  $1/m_c^2$  effect has been found independently in the exclusive mode  $B \rightarrow K^* \gamma$  in ref. [95]. Numerically, the effect there is also at the few percent level.

As was emphasized by Misiak [102], an analogous systematic analysis of terms like  $\Gamma_{B \rightarrow X_s \gamma}^{(\mathcal{O}_2, \mathcal{O}_2)}$  at first order in  $\alpha_s(m_b)$  is still missing. Rigorous techniques such as OPEs do not seem to be applicable in this case.

The analysis of the  $1/m_b^2$  and  $1/m_c^2$  effects was extended to the decay  $B \rightarrow X_s \ell^+ \ell^-$  in [89, 90, 94, 96, 97, 99]. They can be calculated quite analogously to those in the decay  $B \rightarrow X_s \gamma$ . As was first noticed in [90], the relative  $\Lambda_{QCD}^2/m_b^2$  correction diverges in the high- $q_{\ell^+ \ell^-}$  endpoint, which indicates the breakdown of the heavy mass expansion.

There are also on-shell  $c\bar{c}$  resonances, which have to be taken into account. While in the decay  $B \rightarrow X_s \gamma$  (on-shell photon) the intermediate  $\psi$  background for example, namely  $B \rightarrow \psi X_s$  followed by  $\psi \rightarrow X' \gamma$ , is suppressed for a high energy cut  $E_\gamma$  and can be subtracted from the  $B \rightarrow X_s \gamma$  decay rate (see section III A), the  $c\bar{c}$  resonances show up

as large peaks in the dilepton invariant mass spectrum in the decay  $B \rightarrow X_s \ell^+ \ell^-$  (off-shell photon) [100]. These resonances can be removed by appropriate kinematic cuts in the invariant mass spectrum.

Also the non-perturbative contributions in the decay  $B \rightarrow X_d \gamma$  can be treated in analogy to the ones in the decay  $B \rightarrow X_s \gamma$ . The power corrections in  $1/m_b^2$  and  $1/m_c^2$  (besides the CKM factors) are the same for the two modes. But the long-distance contributions from the intermediate  $u$ -quark in the penguin loops are different. These are suppressed in the  $B \rightarrow X_s \gamma$  mode by the unfavourable CKM matrix elements. In  $B \rightarrow X_d \gamma$ , there is no CKM suppression and one has to include the long-distance intermediate  $u$ -quark contributions.

Naively, one could expect that these contributions from up-quark loops scale with  $1/m_u^2$ . However, following the approach of [94], one easily shows that the general vertex function cannot in that case be expanded in the parameter  $t = k \cdot q / m_u^2$  (where  $k$  and  $q$  are the gluon and photon momentum respectively). But the expansion in inverse powers of  $t$  is reasonable. The leading term in this expansion scales like  $t^{-1} \sim m_u^2 / k_g k_\gamma$  and therefore cancels the factor  $1/m_u^2$  in the prefactor (see the analogous  $1/m_c^2$  factor in (VI.27)) and one gets a suppression factor  $(\Lambda_{QCD}^2 / m_u^2) \cdot (m_u^2 / k_g k_\gamma)$ . Thus, although the expansion in inverse powers in  $t$  induces non-local operators, one explicitly finds that the leading term scales with  $\Lambda_{QCD} / m_b$ . This indicates no large long-distance intermediate  $u$ -quark contributions.

Model calculations, based on vector meson dominance, also suggest this conclusion [118]. Furthermore, estimates of the long-distance contributions in exclusive decays  $B \rightarrow \rho \gamma$  and  $B \rightarrow \omega \gamma$  in the light-cone sum rule approach do not exceed 15% [120].

Finally, it must be stressed that there is no spurious enhancement of the form  $\log(m_u / \mu_b)$  in the perturbative contribution to the matrix elements of the four-quark operators, as shown by the explicit calculation in [65] (see also [121]). In other words, the limit  $m_u \rightarrow 0$  can be taken.

All these observations exclude very large long-distance intermediate  $u$ -quark contributions in the decay  $B \rightarrow X_d \gamma$ .

## VII. PHENOMENOLOGY

### A. SM prediction of $B \rightarrow X_s \gamma$

The theoretical prediction for the partonic  $b \rightarrow X_s^{\text{parton}} \gamma$  decay rate is usually normalized by the semi-leptonic decay rate in order to get rid of uncertainties related to the CKM matrix elements and the fifth power of the  $b$  quark mass. Moreover, an explicit lower cut on the photon energy in the bremsstrahlung correction has to be made:

$$R_{\text{quark}}(\delta) = \frac{\Gamma[b \rightarrow s\gamma] + \Gamma[b \rightarrow s\gamma\text{gluon}]_\delta}{\Gamma[b \rightarrow X_c e \bar{\nu}_e]}, \quad (\text{VII.29})$$

where the subscript  $\delta$  means that only photons with energy  $E_\gamma > (1-\delta)E_\gamma^{\text{max}} = (1-\delta)\frac{m_b}{2}$  are counted. The ratio  $R_{\text{quark}}$  is divergent in the limit  $\delta \rightarrow 1$ , owing to the soft photon divergence in the subprocess  $b \rightarrow s\gamma\text{gluon}$ . In this limit only the sum of  $\Gamma[b \rightarrow s\gamma]$ ,  $\Gamma[b \rightarrow s\text{gluon}]$  and  $\Gamma[b \rightarrow s\gamma\text{gluon}]$  is a reasonable physical quantity, in which all divergences cancel out. In [46] it was shown that the theoretical result is rather sensitive to the unphysical soft-photon divergence; the choice  $\delta = 0.90$  was suggested as the definition of the ‘total’ decay rate.

It is suggestive to give up the concept of a ‘total’ decay rate of  $b \rightarrow s\gamma$  and compare theory and experiment using the same energy cut. Then also the theoretical uncertainty regarding the photon energy spectrum mentioned in section III B would occur naturally in the theoretical prediction.

Using the measured semi-leptonic branching ratio  $\mathcal{B}_{\text{exp.}}^{\text{sl}}$ , the branching ratio  $\mathcal{B}(B \rightarrow X_s \gamma)$  is given by

$$\mathcal{B}(B \rightarrow X_s \gamma) = R_{\text{quark}} \times \mathcal{B}_{\text{exp.}}^{\text{sl}} (1 + \Delta_{\text{nonpert}}), \quad (\text{VII.30})$$

where the non-perturbative corrections scaling with  $1/m_b^2$  and  $1/m_c^2$ , summed in  $\Delta_{\text{nonpert}}$  (see section VI), have a numerical effect of +1% and +3%, respectively, on the branching ratio only. For a comparison with the ALEPH measurement (III.3), the measured semi-leptonic branching ratio  $\mathcal{B}(H_b \rightarrow X_{c,u} \ell \bar{\nu})$  should be used consistently. This leads to a slightly larger theoretical prediction for the LEP experiments.

Including only the resummed QED corrections and the non-perturbative corrections discussed in section VI, and using the on-shell value of  $\alpha_{\text{em}}$  and the charm pole mass, one ends up with the following theoretical prediction for the  $B \rightarrow X_s \gamma$  branching ratio [108]:

$$\mathcal{B}(B \rightarrow X_s \gamma) = (3.32 \pm 0.30) \times 10^{-4}, \quad (\text{VII.31})$$

where the error has two sources, the uncertainty regarding the scale dependences and the uncertainty due to the input parameters. In the latter the uncertainty due to the parameter  $m_c/m_b$  is dominant. This prediction almost coincides with the prediction of Kagan and Neubert [46].

In [113] two important observations were made. First it was shown that the charm-loop contribution to the decay  $B \rightarrow X_s \gamma$  is numerically dominant, and very stable under logarithmic QCD corrections, and that the strong enhancement of the branching ratio by

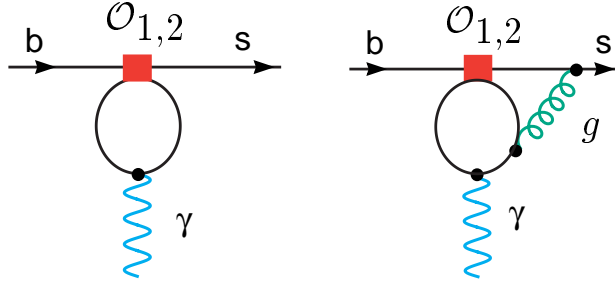


FIG. 22. The one-loop matrix element of the four-quark operators  $\mathcal{O}_{1,2}$  vanishes (left), therefore the charm dependence starts with the two-loop (NLL) contribution (right).

QCD logarithms is mainly due to the  $b$ -quark mass evolution in the top-quark sector. This leads to a better control over the residual scale dependence at NLL.

Secondly, quark mass effects within the decay  $B \rightarrow X_s \gamma$  were further analysed, in particular the definitions of the quark masses  $m_c$  and  $m_b$  in the two-loop matrix element of the four-quark operators  $\mathcal{O}_{1,2}$  (see fig. 22). Since the charm quark in the matrix element  $\langle \mathcal{O}_{1,2} \rangle$  are dominantly off-shell, it is argued that the running charm mass should be chosen instead of the pole mass. The latter choice was used in all previous analyses [65,67,72,46,108].

$$m_c^{pole}/m_b^{pole} \quad \Rightarrow \quad m_c^{\overline{MS}}(\mu)/m_b^{pole}, \quad \mu \in [m_c, m_b]. \quad (\text{VII.32})$$

Numerically, the shift from  $m_c^{pole}/m_b^{pole} = 0.29 \pm 0.02$  to  $m_c^{\overline{MS}}(\mu)/m_b^{pole} = 0.22 \pm 0.04$  is rather important and leads to a  $+11\%$  shift of the central value of the  $B \rightarrow X_s \gamma$  branching ratio. The error in the charm mass within the  $\overline{MS}$  scheme, is due to the uncertainty resulting from the scale variation and due to the uncertainty in  $m_c^{\overline{MS}}(m_c^{\overline{MS}})$ . With their new choice of the charm mass renormalization scheme and with  $\delta = 0.9$ , their theoretical prediction for the ‘total’ branching ratio is<sup>2</sup>

$$\mathcal{B}(B \rightarrow X_s \gamma) = (3.73 \pm 0.30) \times 10^{-4}. \quad (\text{VII.33})$$

Since the matrix element starts at NLL order (see fig. 22) and, thus, the renormalization scheme for  $m_c$  is an NNLL issue, one should regard the choice of the  $\overline{MS}$  scheme as an educated guess of the NNLL corrections. Nevertheless, the new choice is guided by the experience gained from many higher order calculations in perturbation theory. Moreover, the  $\overline{MS}$  mass of the charm quark is also a short-distance quantity which does not suffer from non-perturbative ambiguities, in contrast to its pole mass. Therefore the central value resulting within this scheme, VII.33, is definitely favoured and should be regarded as the present theoretical prediction.

---

<sup>2</sup>Actually, the theoretical prediction in [113] is given for the energy cut  $E\gamma = 1.6$  GeV:  $\mathcal{B}(B \rightarrow X_s \gamma)_{E\gamma > 1.6 \text{ GeV}} = (3.60 \pm 0.30) \times 10^{-4}$ . The theoretical error in (VII.33) might be larger due to nonperturbative corrections (see section III).

One should note that the scheme ambiguity regarding the  $b$  quark mass is under control.

Because the choice of the renormalization scheme for  $m_c$  is a NNLL effect, one has to emphasize that regarding the charm mass scheme the theoretical prediction (VII.31) using the pole mass scheme is in principle as good as the new prediction (VII.33) using the  $\overline{MS}$  scheme; both predictions do not take into account the full impact of charm mass scheme ambiguity. Thus, one has to argue for a larger theoretical uncertainty in  $m_c^{\overline{MS}}(\mu)/m_b^{\text{pole}}$ , which includes also the value of  $m_c^{\text{pole}}$ . This leads to a more appropriate error above 10% in VII.33.

One should emphasize that this present dominant uncertainty is due to a charm mass scheme ambiguity at the NLL level, i.e. to the question if the  $\overline{MS}$  or the pole mass is more appropriate to estimate the unknown NNLL contributions. This uncertainty is of perturbative origin. The second uncertainty is due to the numerical value of  $m_c$  within the specific choice of the charm mass scheme and is a parametrical uncertainty. The Particle Data Review in its latest edition [1] gives the following range for the latter uncertainty within the  $\overline{MS}$  scheme:  $1.0 \text{ GeV} \leq m_c^{\overline{MS}}(m_c^{\overline{MS}}) \leq 1.4 \text{ GeV}$  and has therefore doubled the uncertainty with respect to the one quoted previously [119]. Nevertheless, there are determinations using the sum rule technique [114] and also one that use the lattice technique (in the quenched approximation) [115] which indicate much smaller uncertainties.

The only way to resolve this charm mass scheme ambiguity within the present theoretical NLL prediction and to reduce the uncertainty below 10%, would be a NNLL calculation, which is *not* beyond the power of present technical tools in perturbation theory. Such an ambitious program makes sense only if one is sure that the associated non-perturbative effects are under control. It was argued [116] that the numerical behaviour of the branching ratio of  $B \rightarrow X_s \gamma$  as a function of  $m_c$  suggests that the dominant charm mass dependence originates from distances much smaller than  $\Lambda_{QCD}$ . In such a case, the associated non-perturbative effects would be under control and negligible.

## B. CKM phenomenology with $B \rightarrow X_{s,d}\gamma$

Instead of making a theoretical prediction for the branching ratio  $\mathcal{B}(B \rightarrow X_s \gamma)$ , one can use the experimental data and theory in order to determine the combination  $|V_{tb}V_{ts}^*|/|V_{cb}|$  of CKM matrix elements; in turn, one can determine  $|V_{ts}|$  by making use of the relatively well known CKM matrix elements  $V_{cb}$  and  $V_{tb}$ . But having used the unitarity constraint in the theory prediction already, the  $B \rightarrow X_s \gamma$  constraint on  $V_{ts}$  does not add much to what is already known from the unitarity fit [117,108]. If one does not use the CKM unitarity, the sensitivity of  $B \rightarrow X_s \gamma$  to  $V_{ts}$  gets significantly reduced, because the charm quark contribution is twice as large as the top quark contribution.

A future measurement of the  $B \rightarrow X_d \gamma$  decay rate will help to reduce the currently allowed region of the CKM Wolfenstein parameters  $\rho$  and  $\eta$ . It is also of specific interest with respect to new physics, because its CKM suppression by the factor  $|V_{td}|^2/|V_{ts}|^2$  in the SM may not be true in extended models.

Most of the theoretical improvements carried out in the context of the decay  $B \rightarrow X_s \gamma$  can straightforwardly be adapted for the decay  $B \rightarrow X_d \gamma$  and, thus, the NLL-improved and

power-corrected decay rate for  $B \rightarrow X_d\gamma$  has much reduced theoretical uncertainty, which would allow an extraction of the CKM parameters from the measured branching ratio.

The predictions for the  $B \rightarrow X_d\gamma$  decay given in [82] show that, for the central values of the input parameters, the difference between the LL and NLL results is  $\sim 10\%$ , increasing the branching ratio in the NLL case. Of particular theoretical interest is the ratio of the branching ratios, defined as

$$R(d\gamma/s\gamma) \equiv \frac{\mathcal{B}(B \rightarrow X_d\gamma)}{\mathcal{B}(B \rightarrow X_s\gamma)}, \quad (\text{VII.34})$$

in which a good part of the theoretical uncertainties cancels. This suggests that a future measurement of  $R(d\gamma/s\gamma)$  will have a large impact on the CKM phenomenology: varying the CKM Wolfenstein parameters  $\rho$  and  $\eta$  in the ranges  $-0.1 \leq \rho \leq 0.4$  and  $0.2 \leq \eta \leq 0.46$  and taking into account other parametric dependences stated above, the results (without electroweak corrections) are

$$6.0 \times 10^{-6} \leq \mathcal{B}(B \rightarrow X_d\gamma) \leq 2.6 \times 10^{-5}, \\ 0.017 \leq R(d\gamma/s\gamma) \leq 0.074.$$

In these predictions [82] it is assumed that the long-distance intermediate  $u$ -quark contributions play only a subdominant role (see the discussion at the end of section VI).

As mentioned in section III B, the photon spectrum of  $B \rightarrow X_s\gamma$  plays an important role in the determination of the CKM matrix element  $V_{ub}$ .

### C. Role of $b \rightarrow s$ gluon for $B \rightarrow X_{nocharm}$

Some remarks on the decay mode  $b \rightarrow s$  gluon are in order. The effective Hamiltonian in the decay mode  $b \rightarrow s$  gluon coincides with the one in the decay  $b \rightarrow s\gamma$ . By replacing the photon by the gluon, the NLL QCD calculation of  $b \rightarrow s\gamma$  can also be used. But in the calculation of the matrix element of the operator  $\mathcal{O}_2$ , further diagrams with the nonabelian three-gluon coupling had to be calculated [109]. The NLL calculation [109] leads to  $\mathcal{B}(b \rightarrow s\text{ gluon}) = (5.0 \pm 1.0) \times 10^{-3}$ , which is a factor of more than 2 larger than the former LL result  $\mathcal{B}(b \rightarrow s\text{ gluon}) = (2.2 \pm 0.8) \times 10^{-3}$  [63]. The mode  $b \rightarrow s$  gluon represents one component of the inclusive charmless hadronic decays,  $B \rightarrow X_{nocharm}$ , where  $X_{nocharm}$  denotes any hadronic charmless final state. The corresponding branching ratio allows for the extraction of the ratio  $|V_{ub}/V_{cb}|$  [111]. At the quark level, there are decay modes with three-body final states,  $b \rightarrow q'\bar{q}'q$  ( $q' = u, d, s$ ;  $q = d, s$ ) and the modes  $b \rightarrow qg$ , with two-body final-state topology. The component  $b \rightarrow sg$  of the charmless hadronic decays is expected to manifest itself in kaons with high momenta (of order  $m_b/2$ ), owing to its two-body nature [112]. The impact of the NLL corrections in  $b \rightarrow sg$  on the inclusive charmless hadronic decays,  $B \rightarrow X_{nocharm}$ , turns out to be as big as the NLL corrections to the  $b$  quark decay modes with three quarks [109].

There is still only marginal overlap between theory and experiment for the inclusive semi-leptonic branching ratio and the charm multiplicity in  $B$  meson decays [110], if usual scale variations are used in the theoretical predictions [109]. A possible reinforcement of the

decay  $b \rightarrow sg$  due to new physics through the chromomagnetic ( $\mathcal{O}_8$ ) contribution would lead to a natural explanation of these effects [112]. There is still room for such a scenario, which would be also compatible with the present  $B \rightarrow X_s \gamma$  constraint [16].

#### D. Phenomenology of $B \rightarrow X_s \ell^+ \ell^-$

In comparison with the  $B \rightarrow X_s \gamma$ , the inclusive  $B \rightarrow X_s \ell^+ \ell^-$  decay presents a complementary and also more complex test of the SM. As mentioned above, also this decay is dominated by perturbative contributions if the  $c\bar{c}$  resonances that show up as large peaks in the dilepton invariant mass spectrum (see fig. 23 [98]) are removed by appropriate kinematic cuts. In the 'perturbative windows', namely in the low- $s$  region  $0.05 < s = q^2/m_b^2 < 0.25$  and also in the high- $s$  region with  $0.65 < s < s_{max}$  (for  $s_{max}$  see section VI), theoretical predictions for the invariant mass spectrum are dominated by the purely perturbative contributions, and a theoretical precision comparable with the one reached in the decay  $B \rightarrow X_s \gamma$  is in principle possible. Regarding the choice of precise cuts in the dilepton mass spectrum, it is important that one directly compares theory and experiment using the same energy cuts and avoids any kind of extrapolation.

In the high- $s$  region, one should encounter the breakdown of the heavy mass expansion at the endpoint (see section VI). This fact leads to sizeable  $\Lambda_{QCD}^2/m_b^2$  non-perturbative corrections in this region. In [99] rather large Wilson coefficients to order  $\Lambda_{QCD}^3/m_b^3$  were found. The latter can be used to give an estimate of these corrections while the corresponding matrix elements are unknown. Following an argument in [101], one can show that this  $\Lambda_{QCD}/m_b$  expansion is effectively a  $\Lambda_{QCD}/m_c$  one in the high- $s$  region.

The kinematic observables, the invariant dilepton mass spectrum and the forward–backward (FB) asymmetry are usually normalized by the semi-leptonic decay rate in order to reduce the uncertainties due to bottom quark mass and CKM angles. The normalized dilepton invariant mass spectrum and the FB asymmetry are defined as

$$R(s) = \frac{d}{ds} \Gamma(B \rightarrow X_s \ell^+ \ell^-) / \Gamma(B \rightarrow X_c e \bar{\nu}), \quad (\text{VII.35})$$

$$A_{FB}(s) = \frac{1}{\Gamma(B \rightarrow X_c e \bar{\nu})} \times \int_{-1}^1 d \cos \theta_\ell \frac{d^2 \Gamma(B \rightarrow X_s \ell^+ \ell^-)}{ds d \cos \theta_\ell} \text{sgn}(\cos \theta_\ell), \quad (\text{VII.36})$$

where  $\theta_\ell$  is the angle between  $\ell^+$  and  $B$  momenta in the dilepton centre-of-mass frame <sup>3</sup>

It was shown in [90] that  $A_{FB}(s)$  is equivalent to the energy asymmetry introduced in [154]:

$$A_{energy} = \frac{N(E_{\ell^-} > E_{\ell^+}) - N(E_{\ell^+} > E_{\ell^-})}{N(E_{\ell^-} > E_{\ell^+}) + N(E_{\ell^+} > E_{\ell^-})} \quad (\text{VII.37})$$

---

<sup>3</sup>The so-called 'normalized' FB asymmetry, which is also often used, is given by  $\overline{A}_{FB}(s) = \int_{-1}^1 d \cos \theta_\ell \frac{d^2 \Gamma(B \rightarrow X_s \ell^+ \ell^-)}{ds d \cos \theta_\ell} \text{sgn}(\cos \theta_\ell) / \int_{-1}^1 d \cos \theta_\ell \frac{d^2 \Gamma(B \rightarrow X_s \ell^+ \ell^-)}{ds d \cos \theta_\ell}$

$\frac{d}{ds} BR(B \rightarrow X_s l^+ l^-) \times 10^{-5}$

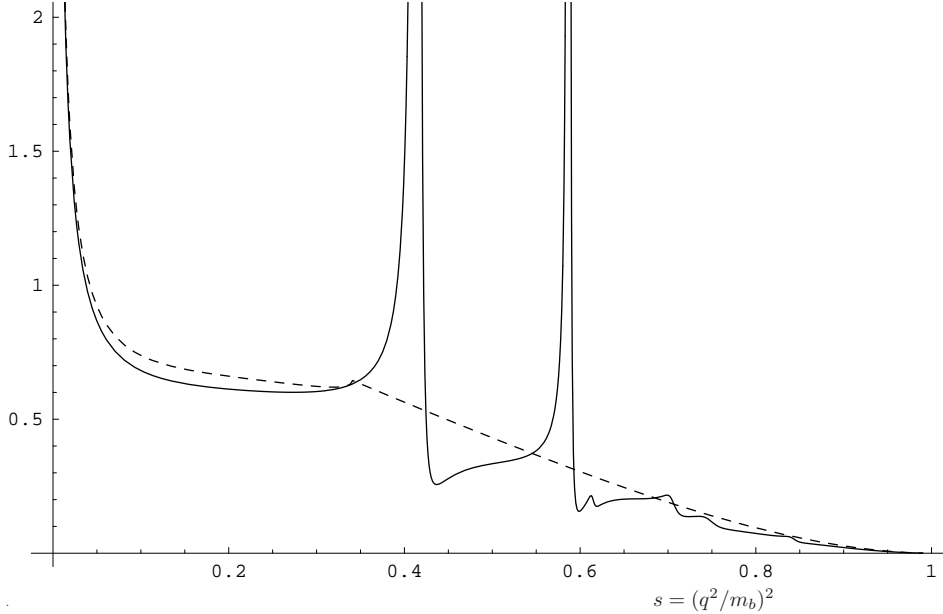


FIG. 23. Schematic dilepton mass spectrum of  $B \rightarrow X_s \ell^+ \ell^-$ , the dashed line corresponds to the perturbative contribution.

where  $N(E_{\ell^-} > E_{\ell^+})$  denotes the number of lepton pairs whose negatively charged member is more energetic in the  $B$  meson rest frame than its positive partner. From the experimental point of view, there is no significant difference either between measuring the inherent asymmetry using the lepton energy distribution or using the three-momentum information.

For the low- $s$  region the present partonic NNLL prediction is given in [76,78]:

$$\int_{0.05}^{0.25} d\hat{s} R_{quark}^{\ell^+ \ell^-}(\hat{s}) = (1.28 \pm 0.08_{scale}) \times 10^{-5} \quad (\text{VII.38})$$

The error quoted in (VII.38) reflects only the renormalization scale uncertainty and is purely perturbative. There is no additional problem due to the charm mass renormalization scheme ambiguity within the decay  $B \rightarrow X_s \ell^+ \ell^-$  because the charm dependence starts already at one loop, in contrast to the case of the decay  $B \rightarrow X_s \gamma$  (see fig. 16). The charm dependence itself leads to an additional uncertainty of  $\sim 7.6\%$  within the partonic quantity (VII.38), if the pole mass is varied,  $m_c^{pole}/m_b^{pole} = 0.29 \pm 0.02$ .

As discussed in section V, the impact of the NNLL contributions is significant. The large matching scale  $\mu_W$  uncertainty of 16% of the NLL result was removed; the low-scale uncertainty  $\mu_b$  of 13% was cut in half; and also the central value of the integrated low dilepton spectrum (VII.38) was significantly changed by  $\approx -14\%$  due to NNLL corrections.

These small uncertainties in the inclusive mode should be compared with the ones of the

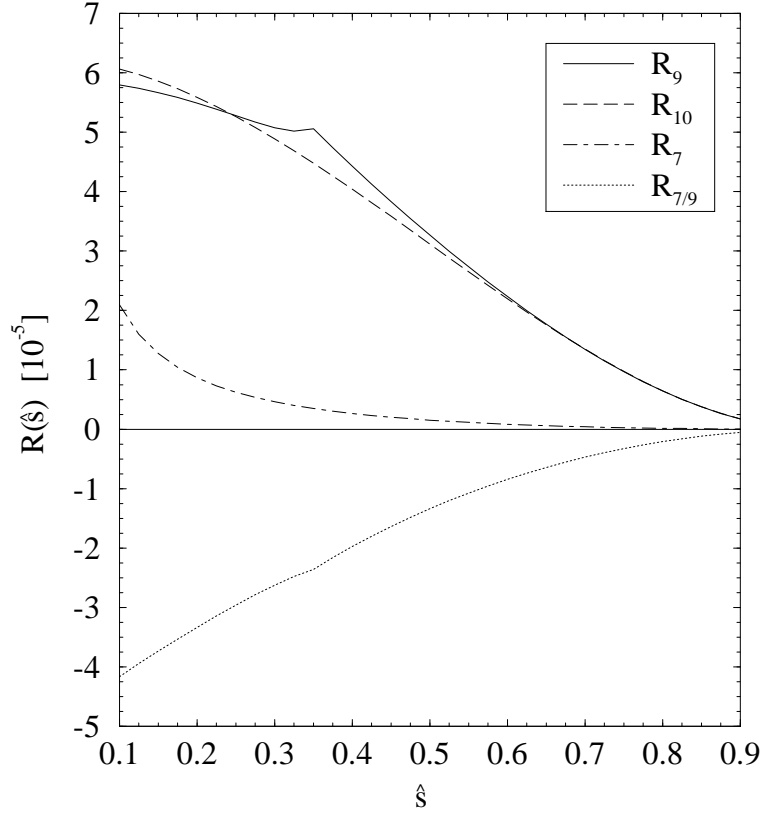


FIG. 24. Comparison of the different short-distance contributions to  $R_{\text{quark}}(\hat{s})$  (NLL precision), from [87].

corresponding exclusive mode  $B \rightarrow K^* \mu^+ \mu^-$  given in [122];  $\Delta BR = ({}^{+26}_{-17}, {}^{\pm 6}_{-4}, {}^{\pm 0.7}_{+0.4}, \pm 2)\%$ . The first dominant error represents the hadronic uncertainty due to the form factors.

Using the measured semi-leptonic branching ratio  $\mathcal{B}_{\text{exp.}}^{\text{sl}}$ , the prediction for the corresponding branching ratio is given by

$$\begin{aligned}
 \mathcal{B}(B \rightarrow X_s \ell^+ \ell^-)_{\text{Cut: } \hat{s} \in [0.05, 0.25]} &= \\
 &= \mathcal{B}_{\text{exp.}}^{\text{sl}} \int_{0.05}^{0.25} d\hat{s} [R_{\text{quark}}^{\ell^+ \ell^-}(\hat{s}) + \delta_{1/m_b^2} R(\hat{s}) + \delta_{1/m_c^2} R(\hat{s})] \\
 &= 0.104 [(1.27 \pm 0.08_{\text{scale}}) + 0.06 - 0.02] \times 10^{-5} \\
 &= (1.36 \pm 0.08_{\text{scale}}) \times 10^{-6}.
 \end{aligned} \tag{VII.39}$$

$\delta_{1/m_b^2} R(\hat{s})$  and  $\delta_{1/m_c^2} R(\hat{s})$  are the non-perturbative contributions discussed in section VI. The recent first measurement of BELLE, with a rather large uncertainty [55], is compatible with this SM prediction.

One could think that within the perturbative window at low  $\hat{s} \in [0.05, 0.25]$ , one is only sensitive to  $C_7$ , which would be redundant information, since we already know it from the decay  $B \rightarrow X_s \gamma$ . But, as was explicitly shown in [86,87], one is also sensitive to the new Wilson coefficients  $C_9$  and  $C_{10}$  and interference terms in the low  $\hat{s}$  regime with

$\hat{s} = m_{\ell^+\ell^-}/m_b^2 \in [0.05, 0.25]$  (see fig. 24 where the various perturbative contributions to  $R_{quark}$  (with NLL precision) are plotted).

A phenomenological NNLL analysis including also the high dilepton mass region will be presented in [79]. Clearly, the kinematical cuts should be adjusted to the experimental choices.

The phenomenological impact of the NNLL contributions on the FB asymmetry is also significant [75,77]. The position of the zero of the FB asymmetry, defined by  $A_{FB}(s_0) = 0$ , is particularly interesting to determine relative sign and magnitude of the Wilson coefficients  $C_7$  and  $C_9$  and it is therefore extremely sensitive to possible new physics effects.

Employing the counting rule proposed in [85], i.e. treating the formally  $O(1/\alpha_s)$  term of  $C_9$  as  $O(1)$  (see discussion at the end of section V), the lowest-order value of  $s_0$  – formally derived by the NLL expression of  $A_{FB}$  – is determined by the solution of

$$s_0 C_9^{eff}(s_0) + 2C_7^{eff} = 0 , \quad (\text{VII.40})$$

where the effective coefficients  $C_i^{eff}$  encode also all dominant matrix element corrections, which leads to an explicit  $s$  dependence (see [75], (A.1)) One arrives at

$$s_0^{NLL} = 0.14 \pm 0.02 , \quad (\text{VII.41})$$

where the error is determined by the scale dependence. That NLL result is now modified by the NNLL contributions to [75,77]

$$s_0^{NNLL} = 0.162 \pm 0.008 . \quad (\text{VII.42})$$

In this case the variation of the result induced by the scale dependence is accidentally very small (about  $\pm 1\%$ ) and cannot be regarded as a good estimate of missing higher-order effects. Taking into account the separate scale variation of both Wilson coefficients  $C_9$  and  $C_7$ , and the charm-mass dependence, one estimates a conservative overall error on  $s_0$  of about 5% [75]. In this  $s$  region the non-perturbative  $1/m_b^2$  and  $1/m_c^2$  corrections to  $A_{FB}(s)$  are very small and also under control (see section VI).

An illustration of the shift of the central value and the reduced scale dependence between NNL and NNLL expressions of  $A_{FB}(s)$ , in the low  $s$  region, is presented in fig. 25. The complete effect of NNLL contributions to the FB asymmetry adds up to a 16% shift compared with the NLL result, with a residual error due to higher-order terms reduced at the 5% level. Thus, the zero of the FB asymmetry in the inclusive mode turns out to be one of the most sensitive tests for new physics beyond the SM.

The  $B$  factories will soon provide statistics and resolution needed for the measurements of  $B \rightarrow X_s \ell^+ \ell^-$  kinematic distributions. Precise theoretical estimates of the SM expectations are therefore needed in order to perform new significant tests of flavour physics. The recently calculated new (NNLL) contributions [84,85,78,76,75,77,79] have significantly improved the sensitivity of the inclusive  $B \rightarrow X_s \ell^+ \ell^-$  decay in testing extensions of the SM in the sector of flavour dynamics. Together with the decay  $B \rightarrow X_s \gamma$ , the inclusive  $B \rightarrow X_s \ell^+ \ell^-$  decay will make precision flavour physics possible, if one can measure the kinematic variables in the  $B \rightarrow X_s \ell^+ \ell^-$  decay precisely.

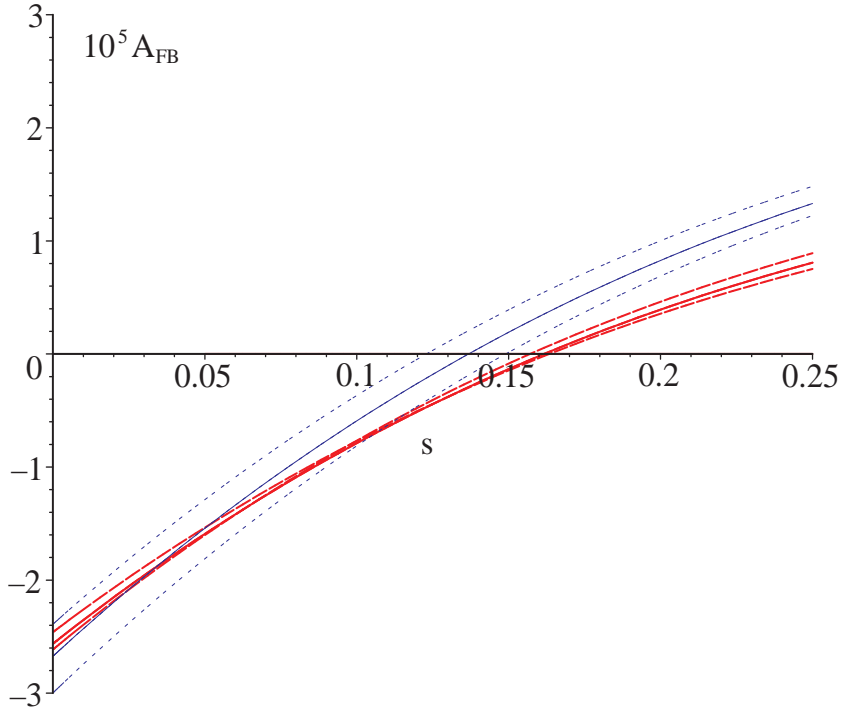


FIG. 25. Comparison between NNLL and NLL results for  $A_{FB}(s)$  in the low  $s$  region. The three thick lines are the NNLL predictions for  $\mu = 5$  GeV (full), and  $\mu = 2.5$  and  $10$  GeV (dashed); the dotted curves are the corresponding NLL results. All curves for  $m_c/m_b = 0.29$ . Note that  $A_{FB}(s)$  is normalized by the semi-leptonic decay rate, see (VII.36).

### E. Golden mode $B \rightarrow X_s \bar{\nu} \nu$

The decay  $B \rightarrow X_s \nu \bar{\nu}$  is the theoretically cleanest rare  $B$  decay, but also the most difficult experimentally.

As discussed in section V, the partonic decay is completely dominated by the internal top contribution due to the hard GIM mechanism. The perturbative scale uncertainty is  $O(1\%)$ . Moreover, the non-perturbative contributions scaling with  $1/m_b^2$  are under control and small [89,90,97]. Because of the absence of the photon-penguin contribution, the non-perturbative contributions scaling with  $1/m_c^2$  can be estimated to be at the level of  $10^{-3}$  at most [94].

After normalizing to the semi-leptonic branching ratio and summing over the three neutrino flavours, the branching ratio of the decay  $B \rightarrow X_s \nu \bar{\nu}$  is given by [88,34]:

$$\mathcal{B}(B \rightarrow X_s \nu \bar{\nu}) = \mathcal{B}_{exp.}^{sl} \frac{12\alpha^2}{\pi^2 \sin^4 \Theta_W} \frac{|V_{ts}|^2}{|V_{cb}|^2} \frac{C(m_t^2/m_W^2) \bar{\eta}}{f(m_c^2/m_b^2) \kappa(m_c^2/m_b^2)}. \quad (\text{VII.43})$$

Using the measured semi-leptonic branching ratio and the phase-space factor of the semi-leptonic decay  $f$ , the corresponding QCD correction  $\kappa$ , the QCD correction of the matrix

element of the decay  $B \rightarrow X_s \nu \bar{\nu}$ , namely  $\bar{\eta} = \kappa(0)$ , and scanning the input parameters, one ends up with the theoretical prediction [34]:

$$\mathcal{B}(B \rightarrow X_s \nu \bar{\nu}) = (3.5 \pm 0.7) \times 10^{-5}. \quad (\text{VII.44})$$

The replacement of  $V_{ts}$  by  $V_{td}$  in (VII.43) leads to the case of the decay  $B \rightarrow X_d \nu \bar{\nu}$ . Obviously all uncertainties cancel out in the ratio of the two branching ratios of  $B \rightarrow X_d \nu \bar{\nu}$  and  $B \rightarrow X_s \nu \bar{\nu}$ . Thus, it allows for the cleanest direct determination of the ratio of the two corresponding CKM matrix elements.

The measurement of these decay modes is rather difficult. The neutrinos escape detection; one, thus, has to search for the decays  $B \rightarrow X_{s,d} \nu \bar{\nu}$  through large missing energy associated with the two neutrinos. Clearly, background control is more than difficult in these channels. Hopefully, the  $B$  factories, with their high statistics and their clean environment, will be able to measure these decays in the future.

However, the lack of an excess of events with large missing energy in a sample of  $0.5 \times 10^6$   $b\bar{b}$  pairs at LEP already allowed ALEPH to establish an upper bound on the branching ratio of  $B \rightarrow X_s \nu \bar{\nu}$  [123,124] at 90% C.L.,

$$\mathcal{B}(B \rightarrow X_s \nu \bar{\nu}) < 7.7 \times 10^{-4}. \quad (\text{VII.45})$$

This upper bound is still an order of magnitude above the SM prediction, but it already leads to constraints on new physics models [124]. For this purpose, the QCD corrections to the decays  $B \rightarrow X_{s,d} \nu \bar{\nu}$  in supersymmetric theories (MSSM) have recently been presented [125].

## VIII. INDIRECT SEARCH FOR SUPERSYMMETRY

### A. Generalities

Today supersymmetric models are given priority in our search for new physics beyond the SM. This is primarily suggested by theoretical arguments related to the well-known hierarchy problem. Supersymmetry eliminates the sensitivity for the highest scale in the theory and, thus, stabilizes the low energy theory. The precise mechanism of the necessary supersymmetry breaking is unknown. A reasonable approach to this problem is the inclusion of the most general soft breaking term consistent with the SM gauge symmetries in the so-called unconstrained minimal supersymmetric standard model (MSSM). This leads to a proliferation of free parameters in the theory.

In the MSSM there are new sources of FCNC transitions. Besides the CKM-induced contributions, which are brought about by a charged Higgs or a chargino, there are generic supersymmetric contributions that arise from flavour mixing in the squark mass matrices. The structure of the MSSM does not explain the suppression of FCNC processes, which is observed in experiments; the gauge symmetry within the supersymmetric framework does not protect the observed strong suppression of the FCNC transitions. This is the crucial point of the well-known supersymmetric flavour problem. Clearly, the origin of flavour violation is highly model-dependent.

Within the framework of the MSSM there are at present three favoured supersymmetric models that solve the supersymmetric flavour problem by a specific mechanism through which the sector of supersymmetry breaking communicates with the sector accessible to experiments: in the minimal supergravity model (mSUGRA) [127], supergravity is the corresponding mediator; in the other two models, this is achieved by gauge interactions (GMSB) [128] and by anomalies (AMSB) [129]. Furthermore, there are other classes of models in which the flavour problem is solved by particular flavour symmetries [130].

The decay  $B \rightarrow X_s \gamma$  is sensitive to the mechanism of supersymmetry breaking because, in the limit of exact supersymmetry, the decay rate would be just zero:

$$\mathcal{B}(B \rightarrow X_s \gamma)_{Exact\,Susy} = 0. \quad (\text{VIII.1})$$

This follows from an argument first given by Ferrara and Remiddi in 1974 [126]. In that work the absence of the anomalous magnetic moment in a supersymmetric abelian gauge theory was shown.

Flavour violation thus originates from the interplay between the dynamics of flavour and the mechanism of supersymmetry breaking. FCNC processes therefore yield important (indirect) information on the construction of supersymmetric extensions of the SM and can contribute to the question of which mechanism ultimately breaks supersymmetry and will thus yield important (indirect) information on the construction of supersymmetric extensions of the SM. In this context it is important to analyse the correlations between the different sets of information from rare  $B$  and  $K$  decays. Moreover, tight experimental bounds on some flavour-diagonal transitions, such as the electric dipole moment of the electron and of the neutron, as well as  $g-2$ , help constraining the soft terms that induce chirality violations.

As was already emphasized in the introduction, inclusive rare decays, as loop-induced processes, are particularly sensitive to new physics and theoretically clean. Neutral flavour transitions involving third-generation quarks, typically in the  $B$  system, do not yet pose serious threats to specific models. However, the rare decay  $B \rightarrow X_s \gamma$  has already carved out large regions in the space of free parameters of most of the models in the classes mentioned above. Once more precise data from the  $B$  factories are available, this decay will undoubtedly gain even more efficiency in selecting the viable regions of the parameter space in the various classes of models. This indirect search for new physics is a model-dependent issue; especially in the MSSM with its 43 new CP-violating phases. Simplifying assumptions about the parameters often introduce model-dependent correlations between different observables. Thus, flavour physics will also help in discriminating between the models that will be proposed by then. In view of this, it is important to calculate the rate of the rare  $B$  decays, with theoretical uncertainties as reduced as possible and general enough for generic supersymmetric models.

In the analysis of FCNC processes within supersymmetry, the additional assumption of minimal flavour violation (MFV) is often introduced. Minimal flavour violation is then loosely defined as 'the flavour violation that is completely dictated by the CKM angles'. In a top/bottom approach, one starts with a specific model of supersymmetry breaking and then one can try to justify the simplifying assumption of MFV explicitly within the specific model. In a bottom/top approach, the naive assumption of MFV is problematic, since it is not stable, within the MSSM, under radiative corrections and calls for a more precise concept. In [131], a consistent definition was presented, which essentially requires that all flavour and CP-violating interactions be linked to the known structure of Yukawa couplings. The constraint within an effective field approach is introduced with the help of a symmetry concept and can be shown to be renormalization-group-invariant; it is also a valid concept beyond supersymmetric models [131]. This consistent MFV assumption for example is valid if the soft terms of the scalar mass are universal and the trilinear soft terms are proportional to Yukawa couplings, at an arbitrary high scale. Then the physical squark masses are not equal, but the induced flavour violation is described in terms of the usual CKM parameters.

Perhaps this MFV-based effective field theory approach is too pessimistic from the current point of view. One of the key predictions of the MFV is the direct link between the  $b \rightarrow s$ ,  $b \rightarrow d$  and  $s \rightarrow d$  transitions. This prediction within the  $\Delta F = 1$  sector is definitely not well-tested at the moment.

In contrast to the scale of the electroweak symmetry breaking, there is no similarly strong argument that new flavour structures have to appear at the electroweak scale.

## B. Constraints from $B \rightarrow X_s \gamma$

While in the SM, the rate for  $B \rightarrow X_s \gamma$  is known up to NLL in QCD, the calculation of this decay rate within supersymmetric models is still far from this level of sophistication. There are several contributions to the decay amplitude: besides the  $W$   $t$ -quark and the  $H$   $t$ -quark contributions, there are also the chargino, gluino and neutralino contributions. The first systematic MSSM analysis of the decay  $B \rightarrow X_s \gamma$  was presented in [132].

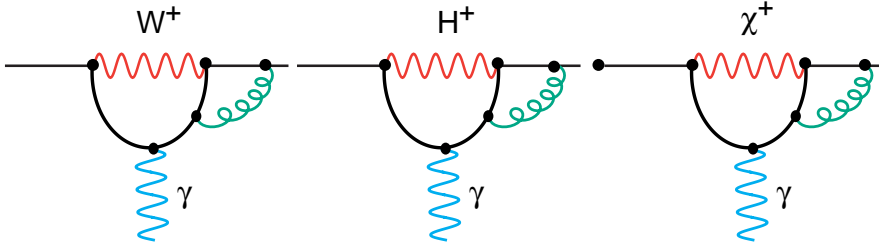


FIG. 26. SM, charged Higgs and chargino contribution at the matching scale.

The phenomenological analyses of the decay  $B \rightarrow X_s\gamma$  in the mSUGRA model [133,134,176] already excluded large parts of the parameter space of this model. However, within many analyses the non-standard contributions were often not investigated with NLL precision as the SM contribution. Besides the large uncertainties in the LL predictions, the step from the LL to the NLL precision is also necessary in order to check the validity of the perturbative approach in the model under consideration. Moreover, it was already shown in specific new-physics scenarios that bounds on the parameter space of non-standard models are very sensitive to NLL contributions (see below).

Nevertheless, within supersymmetric models, partial NLL results are available. The gluonic NLL two-loop matching contributions were presented some time ago [136]. A complete NLL calculation of the  $B \rightarrow X_s\gamma$  branching ratio in the simplest extension of the SM, namely the two-Higgs-doublet model (2HDM), is already available [72,137,113]: in the 2HDM of Type II (which already represents a good approximation for gauge-mediated supersymmetric models with large  $\tan\beta$ , where the charged Higgs contribution dominates the chargino contribution), the  $B \rightarrow X_s\gamma$  is only sensitive to two parameters of this model, the mass of the charged Higgs boson and  $\tan\beta$ . Thus, the experimental data of the decay  $B \rightarrow X_s\gamma$  allow for stringent bounds on these two parameters, which are much more restrictive than the lower bound on the charged Higgs mass found in the direct search at LEP (see fig. 27).

One finds that these indirect bounds are very sensitive to NLL QCD corrections and even to the two-loop electroweak contributions (see [72,137]). Using the latest theoretical NLL prediction (VII.33) and the latest CLEO measurement (III.2), one finds the  $\tan\beta$  independent bound  $M_H > 350$  GeV [113]. But this bound gets weakened if the charm mass renormalization scheme ambiguity of the present NLL prediction (see section VII A) is taken into account. For example, if the pole mass scheme is adapted as in the theoretical prediction (VII.31), then the weaker bound  $M_H > 280$  GeV is found [113].

In [138] a specific supersymmetric scenario is presented, where in particular the possibility of destructive interference of the chargino and the charged Higgs contribution is analysed. The analysis has been done under two assumptions. First, that the only source of flavour violation at the electroweak scale is that of the SM, encoded in the CKM matrix (MFV). Therefore, the analysis applies to mSUGRA, GMSB and AMSB models (in which the same features are assumed at the messenger scale) only when the sources of flavour violation,

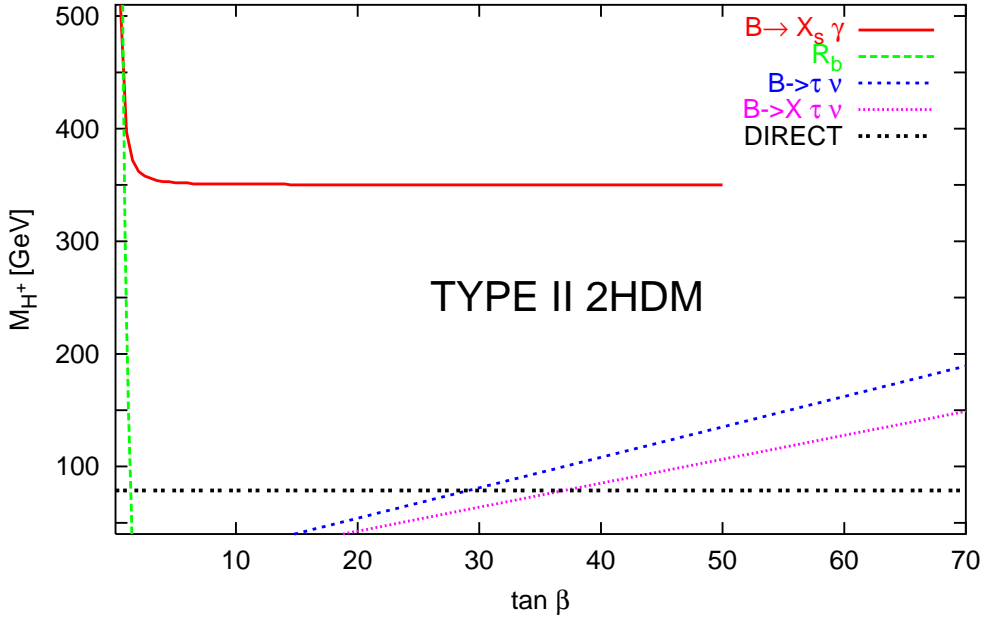


FIG. 27. Direct and indirect lower bounds on  $M_{H^+}$  from different processes in the 2HDM of Type II as a function of  $\tan \beta$ . The  $B \rightarrow X_s \gamma$  bound is based on the latest CLEO measurement (III.2), from [113].

generated radiatively between the supersymmetry-breaking scale and the electroweak scale, can be neglected with respect to those induced by the CKM matrix. The second assumption is that there exists a specific mass hierarchy, in particular the heavy gluino limit. Indeed, the NLL calculation has been done in the limit

$$\mu_{\tilde{g}} \sim O(m_{\tilde{g}}, m_{\tilde{q}}, m_{\tilde{t}_1}) \gg \mu_W \sim O(m_W, m_{H^+}, m_t, m_\chi, m_{\tilde{t}_2}). \quad (\text{VIII.2})$$

The mass scale of the charginos ( $\chi$ ) and of the lighter stop ( $\tilde{t}_2$ ) is the ordinary electroweak scale  $\mu_W$ , while the scale  $\mu_g$  is characteristic of all other strongly interacting supersymmetric particles (squarks and gluinos) and is assumed to be of the order of 1 TeV. NLL QCD corrections have been calculated up to first order in  $\mu_W/\mu_{\tilde{g}}$ , including the important non-decoupling effects [138].

At the electroweak scale  $\mu_W$ , the new contributions do not induce any new operators in this scenario. Thus, the only step in the new NLL calculation beyond the one within the SM is Step 1, the matching calculation at the scale  $\mu_W$ , where we encounter the two new CKM-induced contributions of the charged Higgs and the chargino (see fig. 26):

$$C_{NLL}(\mu_W) = C_{NLL}^{SM}(\mu_W) + C_{NLL}^{H^+}(\mu_W) + C_{NLL}^\chi(\mu_W). \quad (\text{VIII.3})$$

It was found [138] that, in this specific supersymmetric scenario, bounds on the parameter space are rather sensitive to NLL contributions and they lead to a significant reduction of the stop-chargino mass region, where the supersymmetric contribution has a large destructive interference with the charged-Higgs boson contribution. In fig. 28 the upper bounds on

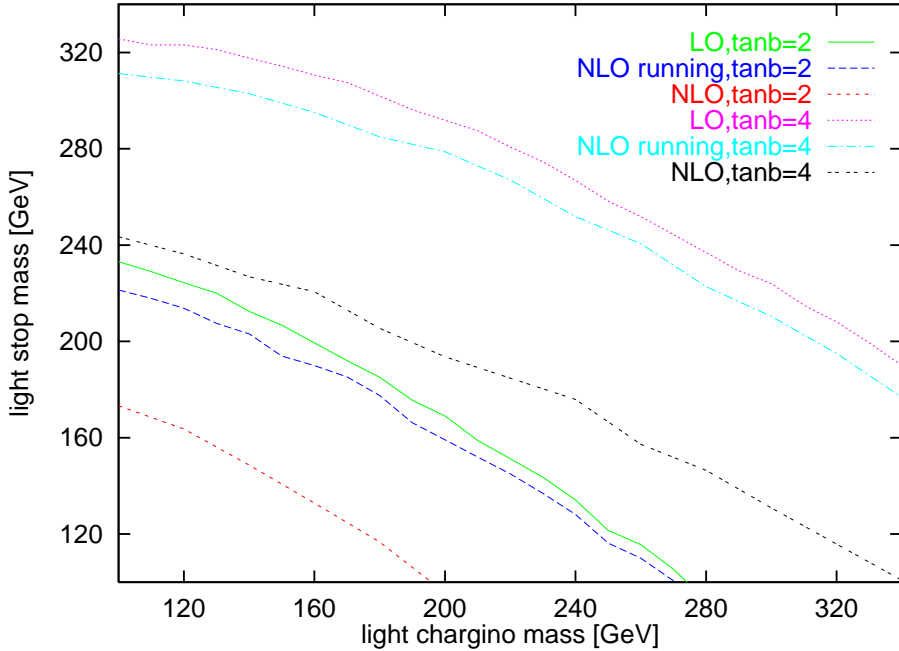


FIG. 28. Upper bounds on the lighter chargino and stop masses from  $B \rightarrow X_s \gamma$  data in the scenario (VIII.2) if a light charged Higgs mass is assumed; for  $\tan \beta = 2$  (three lower curves) and 4 (three upper plots) the LL, NLL-running and NLL results (from the top to the bottom) are shown (see text), from [138].

the lighter chargino and stop masses from  $B \rightarrow X_s \gamma$  data in the scenario of (VIII.2) are illustrated if a light charged Higgs mass of  $m_{H^\pm} = 100$  GeV is assumed. The stop mixing is set to  $|\theta_{\tilde{t}}| < \pi/10$ , which corresponds to the assumption of a mainly right-handed light stop. Moreover,  $|\mu| < 500$  GeV and all heavy masses are around 1 TeV. For  $\tan \beta = 2$  and 4 the results of the LL, ‘NLL running’ and NLL calculations are given. The result of neglecting the new NLL supersymmetric contributions to the Wilson coefficients is labelled as ‘NLL running’ and illustrates the importance of the NLL chargino contribution [138].

This specific MFV scenario was refined and extended to the large  $\tan \beta$  regime by the resummations of terms of the form  $\alpha_s^n \tan^{n+1} \beta$  [13,14]. Additional  $\tan \beta$  terms, which have to be summed in the large  $\tan \beta$  regime were singled out in [131]. The stability of the renormalization-group-improved perturbation theory was re-assured for this specific scenario: the resummed NLL results in the large  $\tan \beta$  regime show constraints similar to the LL results (see [139]). For example, it is a well-known feature in the mSUGRA model that, depending on the sign of  $A_t \cdot \mu$  (where  $A_t$  denotes the stop mixing parameter) the chargino contribution can interfere constructively ( $A_t \cdot \mu > 0$ ) or destructively ( $A_t \cdot \mu < 0$ ) with the SM and the charged Higgs contribution. Therefore, the scenario  $A_t \cdot \mu > 0$  within this model requires very heavy superpartners in order to accommodate the  $B \rightarrow X_s \gamma$  data. But also the case  $A_t \cdot \mu < 0$  is constrained in the large  $\tan \beta$  regime where the chargino contribution is strongly enhanced [13,14,139] (see fig. 29).

However, all these NLL analyses are valid only in the heavy gluino regime. Thus, they

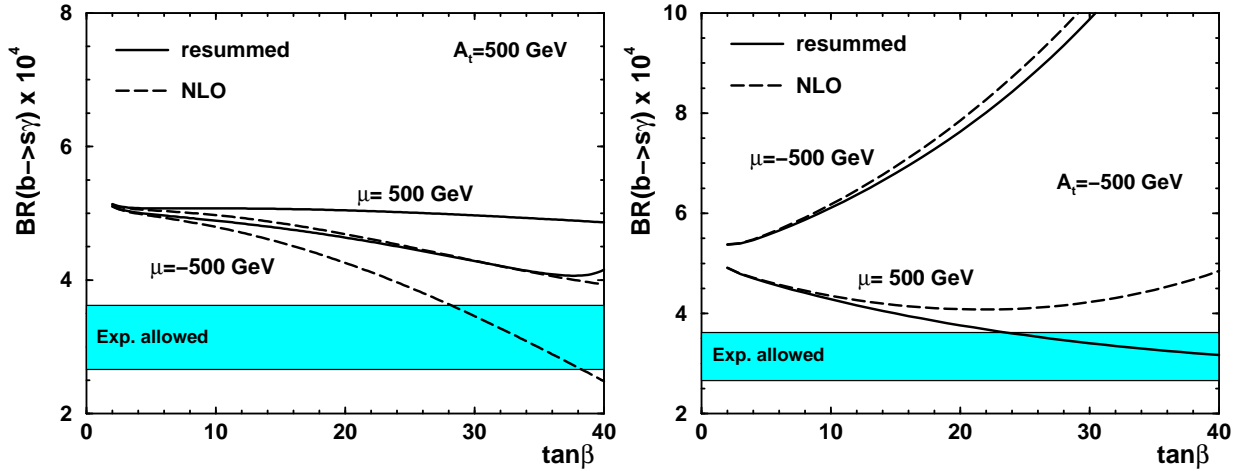


FIG. 29. Comparison of the theoretical NLL predictions within a special MSSM scenario (similar to VIII.2) *with* and *without* the resummed large  $\tan\beta$  terms; the charged Higgs boson mass is 200 GeV and the light stop mass is 250 GeV. The values of  $\mu$  and  $A_t$  are indicated in the plot, while the gluino, heavy stop and down-squark masses are set at 800 GeV; from [13].

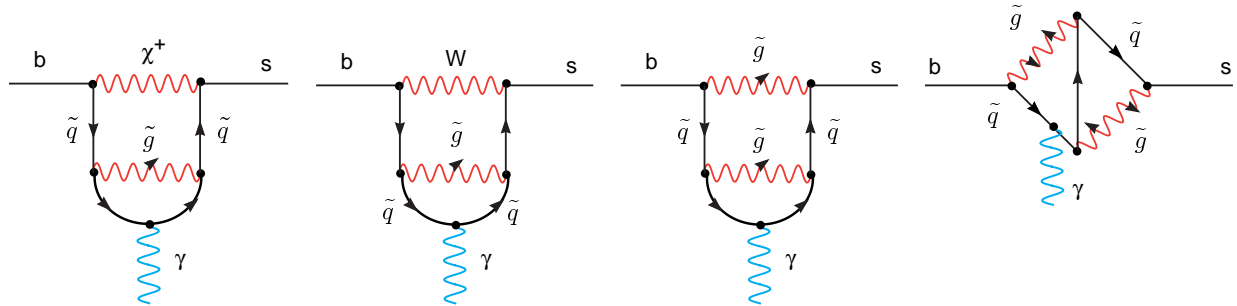


FIG. 30. NLL gluino contributions to the decay  $B \rightarrow X_s \gamma$ .

cannot be used in particular directions of the parameter space of the above-listed models in which quantum effects induce a gluino contribution as large as the chargino or the SM contributions. Nor can it be used as a model-discriminator tool, able to constrain the potentially large sources of flavour violation typical of generic supersymmetric models. Therefore, a complete NLL calculation, also within the MFV approach, should include contributions where the gluon is replaced by its superpartner gluino (see fig. 30) [140].

The flavour non-diagonal gluino–quark–squark vertex induced by the flavour violating scalar mass term and trilinear terms is particularly interesting. This vertex is generically assumed to induce the dominant contribution to quark flavour transitions, as this vertex is weighted by the strong coupling constant  $g_s$ . Therefore, it is often taken as the only contribution to these transitions and in particular to the  $B \rightarrow X_s \gamma$  decay, when attempting to obtain order-of-magnitude upper bounds on flavour violating terms in the scalar potential.

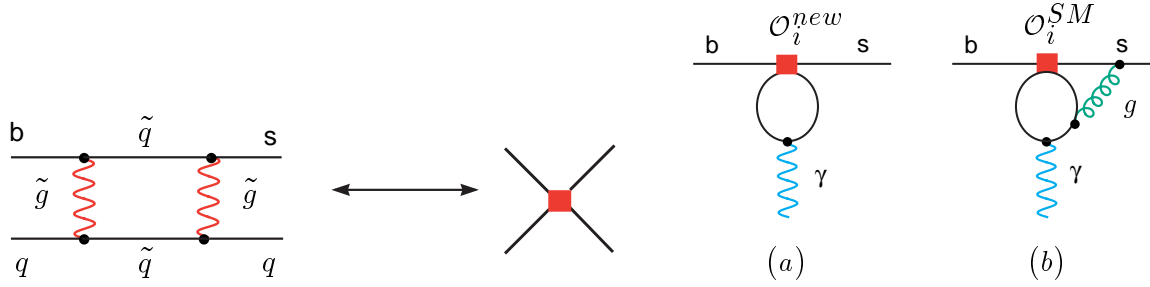


FIG. 31. Left: matching of gluino–squark box on new scalar operators. Right: mixing of new (scalar) operators at one loop (a) in contrast to the vectorial operators of the SM (b) which mix at two loop only.

Once the experimental constraints are imposed, however, the gluino contribution is reduced to values such that the SM and the other supersymmetric contributions can no longer be neglected. Any LL and NLL calculation of the  $B \rightarrow X_s \gamma$  rate in generic supersymmetric models, therefore, should then include all possible contributions.

The gluino contribution presents some peculiar features related to the implementation of the QCD corrections. In ref. [15] this contribution to the decay  $B \rightarrow X_s \gamma$  has been investigated in great detail for supersymmetric models with generic soft terms. The gluino-induced contributions to the decay amplitude for  $B \rightarrow X_s \gamma$  are of the following form:

$$\alpha_s(m_b) (\alpha_s(m_b) \log(m_b/M))^n \quad (LL), \quad (\text{VIII.4})$$

$$\alpha_s^2(m_b) (\alpha_s(m_b) \log(m_b/M))^n \quad (NLL). \quad (\text{VIII.5})$$

The relevant operator basis of the SM effective Hamiltonian gets enlarged to contain magnetic and chromomagnetic operators with an extra factor of  $\alpha_s$ . Furthermore, one finds that gluino–squark boxes induce new scalar and tensorial four-quark operators, which are shown to mix into the magnetic operators without gluons already at one loop. On the other hand, the vectorial four-quark operators mix only with an additional gluon into magnetic ones (fig. 31). Thus, they will contribute at NLL order only. But from the numerical point of view the contributions of the vectorial operators (although NLL) are not necessarily suppressed w.r.t. the new four-quark contributions; this is due to the expectation that the flavour-violation parameters present in the Wilson coefficients of the new operators are expected to be much smaller (or much more stringently constrained) than the corresponding ones in the coefficients of the vectorial operators. This feature shows that a complete NLL calculation is important.

To understand the sources of flavour violation that may be present in supersymmetric models in addition to those enclosed in the CKM matrix, one has to consider the contributions to the squark mass matrices

$$\mathcal{M}_f^2 \equiv \begin{pmatrix} m_{f,LL}^2 + F_{fLL} + D_{fLL} & (m_{f,LR}^2) + F_{fLR} \\ (m_{f,LR}^2)^\dagger + F_{fRL} & m_{f,RR}^2 + F_{fRR} + D_{fRR} \end{pmatrix}, \quad (\text{VIII.6})$$

where  $f$  stands for up- or down-type squarks. In the super-CKM basis, where the quark mass matrices are diagonal and the squarks are rotated in parallel to their superpartners, the  $F$  terms from the superpotential and the  $D$  terms turn out to be diagonal  $3 \times 3$  submatrices of the  $6 \times 6$  mass matrices  $\mathcal{M}_f^2$ . This is in general not true for the additional terms  $m_f^2$ , originating from the soft supersymmetric breaking potential. Because all neutral gaugino couplings are flavour diagonal in the super CKM basis, the gluino contributions to the decay  $b \rightarrow s\gamma$  are induced by the off-diagonal elements of the soft terms  $m_{f,LL}^2$ ,  $m_{f,RR}^2$ ,  $m_{f,RL}^2$ .

As a first step, it is convenient to select *one* possible source of flavour violation in the squark sector at a time and assume that all the remaining ones are vanishing. Following refs. [142,143], all diagonal entries in  $m_{d,LL}^2$ ,  $m_{d,RR}^2$ , and  $m_{u,RR}^2$  are set to be equal and their common value is denoted by  $m_{\tilde{q}}^2$ . The branching ratio can then be studied as a function of

$$\delta_{LL,ij} = \frac{(m_{d,LL}^2)_{ij}}{m_{\tilde{q}}^2}, \delta_{RR,ij} = \frac{(m_{d,RR}^2)_{ij}}{m_{\tilde{q}}^2}, \delta_{LR,ij} = \frac{(m_{d,LR}^2)_{ij}}{m_{\tilde{q}}^2} \quad (i \neq j). \quad (\text{VIII.7})$$

Phenomenological analyses in the so-called unconstrained MSSM [141,143,144] neglected QCD corrections and only used the gluino contribution to saturate the experimental bounds. Moreover, no correlations between different sources of flavour violation were taken into account. In this way, one arrived at ‘order-of-magnitude bounds’ on the soft parameters [143,144]. The  $B \rightarrow X_s\gamma$  decay is mainly sensitive to the off-diagonal elements  $\delta_{LR,23}$  and  $\delta_{RL,23}$  and constrains them to values of order  $10^{-2}$ . In [15], the sensitivity of the bounds on the down squark mass matrix to radiative QCD LL corrections was systematically analysed, including the SM and the gluino contributions. Some leading NLL contributions were considered in [146] and the large impact of the NLL corrections for non-minimal models, in particular for large  $\tan\beta$  was demonstrated.

A consistent analysis of the bounds on the sfermion mass matrix should also include interference effects between the various contributions. In [16], the interplay between the various sources of flavour violation and the interference effects of SM, gluino, chargino, neutralino and charged Higgs boson contributions is analysed. New bounds on simple combinations of elements of the soft part of the squark mass matrices are found to be, in general, one order of magnitude weaker than the bound on the single off-diagonal element  $\delta_{LR,23}$ , which was derived in previous work [143,145] by neglecting any kind of interference effects. Thus, it turns out that — at least within the decay  $B \rightarrow X_s\gamma$  — the flavour problem is less severe than often stated.

The measurement of the photon polarization within the decay  $B \rightarrow X_s\gamma$  allows for another important SM test. Assuming that the decay is induced by the magnetic dipole operator only, one starts with the effective Hamiltonian

$$\mathcal{H} = -\frac{4G_F}{\sqrt{2}}\lambda_t(C_{7L}\mathcal{O}_{7L} + C_{7R}\mathcal{O}_{7R}), \quad (\text{VIII.8})$$

where  $\mathcal{O}_{7L,R} \equiv \frac{e}{16\pi^2} \overline{m}_b \bar{s} \sigma_{\mu\nu} \frac{1 \pm \gamma_5}{2} b F^{\mu\nu}$ . Then the photon polarization is defined by

$$\lambda_\gamma \equiv \frac{|C_{7R}|^2 - |C_{7L}|^2}{|C_{7R}|^2 + |C_{7L}|^2}. \quad (\text{VIII.9})$$

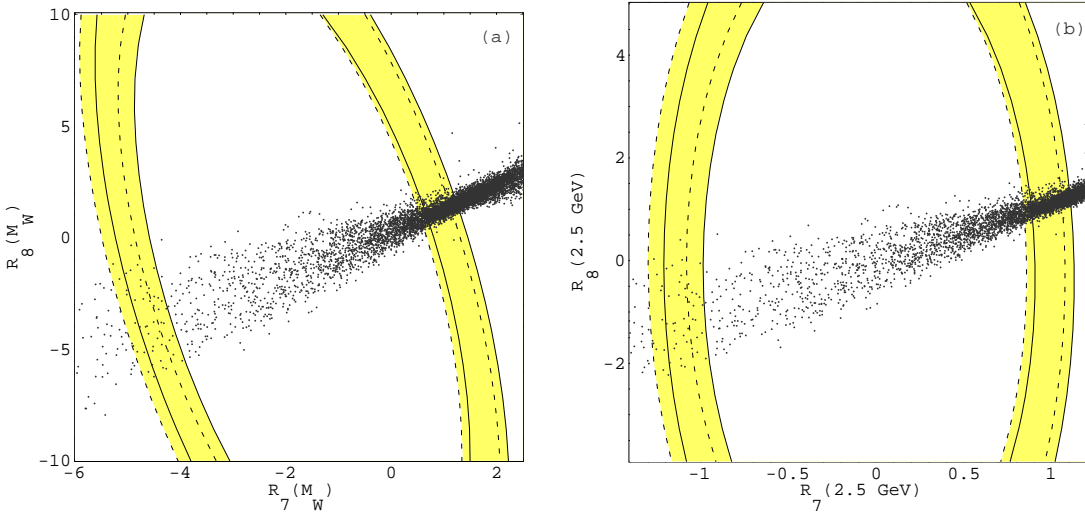


FIG. 32. 90% C.L. bounds in the  $[R_7(\mu), R_8(\mu)]$  plane following from the measurement of the  $B \rightarrow X_s \gamma$  branching ratio for  $\mu = m_W$  (left) and  $\mu = 2.5$  GeV (right), where  $R_{7,8} = C_{7,8}^{total}/C_{7,8}^{SM}$ . Theoretical uncertainties are taken into account. The solid and dashed lines correspond to the  $m_c = m_c^{pole}$  and  $m_c = m_c^{\overline{MS}}(\mu_b)$  cases respectively. The scatter points correspond to the expectation in MFV models; from [160].

In the SM, one has  $C_{7R}/C_{7L} = m_s/m_b \approx 0$  and therefore a mostly left-handed photon. But in many supersymmetric scenarios, and also in left-right-symmetric models, the photon may have a large right-handed component. In [147] the possibility of a strictly right-handed photon within the framework of the MSSM was discussed. Clearly, only in non-minimal models is such an extreme deviation from the SM prediction possible.

There are many suggestions for measuring  $\lambda_\gamma$  in the literature [148–152]. However, they all rely on very high statistics or on new experimental settings and will not be possible in the near future. Quite recently, a new method has been proposed, which can be realized with the present statistics available at the  $B$  factories. The photon polarization can be measured in radiative  $B$  decays to excited kaons, using angular correlations among the three-body decay products of the excited kaons [153]. It is essential for a helicity measurement to have a three-particle decay mode because  $\lambda_\gamma$  is a parity-odd variable and there is no odd-momentum correlation in the two-body mode. In the decays  $B^+ \rightarrow (K_1^+(1400) \rightarrow K^0 \pi^+ \pi^0) \gamma$  and  $B^0 \rightarrow (K_1^0(1400) \rightarrow K^+ \pi^- \pi^0) \gamma$ , however, the up-down asymmetry of the photon momentum with respect to the  $K\pi\pi$  decay plane in the frame of the excited kaon measures the photon polarization rather efficiently. The up-down asymmetry can theoretically be predicted to be  $A = (0.33 \pm 0.05) \times \lambda_\gamma$  in the case of the resonance  $K_1(1400)$  [153]. Thus, the method will definitely be sensitive for large deviations from the SM prediction already with the present luminosity at the  $B$  factories.

### C. Constraints from $B \rightarrow X_s \ell^+ \ell^-$

The inclusive  $B \rightarrow X_s \ell^+ \ell^-$  decay is another important tool to understand the nature of physics beyond the SM. In comparison to the decay  $B \rightarrow X_s \gamma$ , it offers complementary information. For example one is able to resolve the sign ambiguity of the Wilson coefficient  $C_7$ , which is not fixed by the  $B \rightarrow X_s \gamma$  constraint. The FB asymmetry, however, has terms proportional to  $\text{Re}(C_{10}C_9^{eff})$  and  $\text{Re}(C_{10}C_7^{eff})$ . As was first advocated in [18], the invariant dilepton mass spectrum, the forward–backward charge asymmetry and the decay rate of  $B \rightarrow X_s \gamma$  determine the magnitude and also the sign of the three Wilson coefficients  $C_7$ ,  $C_9$ , and  $C_{10}$ , and allow for a model-independent analysis of rare  $B$  decays.

There are several mSUGRA models and also several model-independent analyses in the literature [132,154–159]. It was always assumed that the operator basis is not enlarged in comparison to the SM. All the analyses found strong correlations between the decays  $B \rightarrow X_s \gamma$  and  $B \rightarrow X_s \ell^+ \ell^-$ .

Within the mSUGRA model sizeable deviations from the SM values of the  $B \rightarrow X_s \ell^+ \ell^-$  decay are excluded through the severe constraints on  $C_7$  by the  $B \rightarrow X_s \gamma$  measurement. But it was also shown that in less restricted scenarios supersymmetric contributions could potentially enhance the  $B \rightarrow X_s \ell^+ \ell^-$  kinematic distributions, the dilepton mass spectrum and the FB asymmetry, by more than 100% relative to the SM predictions. One of the reasons of the enhancements is that the Wilson coefficient  $C_7$  can change the sign with respect to the SM in some region of the parameter space. Within the mSUGRA model, the experimental bounds have disfavoured the non-SM sign already (see fig. 32).

When the experimental uncertainties are reduced soon, this fact will allow to discriminate between MFV models and non-minimal models and will lead either to evidence of new physics or to very stringent constraints on the parameter space of such models.

Recently these analyses have been updated in [160] based on the new experimental data of the semi-leptonic decays and on partial results in the NNLL theoretical predictions. Within the analysis, the charm mass renormalization scheme ambiguity (see section VII A) in the decay  $B \rightarrow X_s \gamma$  is taken into account. But also a too conservative error estimate regarding the charm mass dependence within the decay  $B \rightarrow X_s \ell^+ \ell^-$  is assumed, which leads to a rather large error of 15% in the inclusive mode.

It was found [160] that with the present experimental knowledge the decay  $B \rightarrow X_s \gamma$  still leads to the most restrictive constraints. Especially, the MFV scenarios are already highly constrained and only small deviations to the SM rates and distributions are possible; therefore no useful additional bounds from the semi-leptonic modes beyond what are already known from the  $B \rightarrow X_s \gamma$  can be deduced for the MFV models at the moment. But in non-minimal models, additional constraints from the semi-leptonic mode already emerge in some parts of the supersymmetric parameter space, namely for the off-diagonal elements within the squark mass matrix in the up-quark sector.

Within the model-independent analysis, the impact of the partial NNLL contributions on the allowed ranges for the Wilson coefficients was already found to be significant. In this analysis, however, only the integrated branching ratios were used to derive constraints. It is clear that one needs measurements of the kinematic distributions of the  $B \rightarrow X_s \ell^+ \ell^-$ , the dilepton mass spectrum and the FB asymmetry in order to determine the exact values

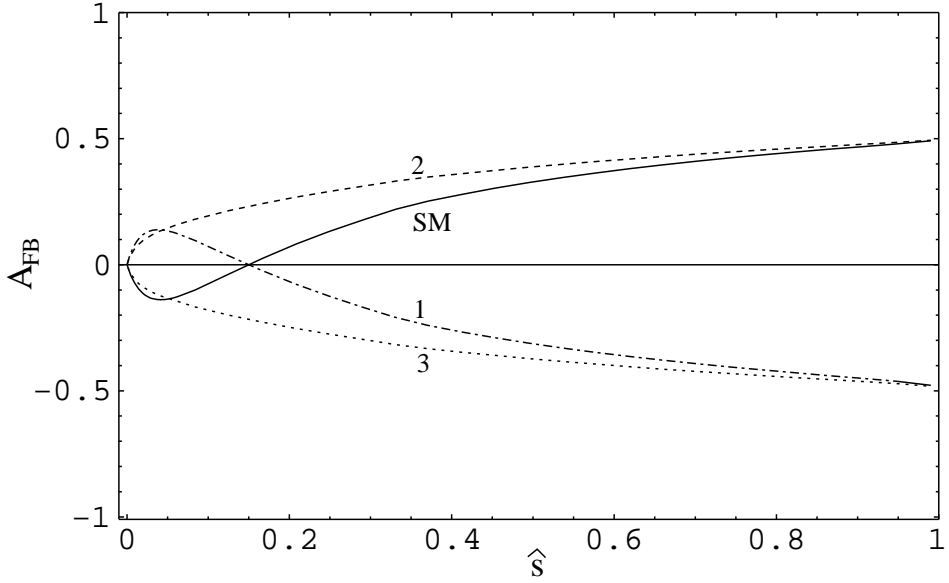


FIG. 33. Four different shapes of the normalized FB asymmetry  $\bar{A}_{FB}$  for the decay  $B \rightarrow X_s \ell^+ \ell^-$ . The four curves correspond to four sample points of the Wilson coefficients that are compatible with the present measurements of the integrated branching ratios; from [160].

and signs of the Wilson coefficients. In fig. 33, the impact of these future measurements is illustrated. It shows the shape of the FB asymmetry for the SM and three additional sample points, which are all still allowed by the present measurements of the branching ratios; thus, even rather rough measurements of the FB asymmetry will either rule out large parts of the parameter space of extended models or show clear evidence for new physics beyond the SM.

## IX. DIRECT CP VIOLATION IN $B \rightarrow S$ TRANSITIONS

The  $B$  system provides us with an independent test of the CKM prescription of CP violation. Until recently, the neutral kaon system was the only environment where CP violation had been observed. Those effects in the kaon system are often plagued by large theoretical uncertainties due to long-range QCD. So it was difficult to decide if the CKM description really accounts quantitatively for CP violation. In contrast, non-perturbative contributions are under control in the  $B$  system thanks to the heavy mass expansion. Moreover, there are gold-plated CP asymmetries like the one in the decay mode  $B \rightarrow \psi K_S$ , which are theoretically very clean, because the direct decay amplitude is dominated by one single weak phase and, thus, most of the hadronic uncertainties drop out in the CP asymmetry.

The CKM prescription of CP violation with one single phase — proposed in 1972 when the second family was not confirmed experimentally [161] — is very predictive and has now passed its first precision test in the golden  $B$  mode,  $B_d \rightarrow \psi K_S$ , at the 10% level [8,9]. Nevertheless, there is still room for non-standard CP phases, especially in the FCNC  $\Delta F = 1$  modes. Actually, detailed measurements of CP asymmetries in rare  $B$  decays will be possible in the near future.

The direct *normalized* CP asymmetries of the inclusive decay modes is given by <sup>4</sup>

$$\alpha_{CP}(B \rightarrow X_{s/d}\gamma) = \frac{\Gamma(\bar{B} \rightarrow X_{s/d}\gamma) - \Gamma(B \rightarrow X_{\bar{s}/\bar{d}}\gamma)}{\Gamma(\bar{B} \rightarrow X_{s/d}\gamma) + \Gamma(B \rightarrow X_{\bar{s}/\bar{d}}\gamma)} \quad (\text{IX.1})$$

CLEO has already presented a measurement of the CP asymmetry in the inclusive decay  $B \rightarrow X_s\gamma$ , actually a measurement of a weighted sum,  $\alpha_{CP} = 0.965\alpha_{CP}(B \rightarrow X_s\gamma) + 0.02\alpha_{CP}(B \rightarrow X_d\gamma)$ , yielding [172]

$$\alpha_{CP} = (-0.079 \pm 0.108 \pm 0.022) \times (1.0 \pm 0.030). \quad (\text{IX.2})$$

The first error is statistical, the second and third errors additive and multiplicative systematic respectively. This measurement is based on  $10^7 B\bar{B}$  events and implies that, at 90% confidence level,  $\alpha_{CP}$  lies between  $-0.27 < \alpha_{CP} < +0.10$ ; very large effects are thus already excluded. The same conclusion can be deduced from the measurements of the CP asymmetry in the exclusive mode  $B \rightarrow K^*(892)\gamma$  of CLEO [174],  $\alpha_{CP} = +0.08 \pm 0.13_{\text{stat}} \pm 0.03_{\text{syst}}$ , of BABAR [175],  $\alpha_{CP} = -0.044 \pm 0.076 \pm 0.082$ , and of BELLE [173],  $\alpha_{CP} = -0.022 \pm 0.048 \pm 0.017$ . The preliminary measurement of BELLE is the best by far, based on  $65.4 \times 10^6 B$  meson pairs and implies that, at 90% confidence level,  $\alpha_{CP}$  in the exclusive  $B \rightarrow K^*\gamma$  lies between  $-0.106 < \alpha_{CP} < +0.062$ .

Theoretical NLL QCD predictions of the *normalized* CP asymmetries of the inclusive channels (see [82,162]) within the SM can be expressed by the approximate formulae [169]

---

<sup>4</sup>There is a sign convention that is generally adopted in theory and experiment: on the partonic level  $\alpha_{CP}(b \rightarrow s\gamma) = (\Gamma(b \rightarrow s\gamma) - \Gamma(\bar{b} \rightarrow \bar{s}\gamma))/(\Gamma(b \rightarrow s\gamma) + \Gamma(\bar{b} \rightarrow \bar{s}\gamma))$ ; analogously  $\alpha_{CP} \sim (\Gamma(\bar{B}^0 \rightarrow \dots) - \Gamma(B^0 \rightarrow \dots))/(\Gamma(\bar{B}^0 \rightarrow \dots) + \Gamma(B^0 \rightarrow \dots))$  and  $\alpha_{CP} \sim (\Gamma(B^- \rightarrow \dots) - \Gamma(B^+ \rightarrow \dots))/(\Gamma(B^- \rightarrow \dots) + \Gamma(B^+ \rightarrow \dots))$ .

$$\begin{aligned}\alpha_{CP}(B \rightarrow X_s \gamma) &\approx 0.334 \times \text{Im}[\epsilon_s] \approx +0.6\%, \\ \alpha_{CP}(B \rightarrow X_d \gamma) &\approx 0.334 \times \text{Im}[\epsilon_d] \approx -16\%\end{aligned}\quad (\text{IX.3})$$

where

$$\epsilon_s = \frac{V_{us}^* V_{ub}}{V_{ts}^* V_{tb}} \simeq -\lambda^2(\rho - i\eta), \quad \epsilon_d = \frac{V_{ud}^* V_{ub}}{V_{td}^* V_{tb}} \simeq \frac{\rho - i\eta}{1 - \rho + i\eta}. \quad (\text{IX.4})$$

Numerically, the best-fit values of the CKM parameters are used [169]. The two CP asymmetries are connected by the relative factor  $\lambda^2((1 - \rho)^2 + \eta^2)$ . Moreover, the small SM prediction for the CP asymmetry in the decay  $B \rightarrow X_s \gamma$  is a result of three suppression factors. There is an  $\alpha_s$  factor needed in order to have a strong phase; moreover, there is a CKM suppression of order  $\lambda^2$  and there is a GIM suppression of order  $(m_c/m_b)^2$  reflecting the fact that in the limit  $m_c = m_u$  any CP asymmetry in the SM would vanish.

An analysis for the leptonic counterparts is presented in [170]. The normalized CP asymmetries may also be calculated for exclusive decays: a model calculation may be found in [171]. Theoretical predictions based on the QCD factorization approach [166,165,164] are also affected by large uncertainties. Only in the case of relatively large new physics effects will one be able to disentangle these effects from the QCD uncertainties. But the available experimental data do not support this scenario in the  $B \rightarrow K^* \gamma$  mode [174,175,173].

Supersymmetric predictions for the CP asymmetries in  $B \rightarrow X_{s/d} \gamma$  depend strongly on what is assumed for the supersymmetry-breaking sector and are, thus, a rather model-dependent issue. The minimal supergravity model cannot account for large CP asymmetries beyond 2% because of the constraints coming from the electron and neutron electric dipole moments [176]. This is generally true in models based on the MFV assumption (see also fig. 34). Non-minimal models with squark mixing or models with R-parity violation allow for larger asymmetries, of the order of 10% or even larger [178,162]. In [162] it is argued that the asymmetry in case of non-minimal models could be even larger than  $\pm 15\%$  if the gluino mass is significantly lighter than the squark masses. Recent studies of the  $B \rightarrow X_d \gamma$  rate asymmetry in specific models led to asymmetries between  $-40\%$  and  $+40\%$  [180] and  $-45\%$  and  $+21\%$  [179]. In general, CP asymmetries may lead to clean evidence for new physics by a significant deviation from the SM prediction.

From (IX.3), it is obvious that a large CP asymmetry in the  $B \rightarrow X_s \gamma$  channel or a positive CP asymmetry in the inclusive  $B \rightarrow X_d \gamma$  channel would be a clear signal for new physics.

The exclusive and inclusive decays of the form  $b \rightarrow s\gamma$  and  $b \rightarrow d\gamma$ , as well as their leptonic counterparts, provide a stringent test, if the CKM matrix is indeed the only source of CP violation. Using U-spin, which is the  $SU(2)$  subgroup of flavour  $SU(3)$  relating the  $s$  and the  $d$  quark and which is already a well-known tool in the context of non-leptonic decays [182,183], one derives relations between the CP asymmetries of the exclusive channels  $B^- \rightarrow K^{*-} \gamma$  and  $B^- \rightarrow \rho^- \gamma$  and of the inclusive channels  $B \rightarrow X_s \gamma$  and  $B \rightarrow X_d \gamma$ .

Any CP violation in the SM has to be proportional to

$$C = i J (m_u - m_c)(m_u - m_t)(m_c - m_t)(m_d - m_s)(m_d - m_b)(m_s - m_b), \quad (\text{IX.5})$$

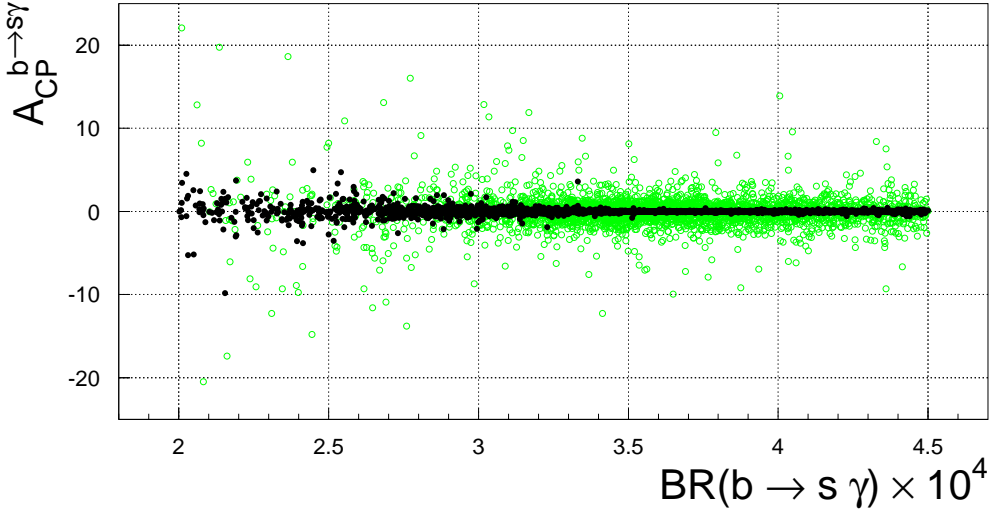


FIG. 34.  $CP$  asymmetry vs ‘total’ width of the decay  $B \rightarrow X_s \gamma$ . The empty circles are computed without any restriction on the phases. The filled black ones show the impact of the EDM’s constraints; from [177].

where  $J = \text{Im}[V_{ub}V_{cb}^*V_{cs}V_{us}^*]$  is the Jarlskog parameter. Therefore, one should make use of the U-spin symmetry only with respect to the strong interactions. Defining the rate asymmetries (not the *normalized*  $CP$  asymmetries) by

$$\Delta\Gamma(B^- \rightarrow V^- \gamma) = \Gamma(B^- \rightarrow V^- \gamma) - \Gamma(B^+ \rightarrow V^+ \gamma) \quad (\text{IX.6})$$

one arrives at the following relation [181]:

$$\Delta\Gamma(B^- \rightarrow K^{*-} \gamma) + \Delta\Gamma(B^- \rightarrow \rho^- \gamma) = b_{exc}\Delta_{exc}, \quad (\text{IX.7})$$

where the right-hand side is written as a product of a relative U-spin breaking  $b_{exc}$  and a typical size  $\Delta_{exc}$  of the  $CP$  violating rate difference. This is a direct consequence of the unitarity of the CKM matrix and, thus, of the fact that the Jarlskog parameter is the only fourth-order quantity that is invariant under rephasing of the quark fields within the SM. The resulting relation between  $b \rightarrow s$  and  $b \rightarrow d$  rate asymmetries due to

$$J = \text{Im}(\lambda_u^{(s)}\lambda_c^{(s)*}) = -\text{Im}(\lambda_u^{(d)}\lambda_c^{(d)*}) \quad (\text{IX.8})$$

was first noticed in [163].

In [181] the SM prediction for the difference of branching ratios, based on model results in [171] and on a sum rule calculation of the form factors [184], was derived:

$$|\Delta\mathcal{B}(B^- \rightarrow K^{*-} \gamma) + \Delta\mathcal{B}(B^- \rightarrow \rho^- \gamma)| \sim 4 \times 10^{-8}. \quad (\text{IX.9})$$

Note that the right-hand side is model-dependent. The U-spin-breaking effects were also estimated in the QCD factorization approach [164]. Within this approach, it was shown

that the U-spin-breaking effect essentially scales with the differences of the two form factors ( $F_{K^*} - F_\rho$ ). Using the form factors from the QCD sum rule calculation in [167] and maximizing the CP asymmetries by a specific choice of the CKM angle  $\gamma$ , the authors of [164] obtain

$$\Delta\mathcal{B}(B^- \rightarrow K^{*-}\gamma) + \Delta\mathcal{B}(B^- \rightarrow \rho^-\gamma) \sim -3 \times 10^{-7}, \quad (\text{IX.10})$$

while for the separate asymmetries they obtain,  $\Delta\mathcal{B}(B \rightarrow K^*\gamma) = -7 \times 10^{-7}$  and  $\Delta\mathcal{B}(B \rightarrow \rho\gamma) = 4 \times 10^{-7}$ , which explicitly shows the limitations of the relation (IX.7) as a test of the SM.

The issue is much more attractive in the inclusive modes. Because of the heavy mass expansion for the inclusive process, the leading contribution is the free  $b$ -quark decay. In particular, there is no sensitivity to the spectator quark and thus one arrives, within the partonic contribution, at the following relation for the CP rate asymmetries as the consequence of the CKM unitarity [163]:

$$\Delta\Gamma(B \rightarrow X_s\gamma) + \Delta\Gamma(B \rightarrow X_d\gamma) = b_{inc}\Delta_{inc}. \quad (\text{IX.11})$$

In this framework one relies on parton–hadron duality. So one can actually compute the breaking of U-spin by keeping a non-vanishing strange quark mass. The typical size of  $b_{inc}$  can be roughly estimated to be of the order of  $|b_{inc}| \sim m_s^2/m_b^2 \sim 5 \times 10^{-4}$ ;  $|\Delta_{inc}|$  is again the average of the moduli of the two CP rate asymmetries. These have been calculated (for vanishing strange quark mass), e.g. in [82], and one arrives at the following estimate within the partonic contribution [181]:

$$|\Delta\mathcal{B}(B \rightarrow X_s\gamma) + \Delta\mathcal{B}(B \rightarrow X_d\gamma)| \sim 1 \times 10^{-9}. \quad (\text{IX.12})$$

Going beyond the leading partonic contribution one has to check if the large suppression factor from the U-spin breaking is still effective in addition to the natural suppression factors already present in the corresponding branching ratios. This question was addressed in [168]. In the leading  $1/m_b^2$  corrections, the U-spin-breaking effects also induce an additional overall factor  $m_s^2/m_b^2$ . In the non-perturbative corrections from the charm quark loop, which scale with  $1/m_c^2$ , one finds again the same overall suppression factor, because the operator  $\tilde{\mathcal{O}}$  (see VI.27) does not contain any information on the strange mass. The corresponding long-distance contributions from up-quark loops, which scale with  $\Lambda_{QCD}/m_b$  (see section VI), follow the same pattern [168]. Thus, in the inclusive mode, the right-hand side in (IX.12) can be computed in a model-independent way with the help of the heavy mass expansion.

Therefore, the prediction (IX.12) provides a very clean SM test, whether generic new CP phases are active or not. Any significant deviation from the estimate (IX.12) would be a direct hint to non-CKM contributions to CP violation.

From the theoretical point of view the *sum* of the CP asymmetries in the inclusive  $b \rightarrow s$  and  $b \rightarrow d$  transitions turns out to be the favourable observable. This might be true also from the experimental point of view.

## X. FURTHER OPPORTUNITIES

Generally, *exclusive* decay modes have large uncertainties due to the hadronic form factors and it might thus be rather difficult to disentangle possible new physics contributions from hadronic uncertainties in these modes — at least in the absence of very large new effects. Therefore exclusive modes often can be used as QCD tests only. However, there are exceptions to this rule. In specific ratios like CP asymmetries, hadronic uncertainties are reduced and large new physics effects might be detectable. There are also exclusive modes that are as clean as inclusive modes because the corresponding hadronic matrix elements can be determined from experiment. The most important examples among them are the exclusive  $B$  decay  $B_s \rightarrow \mu^+ \mu^-$  and the exclusive rare kaon decays  $K_L \rightarrow \pi^0 \nu \bar{\nu}$  and  $K^+ \rightarrow \pi^+ \nu \bar{\nu}$ . The hadronic matrix elements of these FCNC (rare) processes can be related to well-known non-rare semi-leptonic decays.

As the inclusive decay  $B \rightarrow X_s \nu \bar{\nu}$  (see section V), the exclusive decay  $B_s \rightarrow \mu^+ \mu^-$  is completely dominated by the top-quark contribution due to the hard GIM mechanism. QCD corrections within this exclusive mode are already calculated to NLL order. The remaining perturbative uncertainty is not larger than  $\pm 1\%$  [88]. The corresponding hadronic matrix element leads to the decay constant of the  $B_s$  meson,  $f_{B_s}$ , which can be determined on the lattice. The related uncertainty represents the largest part of the theoretical error:  $f_{B_s} = (238 \pm 31) \text{ MeV}$  [21]. The SM prediction for the branching ratio of the decay  $B_s \rightarrow \mu^+ \mu^-$  is of order  $10^{-9}$ . Thus, this decay will be accessible at LHC and also at  $B\text{TeV}$ . However, the branching ratio can be much larger within specific extensions of the SM. For example, the helicity-suppression of the SM contribution leads to an enhanced sensitivity to the Higgs-mediated scalar FCNCs within the 2HDM and, especially within the MSSM. These non-standard contributions lead to a drastic enhancement in the large  $\tan \beta$ -limit [185]. Therefore, this decay might be even detectable at FERMILAB before the LHC experiments and the  $B\text{TeV}$  experiment start to take data (see [186] for further discussions).

The other two important examples of theoretically clean *exclusive* modes,  $K_L \rightarrow \pi^0 \nu \bar{\nu}$  and  $K^+ \rightarrow \pi^+ \nu \bar{\nu}$ , are discussed in more detail in the following section.

### A. $K_L \rightarrow \pi^0 \nu \bar{\nu}$ and $K^+ \rightarrow \pi^+ \nu \bar{\nu}$

The rare decays  $K_L \rightarrow \pi^0 \nu \bar{\nu}$  and  $K^+ \rightarrow \pi^+ \nu \bar{\nu}$  represent complementary opportunities for precision flavour physics. They are also FCNC processes induced at the one-loop level via  $Z^0$  penguin and box diagrams (see fig. 35) and are exceptionally clean processes.

As in the inclusive decay  $B \rightarrow X_s \nu \bar{\nu}$  (see section V), the hard GIM mechanism is active: the short-distance top- and charm-contributions dominate the long-distance up-quark contribution within the charged mode  $K^+ \rightarrow \pi^+ \nu \bar{\nu}$ . The CKM factors of the charm contribution compensates the hard GIM suppression relative to the top contribution in this specific case. The short-distance amplitude is then governed by one single semi-leptonic operator, namely  $(\bar{s} \gamma_\mu P_L d)(\bar{\nu} \gamma_\mu P_L \nu)$ . Its hadronic matrix element can be determined experimentally by the semi-leptonic kaon decay. In fact, the matrix element  $\langle \pi^+ | \bar{s} \gamma_\mu P_L d | K^+ \rangle$  can be related by isospin symmetry to the matrix element  $\sqrt{2} \langle \pi^0 | \bar{s} \gamma_\mu P_L u | K^+ \rangle$  of the semi-leptonic decay

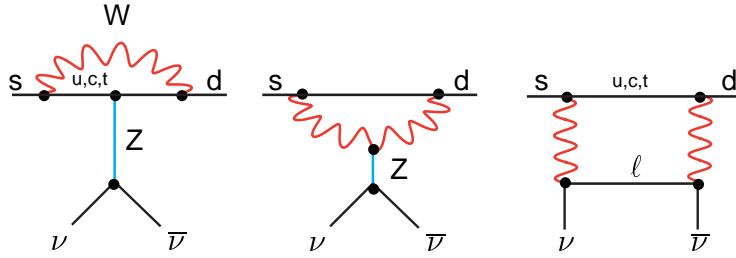


FIG. 35. One-loop diagrams contributing to  $K \rightarrow \pi \nu \bar{\nu}$ .

$K^+ \rightarrow \pi^0 e^+ \nu$ . The corresponding Wilson coefficient is already calculated to NLL QCD [88] and the scale dependence is reduced to 5% in the charged kaon mode.

The situation is even more favourable in the neutral mode, which is dominated by the CP-violating part. There is no relative CKM enhancement of the charm contribution and, thus, the amplitude is completely dominated by the top contribution as in the inclusive rare  $B \rightarrow X_s \bar{\nu} \nu$  decay. The NLL QCD calculation therefore leads to a 1% scale uncertainty only [88].

The validity of the OPE and the renormalization-group-improved perturbation theory in the charm contribution to the charged mode has been critically analysed: the separate scale dependence within the charm contribution of 13% at NLL QCD is consistent with partial NNLL results [195]. Moreover, subleading power corrections within the OPE of order  $m_K^2/m_c^2$  — which might lead to 15% correction — are estimated to be at the level of 5%. However, for a reliable determination of the latter corrections, a lattice calculation of the corresponding hadronic matrix elements will be indispensable [196].

The latest numerical SM predictions are [206,194]

$$\begin{aligned} \mathcal{B}(K^+ \rightarrow \pi^+ \nu \bar{\nu}) &= (7.2 \pm 2.1) \times 10^{-11} \\ \mathcal{B}(K_L \rightarrow \pi^0 \nu \bar{\nu}) &= (2.8 \pm 1.1) \times 10^{-11} \end{aligned} \quad (\text{X.1})$$

The uncertainties of the present SM predictions are dominated by the current errors of the CKM parameters, while the intrinsic error in the charged mode is about 6% (mainly from the charm contribution) and in the neutral mode about 2% only. This implies the important role of these decay modes for CKM phenomenology: they play a unique role among  $K$  decays, as does the  $B_d \rightarrow \psi K_S$  mode among  $B$  decays. The measurements of the two kaon decay modes allow for a measurement of the angle  $\beta$  of the unitarity triangle to a precision comparable to that obtained with the  $B_d \rightarrow \psi K_S$  mode before the LHC era [188]. The only necessary theoretical input is the internal charm contribution to  $K^+ \rightarrow \pi^+ \nu \bar{\nu}$ , which introduces some theoretical uncertainty (see above).

The relation  $(\sin 2\beta)_{\pi \nu \bar{\nu}} = (\sin 2\beta)_{\psi K_S}$  implies a very interesting connection between rare  $K$  decays and  $B$  physics, which must be satisfied in the SM:

$$(\sin 2\beta)_{\pi \nu \bar{\nu}} = (\sin 2\beta)_{\psi K_S} = -A_{CP}(\psi K_S) \frac{1 + x_d^2}{x_d}. \quad (\text{X.2})$$

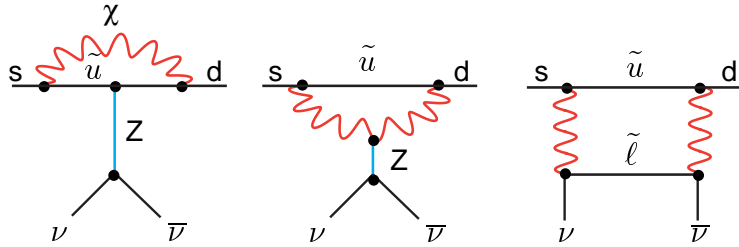


FIG. 36. Supersymmetric contributions to  $K \rightarrow \pi \nu \bar{\nu}$ .

$A_{CP}(\psi K_S)$  denotes the time-integrated CP-violating asymmetry in  $B_d^0 \rightarrow \psi K_S$  and  $x_d = \Delta m/\Gamma$  gives the size of  $B_d^0 - \bar{B}_d^0$  mixing. As was stressed in [188], besides the internal charm contribution to the charged kaon mode, all quantities in (X.2) can be directly measured experimentally, and their relation is almost independent of  $V_{cb}$ .

Besides their rich CKM phenomenology, the decays  $K_L \rightarrow \pi^0 \nu \bar{\nu}$  and  $K^+ \rightarrow \pi^+ \nu \bar{\nu}$  as loop-induced processes are very sensitive to new physics beyond the SM. In addition, the theoretical information is very clean and the measurement of these decays thus leads to very accurate constraints on any new physics model. Moreover, there is the possibility that these clean rare decay modes themselves lead to first evidence of new physics when the measured decay rates are not compatible with the SM.

New physics contributions in  $K_L \rightarrow \pi^0 \nu \bar{\nu}$  and  $K^+ \rightarrow \pi^+ \nu \bar{\nu}$  can be parametrized in a model-independent way by two parameters that quantify the violation of the relation (X.2) [189,190]. New effects in supersymmetric models can be induced through new box- and penguin-diagram contributions which involve new particles such as charged Higgs or charginos and stops (fig. 36) that replace the  $W$  boson and the up-type quark of the SM (fig. 35).

Under the simplifying MFV assumption [206] (see section VIII A), the relation (X.2) is valid. Thus, the measurements of  $\mathcal{B}(K_L \rightarrow \pi^0 \nu \bar{\nu})$  and  $\mathcal{B}(K^+ \rightarrow \pi^+ \nu \bar{\nu})$  still directly determine the angle  $\beta$ , and a significant violation of the relation (X.2) would rule out this assumption.

For the present experimental status of supersymmetry, however, a model-independent analysis that includes also a general flavour change through the squark mass matrices is more suitable. If the new sources of flavour change are parametrized by the mass-insertion approximation, an expansion of the squark mass matrices around their diagonal, it turns out that SUSY contributions in this more general setting of the unconstrained MSSM allow for a significant violation of the relation (X.2). An enhancement of the branching ratios by an order of magnitude (in the case of  $K^+ \rightarrow \pi^+ \nu \bar{\nu}$  by a factor 3) with respect to the SM values is possible, mostly thanks to the chargino-induced Z-penguin contribution [191]. Recent analyses [191–193] within the uMSSM focused on the correlation of rare decays and  $\epsilon'/\epsilon$ , and led to reasonable upper bounds for the branching ratios:  $\mathcal{B}(K_L \rightarrow \pi^0 \nu \bar{\nu}) \leq 1.2 \times 10^{-10}$  and  $\mathcal{B}(K^+ \rightarrow \pi^+ \nu \bar{\nu}) \leq 1.7 \times 10^{-10}$ , which should be compared with the latest numerical SM predictions (X.1).

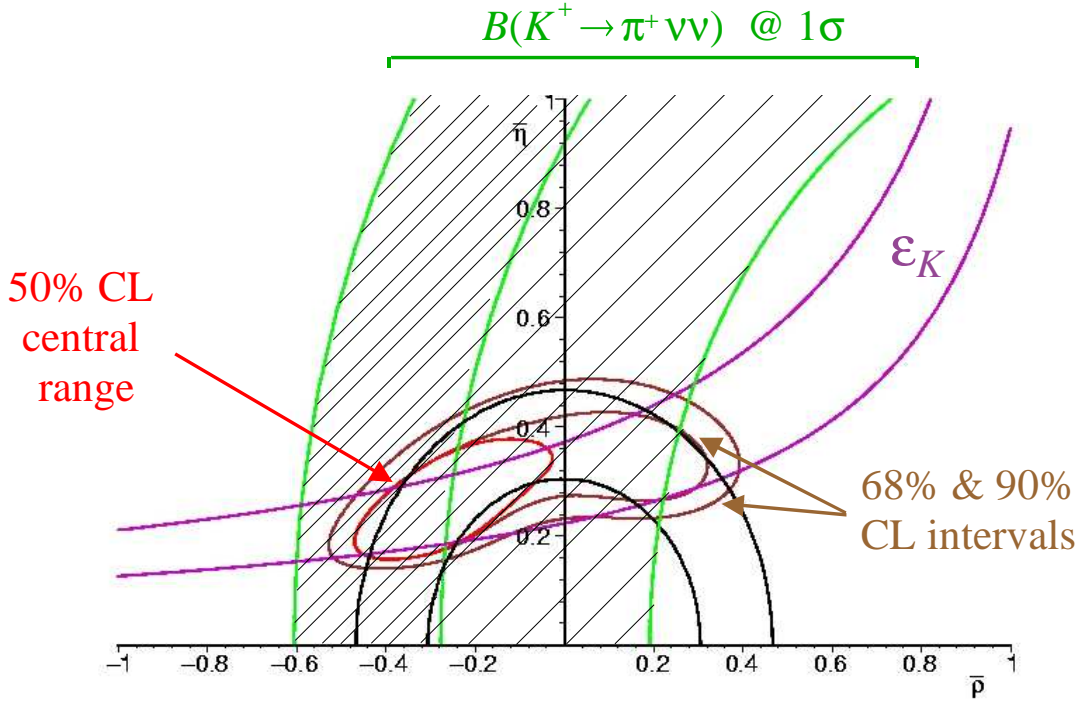


FIG. 37. Allowed region in the  $\bar{\rho}$ - $\bar{\eta}$  plane with the inclusion of the latest  $K^+ \rightarrow \pi^+ \nu \bar{\nu}$  and without  $B_{s,d}$  data. The two external contours denote 68% and 90% confidence intervals; the inner one is the 68% confidence interval *under the assumption* that the experimental error in the present measurement is reduced by a factor 2, from [206].

The rare decays  $K^+ \rightarrow \pi^+ \nu \bar{\nu}$  and  $K_L \rightarrow \pi^0 \nu \bar{\nu}$  are specifically interesting in view of the suggested experiments at the Brookhaven National Laboratory (USA) ([201], [204]) and at FERMILAB ([202]), and at KEK ([203]) (see [205] for a review).

For the neutral  $K_L \rightarrow \pi^0 \nu \bar{\nu}$  mode, the experimental situation is not satisfactory yet; there is only an upper bound available from KTeV [199]:

$$\mathcal{B}(K_L \rightarrow \pi^0 \nu \bar{\nu}) < 5.9 \times 10^{-7}, \quad (\text{X.3})$$

which is four orders of magnitude above the SM expectation. An indirect upper bound on  $\mathcal{B}(K_L \rightarrow \pi^0 \nu \bar{\nu})$ , using the current limit on  $\mathcal{B}(K^+ \rightarrow \pi^+ \nu \bar{\nu})$  and isospin symmetry, can be placed at  $2.6 \times 10^{-9}$  [200]. Future prospects are given by the E391a experiment at KEK with a sensitivity of  $3 \times 10^{-10}$  (possible start 2003) [203] and the E926 experiment (KOPIO) at Brookhaven which aims at a sensitivity of  $10^{-13}$  [204].

For the charged  $K^+ \rightarrow \pi^+ \nu \bar{\nu}$  mode, the experimental situation is more favourable. The current Brookhaven experiment E787 has, to date, observed two clean candidate events for  $K^+ \rightarrow \pi^+ \nu \bar{\nu}$ . The combined analysis including previous data [197] leads to the following branching ratio [198]:

$$\mathcal{B}(K^+ \rightarrow \pi^+ \nu \bar{\nu}) = (1.57^{+1.75}_{-0.82}) \times 10^{-10}. \quad (\text{X.4})$$

The central value is more than twice the central value of the theoretical SM prediction, but the present measurement is still compatible with it, in view of the large error bars on the experimental side. Fig. 37 illustrates the possible future impact of more precise measurements — to be expected from the Brookhaven experiment E949 with a sensitivity of  $10^{-11}/\text{event}$  (started 2001) [201] and from the future high-precision CKM experiment at FERMILAB with yet an order of magnitude higher sensitivity (starting 2007) [202]. If the present central value is confirmed with a smaller error, this will clearly indicate a new-physics contribution either in  $B\bar{B}$  mixing or in the  $K^+ \rightarrow \pi^+ \nu \bar{\nu}$  mode [206].

## XI. SUMMARY

In this paper we have reviewed the status of inclusive rare  $B$  decays, highlighting recent developments. These decays give special insight into the CKM matrix; moreover, as FCNC processes, they are loop-induced and therefore particularly sensitive to new physics.

Decay modes such as  $B \rightarrow X_s \gamma$ ,  $B \rightarrow X_s \nu \bar{\nu}$  and  $B \rightarrow X_s \ell^+ \ell^-$  (with specific kinematic cuts) are dominated by the partonic (perturbative) contributions and are, thus, theoretically very clean in contrast to the corresponding exclusive decay modes and represent laboratories to search for new physics. Non-perturbative contributions play a subdominant role and they are under control thanks to the heavy mass expansion. The inclusive rare  $B$  decays are or will be accessible at the present  $e^+ e^-$  machines (CLEO, BABAR, BELLE), with their low background and their kinematic constraints, and will make precision flavour physics possible in the near future.

Significant theoretical progress has been made during the last years. Calculations of NLL (or even NNLL) QCD corrections to these decay modes have been performed. The theoretical uncertainty has been significantly reduced. As was emphasized, the step from LL to NLL precision within the framework of the renormalization-group-improved perturbation theory is not only a quantitative, but also a qualitative one, which tests the validity of the perturbative approach in a given problem.

Within the theoretical prediction of  $B \rightarrow X_s \gamma$ , the charm mass renormalization scheme ambiguity at NLL order represents the largest uncertainty. In view of the precise experimental data coming up from the  $B$  factories in the near future, this uncertainty should be removed.

Inclusive rare  $B$  decays allow for an indirect search for new physics, a strategy complementary to the direct production of new (supersymmetric) particles, which is reserved for the planned hadronic machines such as the LHC at CERN. But the indirect search at the  $B$  factories already implies significant restrictions for the parameter space of supersymmetric models and, thus, leads to important theoretically clean information for the direct search of supersymmetric particles.

It is even possible that these rare processes give first evidence of new physics outside the neutrino sector by a significant deviation from the SM prediction. But also in the long run, after new physics has already been discovered, inclusive rare  $B$  decays will play an important role in analysing in greater detail the underlying new dynamics.

Within supersymmetric models, the QCD calculation of the inclusive rare  $B$  decays has not reached the sophistication of the corresponding SM calculations. Nevertheless, NLL analyses in specific scenarios already show that bounds on the parameter space of non-standard models are rather sensitive to NLL QCD contributions.

Detailed measurements of CP asymmetries in rare  $B$  decays will also be possible in the near future. They will allow for a stringent and clean test if the CKM matrix is indeed the only source of CP violation. Moreover, a measurement of the photon polarization within the rare  $B$  decays will be possible in order to check the SM prediction of a left-handed photon.

The rare kaon decays,  $K^+ \rightarrow \pi^+ \nu \bar{\nu}$  and  $K_L \rightarrow \pi^0 \nu \bar{\nu}$ , offer complementary opportunities for precision flavour physics. Besides the current Brookhaven experiment, several more are planned or suggested to explore these theoretically clean decay modes.

## ACKNOWLEDGEMENTS

I thank Colin Jessop for many helpful discussions on the experimental aspects of inclusive rare  $B$  decays and Ed Thorndike for useful comments. I am very grateful to Mikolaj Misiak for his careful reading of the manuscript and for useful comments. Discussions with Thomas Besmer, Francesca Borzumati, Giancarlo D'Ambrosio, Paolo Gambino, Adrian Ghinculov, Christoph Greub, Thomas Mannel, Gino Isidori, Daniel Wyler and York-Peng Yao are also gratefully acknowledged.

## REFERENCES

- [1] K. Hagiwara *et al.* [Particle Data Group Collaboration], “Review of Particle Physics,” Phys. Rev. D **66** (2002) 010001.
- [2] CLEO collaboration: <http://www.lns.cornell.edu/public/CLEO/>
- [3] BABAR collaboration: <http://www.slac.stanford.edu/BFROOT/>
- [4] BELLE collaboration: <http://belle.kek.jp/>
- [5] K. Anikeev *et al.*, “B physics at the Tevatron: Run II and beyond,” hep-ph/0201071.
- [6] P. Ball *et al.*, “B decays at the LHC,” hep-ph/0003238.
- [7] J. c. Wang [BTeV collaboration], “The BTeV experiment at the Tevatron collider,” hep-ex/0207009.
- [8] K. Abe *et al.* [Belle Collaboration], “An improved measurement of mixing-induced CP violation in the neutral B meson system,” hep-ex/0208025.
- [9] B. Aubert *et al.* [BABAR Collaboration], “Measurement of the CP-violating asymmetry amplitude  $\sin 2\beta$ ,” hep-ex/0207042.
- [10] T. Hurth *et al.*, “Present and future CP measurements,” J. Phys. G **G27**, 1277 (2001) [hep-ph/0102159].
- [11] J. R. Ellis, M. K. Gaillard, D. V. Nanopoulos and S. Rudaz, “The phenomenology of the next left-handed quarks,” Nucl. Phys. B **131**, 285 (1977) [Erratum-ibid. B **132**, 541 (1978)].
- [12] R. Ammar *et al.* [CLEO Collaboration], “Evidence for penguins: First observation of  $B \rightarrow K^*(892)\gamma$ ,” Phys. Rev. Lett. **71**, 674 (1993).
- [13] M. Carena, D. Garcia, U. Nierste and C. E. Wagner, “ $b \rightarrow s\gamma$  and supersymmetry with large  $\tan(\beta)$ ,” Phys. Lett. B **499**, 141 (2001) [hep-ph/0010003].
- [14] G. Degrassi, P. Gambino and G. F. Giudice, “ $B \rightarrow X_s\gamma$  in supersymmetry: Large contributions beyond the leading order,” JHEP **0012**, 009 (2000) [hep-ph/0009337].
- [15] F. Borzumati, C. Greub, T. Hurth and D. Wyler, “Gluino contribution to radiative B decays: Organization of QCD corrections and leading order results,” Phys. Rev. D **62**, 075005 (2000) [hep-ph/9911245]; “Gluino-mediated rare B decays,” Nucl. Phys. Proc. Suppl. **86**, 503 (2000) [hep-ph/9911304].
- [16] T. Besmer, C. Greub and T. Hurth, “Bounds on flavour violating parameters in supersymmetry,” Nucl. Phys. B **609** (2001) 359 [hep-ph/0105292]; “A new model-independent analysis of  $B \rightarrow X_s\gamma$  in supersymmetry,” hep-ph/0111389.
- [17] T. Hurth, “Inclusive rare B decays,” in *Proc. 5th Int. Symposium on Radiative Corrections (RADCOR 2000)* ed. H.E. Haber, hep-ph/0106050.
- [18] A. Ali, G. F. Giudice and T. Mannel, “Towards a model independent analysis of rare B decays,” Z. Phys. C **67** (1995) 417 [hep-ph/9408213];  
J. L. Hewett, “ $\tau$  polarization asymmetry in  $B \rightarrow X_s\tau^+\tau^-$ ,” Phys. Rev. D **53** (1996) 4964 [hep-ph/9506289];  
F. Kruger and L. M. Sehgal, “Lepton Polarization in the Decays  $B \rightarrow X_s\mu^+\mu^-$  and  $B \rightarrow X_s\tau^+\tau^-$ ,” Phys. Lett. B **380**, 199 (1996) [hep-ph/9603237].
- [19] G. W. Bennett *et al.* [Muon g-2 Collaboration], “Measurement of the positive muon anomalous magnetic moment to 0.7 ppm,” Phys. Rev. Lett. **89**, 101804 (2002) [Erratum-ibid. **89**, 129903 (2002)] [hep-ex/0208001].
- [20] E. de Rafael, “The muon g-2 revisited,” hep-ph/0208251.

- [21] L. Lellouch, “Phenomenology from lattice QCD,” hep-ph/0211359;
- L. Lellouch and M. Luscher, “Weak transition matrix elements from finite-volume correlation functions,” *Commun. Math. Phys.* **219**, 31 (2001) [hep-lat/0003023];
- L. Lellouch, “Light hadron weak matrix elements,” *Nucl. Phys. Proc. Suppl.* **94**, 142 (2001) [hep-lat/0011088];
- C. Bernard, “Heavy quark physics on the lattice,” *Nucl. Phys. Proc. Suppl.* **94**, 159 (2001) [hep-lat/0011064];
- C. T. Sachrajda, “Lattice  $B$  physics,” *Nucl. Instrum. Meth. A* **462**, 23 (2001) [hep-lat/0101003].
- [22] J. D. Bjorken, “Topics In  $B$  Physics,” *Nucl. Phys. Proc. Suppl.* **11**, 325 (1989);
- M. J. Dugan and B. Grinstein, “QCD basis for factorization in decays of heavy mesons,” *Phys. Lett. B* **255**, 583 (1991);
- H. D. Politzer and M. B. Wise, “Perturbative corrections to factorization in  $\bar{B}$  decay,” *Phys. Lett. B* **257**, 399 (1991).
- [23] M. Beneke, G. Buchalla, M. Neubert and C. T. Sachrajda, “QCD factorization for exclusive, non-leptonic  $B$  meson decays: General arguments and the case of heavy-light final states,” *Nucl. Phys. B* **591**, 313 (2000) [hep-ph/0006124];
- C. W. Bauer, D. Pirjol and I. W. Stewart, “A proof of factorization for  $B \rightarrow D\pi$ ,” *Phys. Rev. Lett.* **87**, 201806 (2001) [hep-ph/0107002].
- [24] Y. Y. Keum, H. N. Li and A. I. Sanda, “Penguin enhancement and  $B \rightarrow K\pi$  decays in perturbative QCD,” *Phys. Rev. D* **63**, 054008 (2001) [hep-ph/0004173];
- Y. Y. Keum and A. I. Sanda, “Possible large direct CP violations in charmless  $B$  decays,” hep-ph/0209014.
- [25] M. Beneke, G. Buchalla, M. Neubert and C. T. Sachrajda, “QCD factorization in  $B \rightarrow \pi K, \pi\pi$  decays and extraction of Wolfenstein parameters,” hep-ph/0104110;
- M. Ciuchini, E. Franco, G. Martinelli, M. Pierini and L. Silvestrini, “Charming penguins strike back,” hep-ph/0104126.
- [26] M. Beneke, A. P. Chapovsky, M. Diehl and T. Feldmann, “Soft-collinear effective theory and heavy-to-light currents beyond leading power,” hep-ph/0206152.
- [27] J. Gasser, “Chiral perturbation theory,” hep-ph/9912548;
- G. Colangelo and G. Isidori, “An introduction to CHPT,” hep-ph/0101264.
- [28] P. Colangelo and A. Khodjamirian, “QCD sum rules: A modern perspective,” hep-ph/0010175;
- M. Shifman, “Snapshots of hadrons or the story of how the vacuum medium determines the properties of the classical mesons which are produced, live and die in the QCD vacuum,” *Prog. Theor. Phys. Suppl.* **131**, 1 (1998) [hep-ph/9802214];
- V. M. Braun, “Light-cone sum rules,” hep-ph/9801222;
- A. Khodjamirian and R. Rückl, “QCD sum rules for exclusive decays of heavy mesons,” hep-ph/9801443;
- [29] N. Isgur and M. B. Wise, “Weak decays of heavy mesons in the static quark approximation,” *Phys. Lett. B* **232**, 113 (1989);
- “Weak transition form factors between heavy mesons,” *Phys. Lett. B* **237**, 527 (1990).
- M. Neubert, “Heavy quark symmetry,” *Phys. Rept.* **245** (1994) 259.
- [30] A. V. Manohar, “Large  $N$  QCD,” hep-ph/9802419;
- E. De Rafael, “Large- $N(c)$  QCD and low energy interactions,” *AIP Conf. Proc.* **602**,

14 (2001) [hep-ph/0110195].

[31] Heavy Mass Expansion J. Chay, H. Georgi and B. Grinstein, “Lepton energy distributions in heavy meson decays from QCD,” *Phys. Lett. B* **247**, 399 (1990); I. I. Bigi, N. G. Uraltsev and A. I. Vainshtein, “Non-perturbative corrections to inclusive beauty and charm decays: QCD versus phenomenological models,” *Phys. Lett. B* **293**, 430 (1992) [Erratum-*ibid. B* **297**, 477 (1993)] [hep-ph/9207214]; I. I. Bigi, M. A. Shifman and N. Uraltsev, “Aspects of heavy quark theory,” *Ann. Rev. Nucl. Part. Sci.* **47**, 591 (1997) [hep-ph/9703290]; A. V. Manohar and M. B. Wise, “Heavy Quark Physics,” Cambridge Monogr. Part. Phys. Nucl. Phys. Cosmol. **10** (2000) 1.

[32] I. I. Bigi and N. Uraltsev, “A vademecum on quark hadron duality,” *Int. J. Mod. Phys. A* **16**, 5201 (2001) [hep-ph/0106346]; M. A. Shifman, “Quark-hadron duality,” hep-ph/0009131.

[33] Courtesy of A. Lenz.

[34] A. J. Buras, “Weak Hamiltonian, CP violation and rare decays,” hep-ph/9806471.

[35] A. Ali and C. Greub, “Inclusive photon energy spectrum in rare  $B$  decays,” *Z. Phys. C* **49**, 431 (1991); “Photon energy spectrum in  $B \rightarrow X_s \gamma$  and comparison with data,” *Phys. Lett. B* **361**, 146 (1995) [hep-ph/9506374].

[36] A. Ali and E. Pietarinen, “Semi-leptonic decays of heavy quarks in quantum chromodynamics,” *Nucl. Phys. B* **154**, 519 (1979).  
G. Altarelli, N. Cabibbo, G. Corbo, L. Maiani and G. Martinelli, “Leptonic decay of heavy flavors: A theoretical update,” *Nucl. Phys. B* **208**, 365 (1982);

[37] M. S. Alam *et al.* [CLEO Collaboration], “First measurement of the rate for the inclusive radiative penguin decay  $b \rightarrow s \gamma$ ,” *Phys. Rev. Lett.* **74**, 2885 (1995).

[38] S. Ahmed *et al.* [CLEO Collaboration], “ $b \rightarrow s \gamma$  branching fraction and CP asymmetry,” hep-ex/9908022.

[39] S. Chen *et al.* [CLEO Collaboration], “Branching fraction and photon energy spectrum for  $b \rightarrow s \gamma$ ,” *Phys. Rev. Lett.* **87**, 251807 (2001) [hep-ex/0108032].

[40] R. Barate *et al.* [ALEPH Collaboration], “A Measurement of the inclusive  $b \rightarrow s \gamma$  branching ratio,” *Phys. Lett. B* **429**, 169 (1998).

[41] K. Abe *et al.* [Belle Collaboration], “A measurement of the branching fraction for the inclusive  $B \rightarrow X_s \gamma$  decays with Belle,” *Phys. Lett. B* **511**, 151 (2001) [hep-ex/0103042].

[42] B. Aubert *et al.* [BABAR Collaboration], “Determination of the branching fraction for inclusive decays  $B \rightarrow X_s \gamma$ ,” hep-ex/0207076; B. Aubert *et al.* [BABAR Collaboration], “ $b \rightarrow s \gamma$  using a sum of exclusive modes,” hep-ex/0207074.

[43] K. Lingel, T. Skwarnicki and J. G. Smith, “Penguin decays of  $B$  mesons,” *Ann. Rev. Nucl. Part. Sci.* **48**, 253 (1998) [hep-ex/9804015].

[44] S. Stone, “ $B$  phenomenology,” hep-ph/0112008.

[45] E. H. Thorndike [Cleo collaboration], “Radiative  $B$  decays: An experimental overview,” hep-ex/0206067.

[46] A.L. Kagan and M. Neubert, “QCD anatomy of  $B \rightarrow X_s \gamma$  decays,” *Eur. Phys. J. C* **7**, 5 (1999) [hep-ph/9805303].

[47] I. I. Bigi, M. Shifman, N. G. Uraltsev and A. Vainshtein, “QCD predictions for lepton spectra in inclusive heavy flavor decays,” *Phys. Rev. Lett. B* **71**, 496 (1993) [hep-ph/9304225]; “On the motion of heavy quarks inside hadrons: Universal distributions

and inclusive decays," Int. J. Mod. Phys. **A9**, 2467 (1994) [hep-ph/9312359];  
 A. V. Manohar and M. B. Wise, "Inclusive semi-leptonic  $B$  and polarized  $\Lambda_b$  decays from QCD," Phys. Rev. D **49**, 1310 (1994) [hep-ph/9308246];  
 M. Neubert, "QCD based interpretation of the lepton spectrum in inclusive  $\bar{B} \rightarrow X_u \ell \bar{\nu}$  decays," Phys. Rev. D **49**, 3392 (1994) [hep-ph/9311325]; "Analysis of the photon spectrum in inclusive  $B \rightarrow X_s \gamma$  decays," Phys. Rev. D **49**, 4623 (1994) [hep-ph/9312311];  
 T. Mannel and M. Neubert, "Resummation of non-perturbative corrections to the lepton spectrum in inclusive  $B \rightarrow X \ell \bar{\nu}$  decays," Phys. Rev. D **50**, 2037 (1994) [hep-ph/9402288];  
 U. Aglietti and G. Ricciardi, "The structure function of semi-inclusive heavy flavour decays in field theory," Nucl. Phys. B **587**, 363 (2000) [hep-ph/0003146];  
 U. Aglietti, M. Ciuchini and P. Gambino, "A new model-independent way of extracting  $|V(ub)/V(cb)|$ ," Nucl. Phys. B **637**, 427 (2002) [hep-ph/0204140].

[48] A. Bornheim *et al.* [CLEO Collaboration], "Improved measurement of  $|V(ub)|$  with inclusive semileptonic  $B$  decays," Phys. Rev. Lett. **88**, 231803 (2002) [hep-ex/0202019].

[49] C. W. Bauer, M. Luke and T. Mannel, "Subleading shape functions in  $\bar{B} \rightarrow X_u \ell \bar{\nu}$  and the determination of  $|V(ub)|$ ," Phys. Lett. B **B43**, 261 (2002) [hep-ph/0205150];  
 A. K. Leibovich, Z. Ligeti and M. B. Wise, "Enhanced subleading structure functions in semileptonic  $B$  decay," Phys. Lett. B **539**, 242 (2002) [hep-ph/0205148].

[50] C. Jessop, "A world average for  $B \rightarrow X_s \gamma$ ," SLAC-PUB-9610.

[51] Z. Ligeti, M. E. Luke, A. V. Manohar and M. B. Wise, "The  $\bar{B} \rightarrow X_s \gamma$  photon spectrum," Phys. Rev. D **60**, 034019 (1999) [hep-ph/9903305].

[52] K. Abe *et al.* [BELLE Collaboration], "Observation of the decay  $B \rightarrow K \mu^+ \mu^-$ ," Phys. Rev. Lett. **88**, 021801 (2002) [hep-ex/0109026].

[53] Courtesy of C. Jossip.

[54] B. Aubert *et al.* [BABAR Collaboration], "Evidence for the flavor changing neutral current decays  $B \rightarrow K \ell^+ \ell^-$  and  $B \rightarrow K^* \ell^+ \ell^-$ ," hep-ex/0207082.

[55] J. Kaneko *et al.* [Belle Collaboration], "Measurement of the electroweak penguin process  $B \rightarrow X_s \ell^+ \ell^-$ ," hep-ex/0208029.

[56] K. Abe *et al.* [Belle Collaboration], "Evidence for the electroweak penguin decay  $B \rightarrow X_s \ell^+ \ell^-$ ," hep-ex/0107072.

[57] T. E. Coan *et al.* [CLEO Collaboration], "Study of exclusive radiative  $B$  meson decays," Phys. Rev. Lett. **84**, 5283 (2000) [hep-ex/9912057].

[58] Y. Ushiroda [Belle collaboration], "Radiative  $B$  meson decay," hep-ex/0104045.

[59] B. Aubert *et al.* [BABAR Collaboration], "Search for the exclusive radiative decays  $B \rightarrow \rho \gamma$  and  $B^0 \rightarrow \omega \gamma$ ," hep-ex/0207073.

[60] M. Misiak, "Status of theoretical  $\bar{B} \rightarrow X_s \gamma$  and  $B \rightarrow X_s \ell^+ \ell^-$  analyses," hep-ph/0009033; "Radiative  $B$  decay in the SM," hep-ph/0105312 and private communication.

[61] M. A. Shifman, A. I. Vainshtein and V. I. Zakharov, "On The Weak Radiative Decays (Effects Of Strong Interactions At Short Distances)," Phys. Rev. D **18**, 2583 (1978) [Erratum-ibid. D **19**, 2815 (1979)].

[62] B. Grinstein, R. P. Springer and M. B. Wise, "Effective Hamiltonian for weak radiative  $B$  meson decay," Phys. Lett. B **202**, 138 (1988);  
 B. Grinstein, M. J. Savage and M. B. Wise, " $B \rightarrow X_s e^+ e^-$  in the six quark model,"

Nucl. Phys. B **319**, 271 (1989).

- [63] M. Ciuchini, E. Franco, G. Martinelli, L. Reina and L. Silvestrini, “Scheme independence of the effective Hamiltonian for  $b \rightarrow s\gamma$  and  $b \rightarrow sg$  decays,” Phys. Lett. B **316**, 127 (1993) [hep-ph/9307364];  
 M. Ciuchini, E. Franco, G. Martinelli and L. Reina, “The  $\Delta S = 1$  effective Hamiltonian including next-to-leading order QCD and QED corrections,” Nucl. Phys. B **415**, 403 (1994) [hep-ph/9304257];  
 G. Cella, G. Curci, G. Ricciardi and A. Vicere, “QCD corrections to electroweak processes in an unconventional scheme: Application to the  $b \rightarrow s\gamma$  decay,” Nucl. Phys. B **431**, 417 (1994) [hep-ph/9406203];  
 M. Misiak, “The  $b \rightarrow se^+e^-$  and  $b \rightarrow s\gamma$  decays with next-to-leading logarithmic QCD corrections,” Nucl. Phys. B **393**, 23 (1993) [Erratum-ibid. B **439**, 461 (1993)].
- [64] N. Pott, “Bremsstrahlung corrections to the decay  $b \rightarrow s\gamma$ ,” Phys. Rev. D **54**, 938 (1996) [hep-ph/9512252].
- [65] C. Greub, T. Hurth and D. Wyler, “Virtual corrections to the decay  $b \rightarrow s\gamma$ ,” Phys. Lett. B **380**, 385 (1996) [hep-ph/9602281]; “Virtual  $O(\alpha_s)$  corrections to the inclusive decay  $b \rightarrow s\gamma$ ,” Phys. Rev. D **54**, 3350 (1996) [hep-ph/9603404].
- [66] K. Adel and Y. Yao, “Exact  $\alpha_s$  calculation of  $b \rightarrow s\gamma$ ,  $b \rightarrow s\text{gluon}$ ,” Phys. Rev. D **49**, 4945 (1994) [hep-ph/9308349].
- [67] K. Chetyrkin, M. Misiak and M. Munz, “Weak radiative  $B$  meson decay beyond leading logarithms,” Phys. Lett. B **400**, 206 (1997) [hep-ph/9612313].
- [68] K. G. Chetyrkin, M. Misiak and M. Munz, “Beta functions and anomalous dimensions up to three loops,” Nucl. Phys. B **518**, 473 (1998) [hep-ph/9711266].
- [69] K. G. Chetyrkin, M. Misiak and M. Munz, “ $|\Delta(F)| = 1$  non-leptonic effective Hamiltonian in a simpler scheme,” Nucl. Phys. B **520**, 279 (1998) [hep-ph/9711280].
- [70] P. Gambino, M. Gorbahn and U. Haisch, work in progress (private communication).
- [71] C. Greub and T. Hurth, “Two-loop matching of the dipole operators for  $b \rightarrow s\gamma$  and  $b \rightarrow s\text{gluon}$ ,” Phys. Rev. D **56**, 2934 (1997) [hep-ph/9703349].
- [72] M. Ciuchini, G. Degrassi, P. Gambino and G.F. Giudice, “Next-to-leading QCD corrections to  $B \rightarrow X_s\gamma$ : Standard model and two Higgs doublet model,” Nucl. Phys. B **527**, 21 (1998) [hep-ph/9710335].
- [73] A.J. Buras, A. Kwiatkowski and N. Pott, “Next-to-leading order matching for the magnetic photon penguin operator in the  $B \rightarrow X_s\gamma$  decay,” Nucl. Phys. B **517**, 353 (1998) [hep-ph/9710336].
- [74] A. J. Buras, A. Czarnecki, M. Misiak and J. Urban, “Two-loop matrix element of the current-current operator in the decay  $b \rightarrow X_s\gamma$ ,” Nucl. Phys. B **611**, 488 (2001) [hep-ph/0105160].
- [75] A. Ghinculov, T. Hurth, G. Isidori and Y. P. Yao, “Forward-backward asymmetry in  $B \rightarrow X_s\ell^+\ell^-$  at the NNLL level,” hep-ph/0208088.
- [76] H. H. Asatryan, H. M. Asatrian, C. Greub and M. Walker, “Complete gluon bremsstrahlung corrections to the process  $b \rightarrow s\ell^+\ell^-$ ,” Phys. Rev. D **66**, 034009 (2002) [hep-ph/0204341].
- [77] H. M. Asatrian, K. Bieri, C. Greub and A. Hovhannisyan, “NNLL corrections to the angular distribution and to the forward-backward asymmetries in  $b \rightarrow X_s\ell^+\ell^-$ ,” hep-ph/0209006.

- [78] A. Ghinculov, T. Hurth, G. Isidori and Y. P. Yao, “NNLL QCD corrections to the decay  $B \rightarrow X_s \ell^+ \ell^-$ ,” hep-ph/0211197.
- [79] A. Ghinculov, T. Hurth, G. Isidori and Y. P. Yao, “The decay  $B \rightarrow X_s \ell^+ \ell^-$  at the NNLL level,” in preparation.
- [80] A. J. Buras, A. Czarnecki, M. Misiak and J. Urban, “Completing the NLO QCD calculation of  $\bar{B} \rightarrow X_s \gamma$ ,” Nucl. Phys. B **631**, 219 (2002) [hep-ph/0203135].
- [81] C. Greub and T. Hurth, “Towards a next-to-leading logarithmic result in  $B \rightarrow X_s \gamma$ ,” hep-ph/9608449.
- [82] A. Ali, H. Asatrian and C. Greub, “Inclusive decay rate for  $B \rightarrow X_d \gamma$  in next-to-leading logarithmic order and CP asymmetry in the standard model,” Phys. Lett. B **429**, 87 (1998) [hep-ph/9803314].
- [83] C. Greub, T. Hurth, M. Misiak and D. Wyler, “The  $c \rightarrow u \gamma$  Contribution to Weak Radiative Charm Decay,” Phys. Lett. B **382**, 415 (1996) [hep-ph/9603417].
- [84] C. Bobeth, M. Misiak and J. Urban, “Photonic penguins at two loops and  $m_t$ -dependence of  $\mathcal{B}(B \rightarrow X_s \ell^+ \ell^-)$ ,” Nucl. Phys. B **574**, 291 (2000) [hep-ph/9910220].
- [85] H. H. Asatrian, H. M. Asatrian, C. Greub and M. Walker, “Two-loop virtual corrections to  $B \rightarrow X_s \ell^+ \ell^-$  in the standard model,” Phys. Lett. B **507**, 162 (2001) [hep-ph/0103087].
- [86] M. Misiak, “The  $b \rightarrow se^+e^-$  and  $b \rightarrow s\gamma$  decays with next-to-leading logarithmic QCD corrections,” Nucl. Phys. B **393**, 23 (1993) [Erratum-ibid. B **439**, 461 (1993)].
- [87] A. J. Buras and M. Munz, “Effective Hamiltonian for  $B \rightarrow X_s e^+ e^-$  beyond leading logarithms in the NDR and HV schemes,” Phys. Rev. D **52**, 186 (1995) [hep-ph/9501281].
- [88] G. Buchalla and A. J. Buras, “QCD corrections to rare  $K$  and  $B$  decays for arbitrary top quark mass,” Nucl. Phys. B **400**, 225 (1993);  
M. Misiak and J. Urban, “QCD corrections to FCNC decays mediated by  $Z$ -penguins and  $W$ -boxes,” Phys. Lett. B **451**, 161 (1999) [hep-ph/9901278].
- [89] A. F. Falk, M. Luke and M. J. Savage, “Non-perturbative contributions to the inclusive rare decays  $B \rightarrow X_s \gamma$  and  $B \rightarrow X_s \ell^+ \ell^-$ ,” Phys. Rev. D **49**, 3367 (1994) [hep-ph/9308288].
- [90] A. Ali, G. Hiller, L. T. Handoko and T. Morozumi, “Power corrections in the decay rate and distributions in  $B \rightarrow X_s \ell^+ \ell^-$  in the standard model,” Phys. Rev. D **55**, 4105 (1997) [hep-ph/9609449].
- [91] M.B. Voloshin, “Large  $O(m_c^{-2})$  non-perturbative correction to the inclusive rate of the decay  $B \rightarrow X_s \gamma$ ,” Phys. Lett. B **397**, 275 (1997) [hep-ph/9612483].
- [92] Z. Ligeti, L. Randall and M.B. Wise, “Comment on non-perturbative effects in  $\bar{B} \rightarrow X_s \gamma$ ,” Phys. Lett. B **402**, 178 (1997) [hep-ph/9702322].
- [93] A.K. Grant, A.G. Morgan, S. Nussinov and R.D. Peccei, “Comment on non-perturbative  $O(1/m_c^2)$  corrections to  $\Gamma(\bar{B} \rightarrow X_s \gamma)$ ,” Phys. Rev. D **56**, 3151 (1997) [hep-ph/9702380].
- [94] G. Buchalla, G. Isidori and S. J. Rey, “Corrections of order  $\Lambda_{QCD}^2/m_c^2$  to inclusive rare  $B$  decays,” Nucl. Phys. B **511**, 594 (1998) [hep-ph/9705253].
- [95] A. Khodjamirian, R. Rückl, G. Stoll and D. Wyler, “QCD estimate of the long distance effect in  $B \rightarrow K^* \gamma$ ,” Phys. Lett. B **402**, 167 (1997) [hep-ph/9702318];
- [96] J. W. Chen, G. Rupak and M. J. Savage, “Non- $1/m_b^n$  power suppressed contributions to inclusive  $B \rightarrow X_s \ell^+ \ell^-$  decays,” Phys. Lett. B **410**, 285 (1997) [hep-ph/9705219].

[97] G. Buchalla and G. Isidori, “Non-perturbative effects in  $\bar{B} \rightarrow X_s \ell^+ \ell^-$  for large dilepton invariant mass,” Nucl. Phys. B **525**, 333 (1998) [hep-ph/9801456].

[98] Courtesy of M. Misiak.

[99] C. W. Bauer and C. N. Burrell, “Non-perturbative corrections to moments of the decay  $B \rightarrow X_s \ell^+ \ell^-$ ,” Phys. Rev. D **62**, 114028 (2000) [hep-ph/9911404].

[100] C. S. Lim, T. Morozumi and A. I. Sanda, “A prediction for  $d\Gamma(b \rightarrow s\ell\bar{\ell})/dq^2$  including the long distance effects,” Phys. Lett. B **218**, 343 (1989);  
N. G. Deshpande, J. Trampetic and K. Panose, “Resonance background to the decays  $b \rightarrow s\ell^+ \ell^-$ ,  $B \rightarrow K^* \ell^+ \ell^-$  and  $B \rightarrow K \ell^+ \ell^-$ ,” Phys. Rev. D **39**, 1461 (1989).

[101] M. Neubert, “On the inclusive determination of  $|V(ub)|$  from the lepton invariant mass spectrum,” JHEP **0007**, 022 (2000) [hep-ph/0006068].

[102] M. Misiak, “Theory of radiative  $B$  decays,” hep-ph/0002007.

[103] A. Czarnecki and W.J. Marciano, “Electroweak radiative corrections to  $b \rightarrow s\gamma$ ,” Phys. Rev. Lett. **81**, 277 (1998) [hep-ph/9804252].

[104] K. Baranowski and M. Misiak, “The  $O(\alpha_{em}/\alpha_s)$  correction to  $\mathcal{B}(B \rightarrow X_s \gamma)$ ,” Phys. Lett. B **483**, 410 (2000) [hep-ph/9907427].

[105] A. Strumia, “Two loop heavy top corrections to the  $b \rightarrow s\gamma$  decay,” Nucl. Phys. B **532**, 28 (1998) [hep-ph/9804274].

[106] P. Gambino and U. Haisch, “Electroweak effects in radiative  $B$  decays,” JHEP **0009**, 001 (2000) [hep-ph/0007259];

[107] P. Gambino and U. Haisch, “Complete electroweak matching for radiative  $B$  decays,” JHEP **0110**, 020 (2001) [hep-ph/0109058].

[108] C. Greub and T. Hurth, “Radiative corrections in inclusive rare  $B$  decays,” Nucl. Phys. Proc. Suppl. **74**, 247 (1999) [hep-ph/9809468].

[109] C. Greub and P. Liniger, “Calculation of next-to-leading QCD corrections to  $b \rightarrow s\text{gluon}$ ,” Phys. Rev. D **63**, 054025 (2001) [hep-ph/0009144].

[110] A. Golutvin, plenary talk given at the XXXth International Conference on High Energy Physics, Osaka, Japan, July 2000.

[111] A. Lenz, U. Nierste and G. Ostermaier, “Determination of the CKM angle  $\gamma$  and  $|V(ub)/V(cb)|$  from inclusive direct CP asymmetries and branching ratios in charmless  $B$  decays,” Phys. Rev. D **59**, 034008 (1999) [hep-ph/9802202].

[112] A. L. Kagan and J. Rathsman, “Hints for enhanced  $b \rightarrow s\text{gluon}$  from charm and kaon counting,” hep-ph/9701300.

[113] P. Gambino and M. Misiak, “Quark mass effects in  $\bar{B} \rightarrow X_s \gamma$ ,” Nucl. Phys. B **611**, 338 (2001) [hep-ph/0104034].

[114] A. D. Martin, J. Outhwaite and M. G. Ryskin, “Improving  $\alpha_{em}(M_Z^2)$  and the charm mass by analytic continuation,” Eur. Phys. J. C **19**, 681 (2001) [hep-ph/0012231];  
J. H. Kuhn and M. Steinhauser, “Determination of  $\alpha_s$  and heavy quark masses from recent measurements of  $R(s)$ ,” Nucl. Phys. B **619**, 588 (2001) [Erratum-ibid. B **640**, 415 (2002)] [hep-ph/0109084];  
M. Eidemuller and M. Jamin, “Charm quark mass from QCD sum rules for the charmonium system,” Phys. Lett. B **498**, 203 (2001) [hep-ph/0010334]; S. Narison, “ $c$ ,  $b$  quark masses and  $f(D_s)$ ,  $f(B_s)$  decay constants from pseudoscalar sum rules in full QCD to order  $\alpha_s^2$ ,” Phys. Lett. B **520**, 115 (2001) [hep-ph/0108242];  
J. Penarrocha and K. Schilcher, “QCD duality and the mass of the charm quark,”

Phys. Lett. B **515**, 291 (2001) [hep-ph/0105222].

[115] J. Rolf and S. Sint, “A precise determination of the charm quark’s mass in quenched QCD,” hep-ph/0209255.

[116] M. Misiak, talk given at Radcor 2002, Kloster Banz, Germany, 8.-13.9.2002; see <http://www-zeuthen.desy.de/theory/radcor02>.

[117] A. Ali, “Theory of rare  $B$  decays,” hep-ph/9709507.

[118] G. Ricciardi, “Short and long distance interplay in inclusive  $B \rightarrow X_d \gamma$  decays,” Phys. Lett. B **355**, 313 (1995) [hep-ph/9502286];  
 N. G. Deshpande, X. He and J. Trampetic, “Long distance contributions to penguin processes  $b \rightarrow s \gamma$  and  $b \rightarrow d \gamma$ ,” Phys. Lett. B **367**, 362 (1996).

[119] D. E. Groom *et al.* [Particle Data Group Collaboration], “Review of Particle Physics,” Eur. Phys. J. C **15**, 1 (2000).

[120] A. Khodjamirian, G. Stoll and D. Wyler, “Calculation of long distance effects in exclusive weak radiative decays of  $B$  meson,” Phys. Lett. B **358**, 129 (1995) [hep-ph/9506242];  
 A. Ali and V. M. Braun, “Estimates of the weak annihilation contributions to the decays  $B \rightarrow \rho \gamma$  and  $B \rightarrow \omega \gamma$ ,” Phys. Lett. B **359**, 223 (1995) [hep-ph/9506248].

[121] M. Abud, G. Ricciardi and G. Sterman, “Light masses in short distance penguin loops,” Phys. Lett. **B437**, 169 (1998) [hep-ph/9712346].

[122] A. Ali, P. Ball, L. T. Handoko and G. Hiller, “A comparative study of the decays  $B \rightarrow (K, K^*) \ell^+ \ell^-$  in standard model and supersymmetric theories,” Phys. Rev. D **61**, 074024 (2000) [hep-ph/9910221].

[123] ALEPH Collaboration, report no. PA10-019, presented at the 28th International Conference on High Energy Physics, 25-31 July, 1996, Warsaw, Poland.

[124] Y. Grossman, Z. Ligeti and E. Nardi, “First limit on inclusive  $B \rightarrow X_s \nu \bar{\nu}$  decay and constraints on new physics,” Nucl. Phys. B **465**, 369 (1996) [Erratum-ibid. B **480**, 753 (1996)] [hep-ph/9510378].

[125] C. Bobeth, A. J. Buras, F. Kruger and J. Urban, “QCD corrections to  $\bar{B} \rightarrow X_{d,s} \nu \bar{\nu}$ ,  $B_{d,s} \rightarrow \ell^+ \ell^-$ ,  $K \rightarrow \pi \nu \bar{\nu}$  and  $K_L \rightarrow \mu^+ \mu^-$  in the MSSM,” Nucl. Phys. B **630**, 87 (2002) [hep-ph/0112305].

[126] S. Ferrara and E. Remiddi, “Absence of the anomalous magnetic moment in a supersymmetric abelian gauge theory,” Phys. Lett. B **53**, 347 (1974).

[127] A. H. Chamseddine, R. Arnowitt and P. Nath, “Locally supersymmetric grand unification,” Phys. Rev. Lett. **49**, 970 (1982);  
 R. Barbieri, S. Ferrara and C. A. Savoy, “Gauge models with spontaneously broken local supersymmetry,” Phys. Lett. B **119**, 343 (1982);  
 L. Hall, J. Lykken and S. Weinberg, “Supergravity as the messenger of supersymmetry breaking,” Phys. Rev. D **27** (1983) 2359.

[128] M. Dine, W. Fischler and M. Srednicki, “Supersymmetric technicolor,” Nucl. Phys. B **189**, 575 (1981);  
 S. Dimopoulos and S. Raby, “Supercolor,” Nucl. Phys. B **192**, 353 (1981);  
 M. Dine and A. E. Nelson, “Dynamical supersymmetry breaking at low-energies,” Phys. Rev. D **48**, 1277 (1993) [hep-ph/9303230];  
 M. Dine, A. E. Nelson and Y. Shirman, “Low-energy dynamical supersymmetry breaking simplified,” Phys. Rev. D **51**, 1362 (1995) [hep-ph/9408384];

M. Dine, A. E. Nelson, Y. Nir and Y. Shirman, “New tools for low-energy dynamical supersymmetry breaking,” *Phys. Rev. D* **53**, 2658 (1996) [hep-ph/9507378].

[129] G. F. Giudice, M. A. Luty, H. Murayama and R. Rattazzi, “Gaugino mass without singlets,” *JHEP* **9812**, 027 (1998) [hep-ph/9810442];  
L. Randall and R. Sundrum, “Out of this world supersymmetry breaking,” *Nucl. Phys. B* **557**, 79 (1999) [hep-th/9810155].

[130] M. Dine, R. Leigh and A. Kagan, “Flavor symmetries and the problem of squark degeneracy,” *Phys. Rev. D* **48**, 4269 (1993) [hep-ph/9304299];  
Y. Nir and N. Seiberg, “Should squarks be degenerate?,” *Phys. Lett. B* **309**, 337 (1993) [hep-ph/9304307].  
M. Leurer, Y. Nir and N. Seiberg, “Mass matrix models: The Sequel,” *Nucl. Phys. B* **420**, 468 (1994) [hep-ph/9310320].  
S. Dimopoulos and G. F. Giudice, “Naturalness constraints in supersymmetric theories with non-universal soft terms,” *Phys. Lett. B* **357**, 573 (1995) [hep-ph/9507282];  
A. Pomarol and D. Tommasini, “Horizontal symmetries for the supersymmetric flavour problem,” *Nucl. Phys. B* **466**, 3 (1996) [hep-ph/9507462];  
A. G. Cohen, D. B. Kaplan and A. E. Nelson, “The more minimal supersymmetric standard model,” *Phys. Lett. B* **388**, 588 (1996) [hep-ph/9607394];  
R. Barbieri, G. Dvali and L. J. Hall, “Predictions from a  $U(2)$  flavour symmetry in supersymmetric theories,” *Phys. Lett. B* **377**, 76 (1996) [hep-ph/9512388].

[131] G. D’Ambrosio, G. F. Giudice, G. Isidori and A. Strumia, “Minimal flavour violation: An effective field theory approach,” hep-ph/0207036.

[132] S. Bertolini, F. Borzumati, A. Masiero and G. Ridolfi, “Effects of supergravity induced electroweak breaking on rare  $B$  decays and mixings,” *Nucl. Phys. B* **353**, 591 (1991).

[133] F. M. Borzumati, “The Decay  $b \rightarrow s\gamma$  in the MSSM revisited,” *Z. Phys. C* **63**, 291 (1994) [hep-ph/9310212].

[134] H. Baer, M. Brhlik, D. Castano and X. Tata, “ $b \rightarrow s\gamma$  constraints on the minimal supergravity model with large  $\tan(\beta)$ ,” *Phys. Rev. D* **58**, 015007 (1998) [hep-ph/9712305].

[135] T. Goto, Y. Okada and Y. Shimizu, “Flavor changing neutral current processes in  $B$  and  $K$  decays in the supergravity model,” *Phys. Rev. D* **58**, 094006 (1998) [hep-ph/9804294].

[136] C. Bobeth, M. Misiak and J. Urban, “Matching conditions for  $b \rightarrow s\gamma$  and  $b \rightarrow s\text{gluon}$  in extensions of the standard model,” *Nucl. Phys. B* **567**, 153 (2000) [hep-ph/9904413].

[137] F.M. Borzumati and C. Greub, “2HDMs predictions for  $\bar{B} \rightarrow X_s\gamma$  in NLO QCD,” *Phys. Rev. D* **58**, 074004 (1998) [hep-ph/9802391].

[138] M. Ciuchini, G. Degrassi, P. Gambino and G.F. Giudice, “Next-to-leading QCD corrections to  $B \rightarrow X_s\gamma$  in supersymmetry,” *Nucl. Phys. B* **534**, 3 (1998) [hep-ph/9806308,v2].

[139] W. de Boer, M. Huber, A. V. Gladyshev and D. I. Kazakov, “The  $b \rightarrow X_s\gamma$  rate and Higgs boson limits in the constrained minimal supersymmetric model,” hep-ph/0102163.

[140] C. Greub, T. Hurth and M. Steinhauser, work in progress.

[141] J. F. Donoghue, H. P. Nilles and D. Wyler, “Flavor changes in locally supersymmetric theories,” *Phys. Lett. B* **128**, 55 (1983).

[142] L. J. Hall, V. A. Kostelecky and S. Raby, “New flavor violations in supergravity mod-

els,” Nucl. Phys. B **267**, 415 (1986).

[143] F. Gabbiani, E. Gabrielli, A. Masiero and L. Silvestrini, “A complete analysis of FCNC and CP constraints in general SUSY extensions of the standard model,” Nucl. Phys. B **477**, 321 (1996) [hep-ph/9604387].

[144] J. S. Hagelin, S. Kelley and T. Tanaka, “Supersymmetric flavor changing neutral currents: Exact amplitudes and phenomenological analysis,” Nucl. Phys. B **415** (1994) 293.

[145] A. Masiero and O. Vives, “New physics in CP violation experiments,” hep-ph/0104027.

[146] K. i. Okumura and L. Roszkowski, “De-constraining supersymmetry from  $b \rightarrow s\gamma$ ?,” hep-ph/0208101.

[147] L. Everett, G. L. Kane, S. Rigolin, L. T. Wang and T. T. Wang, “Alternative approach to  $b \rightarrow s\gamma$  in the uMSSM,” JHEP **0201**, 022 (2002) [hep-ph/0112126].

[148] D. Atwood, M. Gronau and A. Soni, “Mixing-induced CP asymmetries in radiative  $B$  decays in and beyond the standard model,” Phys. Rev. Lett. **79**, 185 (1997) [hep-ph/9704272].

[149] D. Melikhov, N. Nikitin and S. Simula, “Probing right-handed currents in  $B \rightarrow K^* \ell^+ \ell^-$  transitions,” Phys. Lett. B **442**, 381 (1998) [hep-ph/9807464];  
 F. Kruger, L. M. Sehgal, N. Sinha and R. Sinha, “Angular distribution and CP asymmetries in the decays  $\bar{B} \rightarrow K^- \pi^+ e^- e^+$  and  $\bar{B} \rightarrow \pi^- \pi^+ e^- e^+$ ,” Phys. Rev. D **61**, 114028 (2000) [Erratum-ibid. D **63**, 019901 (2001)] [hep-ph/9907386];  
 C. S. Kim, Y. G. Kim, C. D. Lu and T. Morozumi, “Azimuthal angle distribution in  $B \rightarrow K^*(\rightarrow K\pi) \ell^+ \ell^-$  at low invariant  $m_{\ell^+ \ell^-}$  region,” Phys. Rev. D **62**, 034013 (2000) [hep-ph/0001151].

[150] Y. Grossman and D. Pirjol, “Extracting and using photon polarization information in radiative  $B$  decays,” JHEP **0006**, 029 (2000) [hep-ph/0005069].

[151] T. Mannel and S. Recksiegel, “Probing the helicity structure of  $b \rightarrow s\gamma$  in  $\Lambda_b \rightarrow \Lambda\gamma$ ,” Acta Phys. Polon. B **28**, 2489 (1997) [hep-ph/9710287].

[152] G. Hiller and A. Kagan, “Probing for new physics in polarized  $\Lambda_b$  decays at the  $Z$ ,” Phys. Rev. D **65**, 074038 (2002) [hep-ph/0108074].

[153] M. Gronau, Y. Grossman, D. Pirjol and A. Ryd, “Measuring the photon helicity in radiative  $B$  decays,” Phys. Rev. Lett. **88**, 051802 (2002) [hep-ph/0107254]; M. Gronau and D. Pirjol, “Photon polarization in radiative  $B$  decays,” Phys. Rev. D **66**, 054008 (2002) [hep-ph/0205065].

[154] P. L. Cho, M. Misiak and D. Wyler, “ $K_L \rightarrow \pi^0 e^+ e^-$  and  $B \rightarrow X_s \ell^+ \ell^-$  decay in the MSSM,” Phys. Rev. D **54**, 3329 (1996) [hep-ph/9601360].

[155] T. Goto, Y. Okada, Y. Shimizu and M. Tanaka, “ $b \rightarrow s\ell\bar{\ell}$  in the minimal supergravity model,” Phys. Rev. D **55**, 4273 (1997) [Erratum-ibid. D **66**, 019901 (2002)] [hep-ph/9609512].

[156] J. L. Hewett and J. D. Wells, “Searching for supersymmetry in rare  $B$  decays,” Phys. Rev. D **55**, 5549 (1997) [hep-ph/9610323].

[157] C. S. Huang, W. Liao and Q. S. Yan, “The promising process to distinguish supersymmetric models with large  $\tan(\beta)$  from the standard model:  $B \rightarrow X_s \mu^+ \mu^-$ ,” Phys. Rev. D **59**, 011701 (1999) [hep-ph/9803460].

[158] Y. G. Kim, P. Ko and J. S. Lee, “Possible new physics signals in  $b \rightarrow s\gamma$  and  $b \rightarrow s\ell^+ \ell^-$ ,” Nucl. Phys. B **544**, 64 (1999) [hep-ph/9810336].

[159] E. Lunghi, A. Masiero, I. Scimemi and L. Silvestrini, “ $B \rightarrow X_s \ell^+ \ell^-$  decays in supersymmetry,” Nucl. Phys. B **568**, 120 (2000) [hep-ph/9906286].

[160] A. Ali, E. Lunghi, C. Greub and G. Hiller, “Improved model-independent analysis of semi-leptonic and radiative rare  $B$  decays,” Phys. Rev. D **66**, 034002 (2002) [hep-ph/0112300].

[161] M. Kobayashi and T. Maskawa, “CP violation in the renormalizable theory of weak interaction,” Prog. Theor. Phys. **49**, 652 (1973).

[162] A. L. Kagan and M. Neubert, “Direct CP violation in  $B \rightarrow X_s \gamma$  decays as a signature of new physics,” Phys. Rev. D **58**, 094012 (1998) [hep-ph/9803368].

[163] J. M. Soares, “CP violation in radiative  $b$  decays,” Nucl. Phys. B **367**, 575 (1991).

[164] S. W. Bosch and G. Buchalla, “The radiative decays  $B \rightarrow V \gamma$  at next-to-leading order in QCD,” Nucl. Phys. B **621**, 459 (2002) [hep-ph/0106081].

[165] M. Beneke, T. Feldmann and D. Seidel, “Systematic approach to exclusive  $B \rightarrow V \ell^+ \ell^-, V \gamma$  decays,” Nucl. Phys. B **612**, 25 (2001) [hep-ph/0106067].

[166] A. Ali and A. Y. Parkhomenko, “Branching ratios for  $B \rightarrow \rho \gamma$  decays in next-to-leading order in  $\alpha_s$  including hard spectator corrections,” Eur. Phys. J. C **23**, 89 (2002) [hep-ph/0105302].

[167] P. Ball and V. M. Braun, “Exclusive semi-leptonic and rare  $B$  meson decays in QCD,” Phys. Rev. D **58**, 094016 (1998) [hep-ph/9805422].

[168] T. Hurth and T. Mannel, “Direct CP violation in radiative  $B$  decays,” AIP Conf. Proc. **602**, 212 (2001) [hep-ph/0109041].

[169] K. Kiers, A. Soni and G. Wu, “Direct CP violation in radiative  $b$  decays in and beyond the standard model,” Phys. Rev. D **62**, 116004 (2000) [hep-ph/0006280].

[170] A. Ali and G. Hiller, “A theoretical reappraisal of branching ratios and CP asymmetries in the decays  $B \rightarrow (X_d, X_s) \ell^+ \ell^-$  and determination of the CKM parameters,” Eur. Phys. J. C **8**, 619 (1999) [hep-ph/9812267].

[171] C. Greub, H. Simma and D. Wyler, “Branching ratio and direct CP violating rate asymmetry of the rare decays  $B \rightarrow K^* \gamma$  and  $B \rightarrow \rho \gamma$ ,” Nucl. Phys. B **434**, 39 (1995) [Erratum-ibid. B **444**, 447 (1995)] [hep-ph/9406421].

[172] T. E. Coan *et al.* [CLEO Collaboration], “CP asymmetry in  $b \rightarrow s \gamma$  decays,” hep-ex/0010075.

[173] K. Abe *et al.* [BELLE Collaboration], “Measurement of the  $B \rightarrow K^* \gamma$  branching fractions,” BELLE-CONF-0239.

[174] T. E. Coan *et al.* [CLEO Collaboration], “Study of exclusive radiative  $B$  meson decays,” Phys. Rev. Lett. **84**, 5283 (2000) [hep-ex/9912057].

[175] B. Aubert *et al.* [BABAR Collaboration], “Measurement of  $B \rightarrow K^* \gamma$  branching fractions and charge asymmetries,” Phys. Rev. Lett. **88**, 101805 (2002) [hep-ex/0110065].

[176] T. Goto, Y. Y. Keum, T. Nihei, Y. Okada and Y. Shimizu, “Effect of supersymmetric CP phases on the  $B \rightarrow X_s \gamma$  and  $B \rightarrow X_s \ell^+ \ell^-$  decays in the minimal supergravity model,” Phys. Lett. B **460**, 333 (1999) [hep-ph/9812369].

[177] A. Bartl, T. Gajdosik, E. Lunghi, A. Masiero, W. Porod, H. Stremnitzer and O. Vives, “General flavor blind MSSM and CP violation,” Phys. Rev. D **64**, 076009 (2001) [hep-ph/0103324].

[178] M. Aoki, G. Cho and N. Oshimo, “CP asymmetry for radiative  $B$  meson decay in the supersymmetric standard model,” Nucl. Phys. B **554**, 50 (1999) [hep-ph/9903385];

C. Chua, X. He and W. Hou, “CP violating  $b \rightarrow s\gamma$  decay in supersymmetric models,” Phys. Rev. D **60**, 014003 (1999) [hep-ph/9808431];  
 Y. G. Kim, P. Ko and J. S. Lee, “Possible new physics signals in  $b \rightarrow s\gamma$  and  $b \rightarrow s\ell^+\ell^-$ ,” Nucl. Phys. B **544**, 64 (1999) [hep-ph/9810336];  
 S. Baek and P. Ko, “Probing SUSY-induced CP violations at  $B$  factories,” Phys. Rev. Lett. **83**, 488 (1999) [hep-ph/9812229];  
 L. Giusti, A. Romanino and A. Strumia, “Natural ranges of supersymmetric signals,” Nucl. Phys. B **550**, 3 (1999) [hep-ph/9811386];  
 E. J. Chun, K. Hwang and J. S. Lee, “CP asymmetries in radiative  $B$  decays with R-parity violation,” Phys. Rev. D **62**, 076006 (2000) [hep-ph/0005013];  
 D. Bailin and S. Khalil, “Flavor-dependent SUSY phases and CP asymmetry in  $B \rightarrow X_s\gamma$  decays,” Phys. Rev. Lett. **86**, 4227 (2001) [hep-ph/0010058];  
 D. A. Demir and K. A. Olive, “ $B \rightarrow X_s\gamma$  in supersymmetry with explicit CP violation,” Phys. Rev. D **65**, 034007 (2002) [hep-ph/0107329].

[179] H. H. Asatrian and H. M. Asatrian, “CP asymmetry for inclusive decay  $B \rightarrow X_d\gamma$  in the minimal supersymmetric standard model,” Phys. Lett. B **460**, 148 (1999) [hep-ph/9906221];  
 H. H. Asatryan, H. M. Asatrian, G. K. Yeghiyan and G. K. Savvidy, “Direct CP-asymmetry in inclusive rare  $B$  decays in 2HDM,” hep-ph/0012085.

[180] A. G. Akeroyd, Y. Y. Keum and S. Recksiegel, “Effect of supersymmetric phases on the direct CP asymmetry of  $B \rightarrow X_d\gamma$ ,” Phys. Lett. B **507**, 252 (2001) [hep-ph/0103008].

[181] T. Hurth and T. Mannel, “CP asymmetries in  $b \rightarrow (s/d)$  transitions as a test of CKM CP violation,” Phys. Lett. B **511**, 196 (2001) [hep-ph/0103331].

[182] R. Fleischer, “New strategies to extract  $\beta$  and  $\gamma$  from  $B_d \rightarrow \pi^+\pi^-$  and  $B_s \rightarrow K^+K^-$ ,” Phys. Lett. B **459**, 306 (1999) [hep-ph/9903456].

[183] M. Gronau and J. L. Rosner, “U-spin symmetry in doubly Cabibbo-suppressed charmed meson decays,” Phys. Lett. B **500**, 247 (2001) [hep-ph/0010237];  
 M. Gronau, “U-spin symmetry in charmless  $B$  decays,” Phys. Lett. B **492**, 297 (2000) [hep-ph/0008292].

[184] A. Ali, V. M. Braun and H. Simma, “Exclusive radiative  $B$  decays in the light cone QCD sum rule approach,” Z. Phys. C **63**, 437 (1994) [hep-ph/9401277];  
 P. Ball and V. M. Braun, “Exclusive semi-leptonic and rare  $B$  meson decays in QCD,” Phys. Rev. D **58**, 094016 (1998) [hep-ph/9805422].

[185] C. S. Huang, W. Liao and Q. S. Yan, “The promising process to distinguish supersymmetric models with large  $\tan(\beta)$  from the standard model:  $B \rightarrow X_s\mu^+\mu^-$ ,” Phys. Rev. D **59**, 011701 (1999) [hep-ph/9803460];  
 C. Hamzaoui, M. Pospelov and M. Toharia, “Higgs-mediated FCNC in supersymmetric models with large  $\tan(\beta)$ ,” Phys. Rev. D **59**, 095005 (1999) [hep-ph/9807350];  
 K. S. Babu and C. F. Kolda, “Higgs-mediated  $B^0 \rightarrow \mu^+\mu^-$  in minimal supersymmetry,” Phys. Rev. Lett. **84**, 228 (2000) [hep-ph/9909476];  
 G. Isidori and A. Retico, “Scalar flavour-changing neutral currents in the large- $\tan(\beta)$  limit,” JHEP **0111**, 001 (2001) [hep-ph/0110121];  
 A. Dedes and A. Pilaftsis, “Resummed effective Lagrangian for Higgs-mediated FCNC interactions in the CP-violating MSSM,” hep-ph/0209306;  
 A. J. Buras, P. H. Chankowski, J. Rosiek and L. Slawianowska, “Correlation between

$\Delta M_s$  and  $B_{s,d}^0 \rightarrow \mu^+ \mu^-$  in supersymmetry at large  $\tan(\beta)$ ,” Phys. Lett. B **546**, 96 (2002) [hep-ph/0207241].

[186] S. R. Choudhury and N. Gaur, “Dileptonic decay of  $B_s$  meson in SUSY models with large  $\tan(\beta)$ ,” Phys. Lett. B **451** (1999) 86 [hep-ph/9810307];  
 C. S. Huang, W. Liao, Q. S. Yan and S. H. Zhu, “ $B_s \rightarrow \ell^+ \ell^-$  in a general 2HDM and MSSM,” Phys. Rev. D **63**, 114021 (2001) [Erratum-ibid. D **64**, 059902 (2001)] [hep-ph/0006250];  
 P. H. Chankowski and L. Slawianowska, “ $B_{d,s}^0 \rightarrow \mu^- \mu^+$  decay in the MSSM,” Phys. Rev. D **63**, 054012 (2001) [hep-ph/0008046];  
 C. Bobeth, T. Ewerth, F. Kruger and J. Urban, “Analysis of neutral Higgs-boson contributions to the decays  $\bar{B}_s \rightarrow \ell^+ \ell^-$  and  $\bar{B} \rightarrow K \ell^+ \ell^-$ ,” Phys. Rev. D **64**, 074014 (2001) [hep-ph/0104284];  
 Z. Xiong and J. M. Yang, “Rare  $B$  meson dileptonic decays in minimal supersymmetric model,” Nucl. Phys. B **628** (2002) 193 [hep-ph/0105260];  
 A. Dedes, H. K. Dreiner and U. Nierste, “Correlation of  $B_s \rightarrow \mu^+ \mu^-$  and  $(g-2)_\mu$  in minimal supergravity,” Phys. Rev. Lett. **87**, 251804 (2001) [hep-ph/0108037].

[187] A. Belyaev *et al.* [Kaon Physics Working Group Collaboration], “Kaon physics with a high-intensity proton driver,” hep-ph/0107046.

[188] G. Buchalla and A. J. Buras, “ $\sin 2\beta$  from  $K \rightarrow \pi \nu \bar{\nu}$ ,” Phys. Lett. B **333**, 221 (1994) [hep-ph/9405259].

[189] Y. Nir and M. P. Worah, “Probing the flavor and CP structure of supersymmetric models with  $K \rightarrow \pi \nu \bar{\nu}$  decays,” Phys. Lett. B **423**, 319 (1998) [hep-ph/9711215].

[190] A. J. Buras, A. Romanino and L. Silvestrini, “ $K \rightarrow \pi \nu \bar{\nu}$ : A model independent analysis and supersymmetry,” Nucl. Phys. B **520**, 3 (1998) [hep-ph/9712398].

[191] G. Colangelo and G. Isidori, “Supersymmetric contributions to rare kaon decays: Beyond the single mass-insertion approximation,” JHEP **9809**, 009 (1998) [hep-ph/9808487].

[192] A. J. Buras and L. Silvestrini, “Upper bounds on  $K \rightarrow \pi \nu \bar{\nu}$  and  $K_L \rightarrow \pi^0 e^+ e^-$  from  $\epsilon'/\epsilon$  and  $K_L \rightarrow \mu^+ \mu^-$ ,” Nucl. Phys. B **546**, 299 (1999) [hep-ph/9811471].

[193] A. J. Buras, G. Colangelo, G. Isidori, A. Romanino and L. Silvestrini, “Connections between  $\epsilon'/\epsilon$  and rare kaon decays in supersymmetry,” Nucl. Phys. B **566**, 3 (2000) [hep-ph/9908371].

[194] G. Buchalla and A. J. Buras, “The rare decays  $K \rightarrow \pi \nu \bar{\nu}$ ,  $B \rightarrow X \nu \bar{\nu}$  and  $B \rightarrow \ell^+ \ell^-$ : An update,” Nucl. Phys. B **548**, 309 (1999) [hep-ph/9901288].

[195] G. Buchalla, “Rare kaon decays: Overview,” hep-ph/0110313.

[196] A. F. Falk, A. Lewandowski and A. A. Petrov, “Effects from the charm scale in  $K^+ \rightarrow \pi^+ \nu \bar{\nu}$ ,” Phys. Lett. B **505**, 107 (2001) [hep-ph/0012099].

[197] S. Adler *et al.* [E787 Collaboration], “Further search for the decay  $K^+ \rightarrow \pi^+ \nu \bar{\nu}$ ,” Phys. Rev. Lett. **84**, 3768 (2000) [hep-ex/0002015]; (see also <http://www.phy.bnl.gov/e787/e787.html>).

[198] S. Adler *et al.* [E787 Collaboration], “Further evidence for the decay  $K^+ \rightarrow \pi^+ \nu \bar{\nu}$ ,” Phys. Rev. Lett. **88**, 041803 (2002) [hep-ex/0111091].

[199] A. Alavi-Harati *et al.* [The E799-II/KTeV Collaboration], “Search for the decay  $K_L \rightarrow \pi^0 \nu \bar{\nu}$  using  $\pi^0 \rightarrow e^+ e^- \gamma$ ,” Phys. Rev. D **61**, 072006 (2000) [hep-ex/9907014]; see also <http://kpasa.fnal.gov:8080/public/ktev.html>.

- [200] Y. Grossman and Y. Nir, “ $K_L \rightarrow \pi^0 \nu \bar{\nu}$  beyond the standard model,” Phys. Lett. B **398**, 163 (1997) [hep-ph/9701313].
- [201] E949 collaboration: <http://www.phy.bnl.gov/e949/>
- [202] P. S. Cooper [CKM Collaboration], “CKM: Charged kaons at the main injector,” Nucl. Phys. Proc. Suppl. **99**, 121 (2001);  
see also <http://www.fnal.gov/projects/ckm/Welcome.html> .
- [203] K. Abe *et al.* [KEK-PS E391a Collaboration], “Status of the  $K_L^0 \rightarrow \pi^0 \nu \bar{\nu}$  experiment at KEK (E391a),” KEK-PREPRINT-2000-89 *Prepared for 30th International Conference on High-Energy Physics (ICHEP 2000), Osaka, Japan, 27 Jul - 2 Aug 2000*.
- [204] Y. G. Kudenko, “KOPIO experiment at BNL,” *Prepared for Kaon Decay Workshop for Young Physicists, Tsukuba, Japan, 14-16 Feb 2001*.
- [205] A. R. Barker and S. H. Kettell, “Developments in rare kaon decay physics,” Ann. Rev. Nucl. Part. Sci. **50**, 249 (2000) [hep-ex/0009024].
- [206] G. D’Ambrosio and G. Isidori, “ $K^+ \rightarrow \pi^+ \nu \bar{\nu}$ : A rising star on the stage of flavour physics,” Phys. Lett. B **530**, 108 (2002) [hep-ph/0112135].